

PREDICTION OF HYDROLOGIC FLUXES OVER THE
MARMOT BASIN USING SMALL SCALE
DISTRIBUTED HYDROLOGIC MODEL

ABU SAYED MD. RASHED



PREDICTION OF HYDROLOGIC FLUXES OVER THE MARMOT BASIN USING
SMALL SCALE DISTRIBUTED HYDROLOGIC MODEL

A thesis submitted to
the Memorial University of Newfoundland

In partial fulfillment of the
requirement for the degree of

Master of Engineering (Civil)

2010

By

Abu Sayed Md. Rashed

Faculty of Engineering and Applied Science

Abstract

The distributed-Hydrology-Soil-Vegetation model (DHSVM) was applied to the Marmot Creek watershed in western Alberta. The purpose of this research was primarily to assess the applicability of the model as hydrologic prediction tool for a snow dominated forested watershed. Climate data from July 2005 to December 2007 were used as forcing data. The model was calibrated and validated for the Marmot Creek watershed conditions using both streamflow and snow water equivalent (SWE). DHSVM was able to accurately simulate the streamflow and snow water equivalent for the simulated years. Because the accuracy of DHSVM simulations was greatly improved through rigorous calibration, this research demonstrates the need for model calibration to a watershed of interest, prior to hydrologic simulations using different landscape scenarios.

Next, two scenario were used to measure the effect of digital elevation model (DEM) and land cover change on streamflow and snow water equivalent. A hydrologically modified DEM was generated using ANUDEM software and was used to assess the sensitivity of DEM source on model simulations. Earth Observation for Sustainable Development (EOSD) and United States Geological Survey (USGS) land cover maps were also applied to evaluate the influence of land cover source on streamflow and SWE results. These sensitivity studies show that differences observed through direct comparisons of topographic parameters are reflected in the shape and timing of simulated streamflow and snow water equivalent (SWE) results. Results also show that the USGS DEM produced lower peak flows than the ANUDEM DEM and USGS land cover underestimate SWE when compared to the EOSD land cover.

Overall, the significance of the study is that it broadens the knowledge of DEM and land cover change effects on hydrological processes in snow dominated mountainous watersheds. It thus provides a framework for assessing the vulnerability of watersheds to altered streamflow and SWE regimes attributable to changes in DEM and land cover that occur over large geographical areas and long time-frames.

ACKNOWLEDGEMENTS

Generous appreciation goes to the IP3 research network and CFCAS for providing partial funding for this study. I especially thank my supervisor Dr. Ken Snelgrove for his support, guidance, and assistance throughout the research project. Thanks to the University of Washington Hydrology Group for making DHSVM an open source software for hydrological modeling. I appreciate kind gestures of Dr. John Pomeroy for providing meteorological forcing needed for numerical modeling. Finally, I would like to thank my friends and colleagues in our research group for their kind support.

Table of Contents

Table of Contents	1
List of Tables.....	3
List of Figures.....	4
Chapter 1.....	7
Introduction.....	7
1.1 Motivation	7
1.2 Objective.....	9
1.3 Chapter Summary.....	10
Chapter 2.....	11
Literature Review	11
2.1 Hydrologically Modified DEM.....	11
2.2 ANUDEM.....	13
2.3 Effect of DEM on Streamflow	15
2.4 Effect of Land Cover Change on Streamflow.....	17
2.5 Development of Distributed Hydrology Soil Vegetation Model	19
2.6 Applications of DHSVM.....	22
Chapter 3.....	24
Research Methodology	24
3.1 Introduction.....	24
3.2 Overview of DHSVM model.....	25
3.3 Evapotranspiration.....	32
3.4 Two-layer Ground Snowpack Model.....	34
3.5 Canopy Snow Interception and Release	35
3.6 Unsaturated Soil Moisture Movement.....	36
3.7 Saturated Subsurface Flow	38
3.8 Surface Overland Flow.....	39
3.9 Channel Flow	39
Chapter 4.....	41
Data Acquisition and Model Setup	41
4.1 Study Area.....	41
4.2 Data Preparation.....	46

4.2.1 Processing with GIS.....	47
4.2.2 Raster Inputs.....	47
4.2.3 Stream Network Input	56
4.2.4 Climate Forcing Inputs	57
4.3 Hydrologically Modified DEM Generation.....	64
4.3.1 Creating the ANUDEM Input Data.....	65
4.3.2 DEM Generation.....	67
4.3.3 DEM Comparison.....	70
4.3.4 Watershed Area and Elevation	70
Chapter 5.....	73
Model Calibration	73
5.1 Calibration of Model.....	74
5.1.1 Calibration Process	74
5.1.2 Statistical Judgment.....	75
5.2 Validation of Model	77
5.3 Results.....	79
5.3.1 Statistical Analysis.....	81
5.3.2 Snow Water Equivalent (SWE)	83
5.4 Discussion.....	86
Chapter 6.....	88
DEM and Land Cover Effects	88
6. Results.....	89
6.1. DEM Effects	89
6.1.1 Streamflow	89
6.1.2 Snow Water Equivalent.....	94
6.2 Land Cover Effect.....	98
6.2.1 Streamflow	98
6.2.2 Snow Water Equivalent.....	100
Chapter 7.....	107
Conclusion.....	107
7.1 Summary of the Results.....	107
7.2 Implication and Recommendation.....	108
Bibliography.....	111

List of Tables

Table		Page
4-1	Soil input parameters for DHSVM	50
4-2	Vegetation type descriptions of USGS land cover map	52
4-3	Land cover classes in Marmot Creek basin used in DHSVM	53
4-4	Vegetation input parameters used for DHSVM	54
4-5	Time-dependent field measurements at field sites in Marmot Creek basin by IP3 network	58
4-6	Parameter files used in DHSVM	63
4-7	User directives were applied to ANUDEM version 5.2	69
4-8	Watershed area and elevation	70
5-1	Statistics of observed and simulated stream discharge during calibration and validation periods	82
5-2	Statistics of snow water equivalent (SWE) simulated and measured at Marmot Creek basin in calibration and validation periods	86
5-3	Statistics of streamflow and snow water equivalent simulation in previous studies	86
6-1	Monthly averaged discharges (cms) for each DEM	90
6-2	Summary of average summer (May-Oct) flows	90

List of Figures

Figure		Page
3-1	Schematic representation of DHSVM inputs, preprocessing requirements, outputs and interaction with GIS software	26
3-2	DHSVM: Model representation	28
3-3	DHSVM: One-dimensional vertical water balance	29
3-4	DHSVM: Snow model (Storck, 2000)	30
3-5	DHSVM: Runoff production (Wigmosta and Perkins, 1997)	31
4-1	Marmot Creek basin location on the Canadian map	42
4-2	Aerial view of the Marmot Creek basin (Swanson et al., 1986)	46
4-3	Digital Elevation Model of Marmot Creek watershed from USGS SRTM data.	48
4-4	Marmot Creek soil type	49
4-5	Marmot Creek soil depths generated by AML script	51
4-6	Land Cover classification from USGS	52
4-7	Land Cover classification from EOSD	53
4-8	Watershed mask is used to extract analysis pixels from input grids	55
4-9	DHSVM vector coverage input of stream networks	56
4-10	DHSVM's AML script generated stream network overlaid by Geogratia stream network.	57
4-11	Climate and stream gauge station site locations	59
4-12	Monthly hyetograph for the Marmot Creek basin	60

4-13	Daily hyetograph and seasonal (May-October) stream flow for the Marmot Creek watershed, for the year 2006 to 2007	61
4-14	Daily discharge and precipitation for the Marmot Creek watershed, seasonal (May-October) year 2006.	62
4-15	Stream flow direction error. Steam segment is flowing in the wrong direction	66
4-16	Corrected directions of streamflow	67
4-17	USGS DEM showing the Marmot Creek boundary	71
4-18	ANUDEM DEM showing the Marmot Creek boundary	72
5-1	Calibrated results for the Marmot Creek basin. Simulated daily streamflow (m ³ /s) versus measured streamflow. Broken lines are due to measured streamflow only available from May to October	79
5-2	Precise simulation period for the year 2006	80
5-3	Scatter plot of daily average simulated streamflow versus measured data	83
5-4	Simulated and measured snow water equivalent for the Marmot Creek basin. Measured data started from Jan 01,2006	84
5-5	Simulated and measured snow water equivalent for the Marmot Creek basin for the year 2007	85
6-1	Simulated streamflows for the ANUDEM DEM and USGS DEM along with measured streamflow from May to October in year 2006 and 200	91
6-2	Simulated high flow event, June 2006	92
6-3	Scatter plot of daily streamflow for USGS vs. ANUDEM simulated	93
6-4	Simulated SWE generated by ANUDEM DEM and USGS DEM	95

6-5	DEM-related mean monthly anomalies in snow water equivalent (SWE) during August 2005 through December 2007	96
6-6	Spatial distribution of DEM source effect in SWE (m) over the Marmot Creek basin	97
6-7	Monthly average stream discharge with EOSD land cover, and USGS land cover scenarios	99
6-8	Scatter plot of daily average streamflow for the control and experimental scenarios	100
6-9	Daily SWE (m) time series for EOSD and USGS land cover simulated and measured	101
6-10	Measured and simulated SWE (m) time-series (month)	102
6-11	Spatial distribution of land cover change effect in SWE (m) over the Marmot Creek basin	104
6-12	Scatter plot of SWE (m) with EOSD land cover versus SWE (m) with USGS land cover	105

Chapter 1

Introduction

1.1 Motivation

Through history, human beings have changed the landscape to meet their various needs. In some cases, they have not only changed the condition of the landscape, but the rates and processes that formed it. The main causes of landscape change are economic and technological factors, demographic factors, institutional factors, cultural factors, globalization, agricultural expansion, and agricultural land use intensification. This land cover change will certainly influence the local and regional hydrologic response, which will in turn affect the environment and human society. Water and land management is a topic of great importance, and the impact of these management decisions play a direct role in the environmental and economic sustainability of the lands on which our lives and livelihoods depend. Informed decision making in the fields of water resource management relies on an accurate understanding of basin hydrology, as well as the dynamics of snow accumulation and melt. It is crucial to understand the hydrology of a snow dominated mountainous watershed and its connection to streamflow, and to have robust toolsets to help evaluate the tradeoffs between different landscape presentations. A comprehensive set of tools, used to accurately predict the impact of land use, is needed in order to make well informed decisions to plan our land use strategies. Developments in the acquisition, processing and storage of digital data

have greatly increased the availability and reliability of digital elevation models (DEMs). The emergence of Geographical Information Systems (GISs) has provided a tool to analyze and manipulate spatial information such as DEMs, land use, soil and vegetation data. This capability has led hydrologic computer models to evolve towards spatially distributed simulations of watershed conditions based on physical processes.

This study is part of the IP3 (Improved Processes and Parameterization for Prediction) research network being funded by the Canadian Foundation for Climate and Atmospheric Sciences (CFCAS) for 2006-2010 and strongly supported by partners in federal, provincial and territorial governments, communities, and private sector. The main goal of IP3 is to undertake fundamental research on processes and parameterisations in Canada's cold regions that remain poorly understood but are critical for developing a predictive capability for weather and water resources. IP3 is devoted to an improved understanding of hydrology and weather systems in cold regions, particularly Canada's Rocky Mountains and Western Arctic. Cold regions' hydrology and weather are of key importance to applied water management and policy development for agriculture, communities, recreation, sustainable industrial development, and environment conservation in western and northern Canada.

The Marmot Creek basin is one of the research basins selected by IP3 for understanding the hydrology of the mountainous watershed. Marmot Creek basin was selected for this study as full sets of meteorological data specifically precipitation, temperature, short and longwave radiation, humidity, wind speed and streamflow are available. Marmot Creek feeds the Kananaskis River and the Bow River system from the Rocky Mountains of Alberta; particularly it is located at 115⁰10'W longitude and 50⁰57'N latitude.

This research focuses on the prediction of watershed characteristics, basin hydrology, streamflow and snow accumulation. This prediction is important for water management and policy development for agriculture, communities, recreation, sustainable industrial development, and environmental conservation.

1.2 Objective

The broad goal of this investigation is to improve the understanding of the connection between spatial scale data sources and hydrologic prediction. The specific objectives of this study are as follows:

- To evaluate the potential of hydrologically modified topographic data generated by ANUDEM.
- To assess the model performance using various spatial scale inputs.
- To build a continuous simulation model to understand hydrological processes in Marmot Creek basin using DHSVM.
- To investigate the influence of spatial scale DEM and land cover data on resulting predictions of hydrologic response.

To address these objectives, a hydrologic modeling simulation was carried out over the Marmot Creek basin with different spatial elevation and land cover data. Subsequently, simulated streamflow and snow water equivalent is compared with observed data.

1.3 Chapter Summary

The remainder of this thesis is organized as follows: Chapter 2 provides a literature review related to this study. The physics of distributed hydrology soil vegetation model and its various sub-models are described in chapter 3. The physical hydrology of the study region, data preparation, and data pre-processing needed to drive the model are described in chapter 4. Hydrologically modified DEM generation is also described in the last section of chapter 4. The results of model calibration versus point observations and validation of basin discharge and snow water equivalent (SWE) are discussed in chapter 5. In chapter 6 the model is applied in the Marmot Creek basin to determine the effect of streamflow and snow water equivalent for different source of DEM and land covers. Conclusion and recommendations are presented in chapter 7.

Chapter 2

Literature Review

2.1 Hydrologically Modified DEM

Digital elevation models (DEMs) are widely used for modelling surface hydrology (Moore et al., 1991). Analyses include the automatic delineation of catchment areas (Martz and De Jong, 1998; O'Callaghan and Mark, 1984), development of terrain characteristics (Moore et al., 1991) and drainage networks (Fairfield and Leymarie, 1991), estimation of hydrology and soil moisture (Beven and Kirkby, 1979; English et al., 2004; McKenzie et al., 2003; O'Loughlin, 1986), determination of flow accumulation (Peucker and Douglas, 1975) and flow direction and routing (Tarboton, 1997 and 2002), and automated extraction of parameters for hydrological and hydraulic modelling (Ackerman, 2002; Doan, 2000).

The accuracy with which a DEM is able to replicate the hydrological reality of a catchment is determined by the scale of capture (cell size), the precision (vertical accuracy and relative accuracy between adjacent, upstream and downstream cells) and strength of the landscape gradient (flatness) (Gallant and Hutchinson, 1997; Gyasi-Agyei et al., 1995; Hutchinson and Dowling, 1994; Quinn et al., 1991; Wolock and Price, 1994; Zhang and Montgomery, 1994).

The minimum resolution and precision of a DEM are important when analysing surface hydrology (Quinn et al., 1991; Hutchinson and Dowling, 1994; Wolock and Price, 1994; Zhang and Montgomery, 1994; Gyasi-Agyei et al., 1995; Gallan and Hutchinson, 1997). However, the required level of resolution and precision is often not available for many areas at the catchment or sub-catchment scale. In these circumstances, methods of DEM hydrological correction must be used.

There are potentially many relatively new data sources from which to generate moderate resolution DEMs ranging from ground survey with kinematic GPS to airborne photogrammetry, interferometry, and radar or laser altimetry (Hutchinson and Gallant, 2000). Recent developments in light detection and ranging (LIDAR) technology provide a new option for generating fine-resolution DEMs (Hill et al., 2000; Liu, 2008; Murphy et al., 2008). Algorithms used to present and extract real-world processes from a DEM are also significant (Gallant and Dowling, 2003; Jones, 1998; Tarboton, 1997). By far the most popular data source is digital topographic data used in an interpolation algorithm to generate a DEM. Typically, these data include contours, spot heights, rivers vectors and lakes. While the use of such topographic data appears straightforward, results can vary greatly as a function of both the quality of the input data and of the processing algorithm used. For example, while a DEM can be generated using a Triangular Irregular Network (TIN) approach, the resultant DEM will often not be hydrologically correct. This can be seen by artificial features being present such as spurious triangular-shaped sinks or peaks, resulting in incorrect derived stream networks, contributing areas and catchment boundaries calculation. To meet the challenge of creating hydrologically correct DEMs from digital topographic data (contours, spot heights, rivers and lakes) an application developed by the Australian National University

called ANUDEM has evolved over the last two decades (Hutchinson, 1988; Hutchinson, 1989; Hutchinson, 2004).

In this study hydrologically modified DEM are generated from contour and stream network by ANUDEM for the analyses.

2.2 ANUDEM

Digital elevation models (DEMs) underpin an extensive range of research and applications in natural resource analysis and assessment (Hutchinson, 2006). They are used to support hydrological applications that depend on accurate representation of surface drainage structure. ANUDEM is a program that calculates regular grid digital elevation models (DEMs) with sensible shape and drainage structure from arbitrarily large topographic data sets. It has been used to develop DEMs ranging from fine scale experimental catchments to continental scale (ANUDEM 5.2 manual).

ANUDEM has many features that are not found in other interpolation programs. These are as follows: a) the process is computationally efficient; hence, DEMs with over a million points can be easily interpolated using a computer workstation. b) the roughness penalty (one of the interpolation parameters) can be modified to allow the fitted DEM to follow the sharp changes in terrain associated with ridges and sometimes with streams and other land features. c) the program uses a drainage enforcement algorithm that attempts to remove all sinks in the fitted DEM which have not been identified by the user. d) drainage enforcement is further enhanced by incorporating user-supplied, stream line data in the interpolation process. e) the program can recognize and

preserve sinks in the landscape. f) the grid spacing of the output DEM is user-controlled.

The ANUDEM interpolation procedure has been designed to take advantage of the types of input data commonly available, and the known characteristics of elevation surfaces. It uses an iterative finite difference interpolation technique, optimized to have the computational efficiency of 'local' interpolation methods such as inverse distance weighted interpolation, without losing the surface continuity of global interpolation methods such as kriging and splines. The technique is essentially a discretised thin plate spline technique (Wahba, 1990), where the roughness penalty has been modified to allow the fitted DEM to follow abrupt changes in terrain, such as streams and ridges.

ANUDEM (Hutchinson, 1988; Hutchinson, 1989; Hutchinson, 2003; Hutchinson, 2004) creates a smooth surface without sinks by imposing a global drainage condition via an iterative drainage enforcement algorithm, which is based on input data that can include irregularly spaced elevation data points (spot heights), contour lines, streamlines, sink points (lakes) and cliff lines. Elevation across the entire DEM can be altered when creating a new surface that enforces drainage and eliminates abrupt jumps between the stream and non stream cells. Although ANUDEM allows the user a larger range of input variables to correct hydrology, for the sake of simplicity and consistency with the other source DEM, only the stream network data was used to enforce drainage. ArcGIS 9.3 was used to prepare all the dataset. The UNGENERATE command was used in ARC/INFO to prepare the contour and stream network data for processing in ANUDEM v5.2 using default values for roughness penalties and standard errors (Hutchinson, 2004).

In this study ANUDEM 5.2 generated 90-m resolution DEM and USGS 90-m resolution DEM is used to analyse hydrologic fluxes over the Marmot Basin.

2.3 Effect of DEM on Streamflow

Predicting spatial patterns, rates of runoff generation and many geomorphic processes requires both a hydrologic model and characterization of the land surface. Most physically based models of hydrologic and geomorphic processes rely on either spatially distributed or lumped characterizations of local slope and drainage area per unit contour length (Beven and Kirkby, 1979; O'Loughlin, 1986; Vertessy et al., 1990; Dietrich et al., 1993). Digital elevation models (DEMs), a common format for representing topography digitally (Jenson and Domingue, 1988; Chang and Tsai, 1991; Jenson, 1991; Florinsky, 1998; Gao, 1998; Schoorl et al., 2000; Claessens et al., 2005; Wechsler, 2007; Murphy et al., 2008), are used for such characterization in a wide variety of scientific, engineering, and planning applications. Although the increasing availability of DEMs allows rapid analysis of topographic attributes over even large drainage basins, topographic and hydrologic inputs can influence simulation results greatly (Renschler and Harbor, 2002).

Topography is recognized as a significant factor in determining the streamflow response of upland, forested watersheds to precipitation (Kirkby and Chorley, 1967; Dunne et al., 1975; O'Loughlin, 1981; Beven and Kirkby, 1979; Beven and Wood, 1983). Topography defines the effects of gravity on the movement of water in a watershed, and therefore it influences many aspects of the hydrologic system. Numerous studies have shown that the reliability of the derived topographic and hydrologic attributes depends on the

resolution and accuracy of the input digital elevation model (DEM). For example, topography has been shown to affect the flow path that precipitation follows before it becomes streamflow (Wolock et al., 1990), the spatial distribution of soil moisture within a watershed (Burt and Butcher, 1985), and the chemical characteristics of streamflow (Wolock et al., 1989 and 1990). Zhang and Montgomery (1994) evaluated the effects of 4-, 10-, 30-, and 90-m resolution DEMs for two watersheds and found that the simulated peak discharge increased and simulated depth to the water table decreased as the grid cell size of the DEM increased. Dubin and Lettenmaier, (1999) assessed the influence of digital elevation model resolution on hydrologic modeling and reported that the simulated peak flows were most sensitive to pixel size for storms. Kenward and Lettenmaier (1997) used 5-m resolution DEM derived from automated stereo correlation from low altitude aerial photography, standard USGS 30-m resolution DEM and 30-m resolution DEM processed by Spaceborne Imaging Radar-C (SIR-C), and found that mean annual runoff volumes for simulations that used the USGS and SIR-C DEMs were 0.3 and 7.0 percent larger, respectively, than simulations produced using the 5-m resolution DEM.

In this study the effects of DEM on hydrology simulation is evaluated at a watershed scale using DHSVM with USGS DEM and ANUDEM generated DEM .

2.4 Effect of Land Cover Change on Streamflow

Forest land cover changes influence hydrologic modelling in two ways. First, vegetation extent increases evapotranspiration since deeper moisture storages may be tapped by roots. Second, more vegetation reduces surface snow pack volumes (Berris and Harr, 1987; Storck and Lettenmaier, 1999; Kattleman, 1990) and reduces the radiative and sensible heat transfers to the surface snow pack by attenuating the wind and short wave solar radiation by the canopy (Black, et al., 1991; Poemeroy and Dion, 1996). These two main effects may lead to secondary hydrologic changes. Decrease in evapotranspiration may lead to increase in soil moisture, which consecutively may increase the extent of saturation and lead to more runoff during snow melt or heavy rainfall events. Additionally, increased snowpack, associated with canopy removal, may melt more rapidly through enhanced heat flux into the pack (Wetherbee and Lettenmaier, 1996).

Different field experiments have examined the localized effects of the land cover change at the sub-catchment scales (Rothacher, 1965, 1970; Megahan, 1972, 1983; Ziemer, 1981; Harr and McCorison, 1979; Troendle and King, 1985; Berris and Harr, 1987; Kattelmann, 1990). Although these investigations have added understanding to the physical processes by which landscape disturbance affects local hydrologic response, extrapolation to the catchment scale is complicated, because a catchment integrates a variety of land use changes. There is also a question as to how changes at the sub-catchment scale are affected by their location within a catchment, which in turn partly determines the effect on catchment outlet hydrographs.

Approaches to quantify the effects of land cover changes on catchment hydrology can be classified into one of three methods (Bates and Henry, 1928). Firstly, paired catchment studies, in which one catchment is maintained as control while the other nearby catchment receive some treatment. The discharge records before and after the treatment are compared, from which the significance of the treatment is deduced; secondly, retrospective studies, which are similar in nature to paired catchment studies, but use stream and land cover records which are not subject to careful scientific control. Statistical methods can be used to extract the signal from the records, which often will be smaller than if there were a true control, as changes in land cover occur simultaneously in all catchments (Jones and Grant, 1996; Bowling et al., 2000). Finally, computer modeling, in which the output from a mathematical model of the natural system is compared with the output from an alternative land cover parameterization of the model. The difference between the two sets of output is attributed to the change in land cover. (Wetherbee and Lettenmaier, 1996, 1997; Bowling and Lettenmaier, 1997; Storck and Lettenmaier, 1999; Matheussen, et al., 2000; Storck, 2000; Bowling, et al., 2000)

As it is impossible to isolate the variables in the natural system, the ability of the first two methods are limited in their determination of cause and effect (Eberhardt and Thomas, 1991). The third method, use of physically-based, spatially distributed hydrological model to describe the hydrologic processes that are related to land cover in such a way that individual variables can be isolated and modified, allowing direct interpolation of the effects. Metheussen et al., (2000) investigated the effects of historical land cover change on the hydrology of the Columbia River basin using Variable Infiltration Capacity

(VIC) model, a macro scale hydrological model. In this study DHSVM was applied to address the effects of land cover changes on streamflow for Marmot Creek basin.

2.5 Development of Distributed Hydrology Soil Vegetation Model

Since the mid 1960s there has been a steady growth of development of computer applications that model hydrologic response (Ward and Elliot, 1995). With the arrival of the personal computer in the early 1980s, and with further advances in computing capability and storage space, accuracy and accessibility of spatial data sets, a wide variety of increasingly complex hydrologic models have appeared. Twenty-three different computer based hydrologic models are described in *Mathematical Models of Small Watershed Hydrology and Applications* (Singh and Frevert, 2002). While this is not a comprehensive list, many of the models illustrated represent the most widely used and accepted, as well as the most innovative hydrologic models of the day. At this time, there exists a daunting array of choices of hydrologic simulation tools available to researchers; however, each tool is not appropriate for all objectives, in all scenarios, or every landscape. The hydrologist or researcher is reliant on judgment to choose the model that is most capable of simulating the landscape processes for the area and scale of interest.

Basically, a hydrologic model can be empirical, stochastic or deterministic in nature (Ward and Elliot, 1995). Empirical models are based on observed or experimentally derived data and are also called regression, or black-box models. These models utilize

basic relationships between the inputs and outputs to model a specific physical process (Grayson and Blöschl, 2000). In contrast, stochastic hydrologic models are essentially statistical models. These models utilize statistical theory to identify probabilities of specific hydrologic events, such as floods or hill slope failures. Some, or all, of the inputs into stochastic model are represented by statistical distributions instead of single values (Grayson and Blöschl, 2000). Finally, deterministic models, also described as physically-based models, tend to be the most complex of the three. These models represent the most important physical and chemical processes taking place on the landscape by using mathematical equations. Many of the physical landscape processes are empirically described within the context of the larger deterministic model. Therefore, these models are not truly physically-based, but are instead, theoretical in nature (Ward and Elliot, 1995). Until very recently, few spatially distributed deterministic hydrologic models were in existence (Yeh et al., 2006). Developments of these types of models were necessary to address explicitly the complicated interactions of the atmosphere, topography, soil, water, and vegetation at the watershed scale. Non-distributed or lumped models, do not explicitly represent the landscape, but instead, employ average values of watershed characteristics affecting runoff volumes. In some cases, this averaging may be source of significant error. However, the benefits of lumped models include low data and computation time requirements, relatively simple algorithms, and the resulting ease of use benefit. On the other hand, distributed models tend to be highly input-intensive, and the advantages of the spatial and temporal complexity provided by these types of models may be lost. This is especially true if high resolution data is not used within the distributed model simulations. However, for areas with high degrees of spatial and temporal landscape heterogeneity, the lack of complexity in lumped models may come at the cost of accuracy in hydrologic simulations. Distributed

deterministic models may prove particularly useful in modeling the physical processes governing the hydrology of mountainous, forested landscapes in Alberta, Canada, because of their ability to capture landscape variability. This assumes that high resolution spatial data is available to drive simulations.

The Distributed Hydrology Soil Vegetation Model (DHSVM) was originally designed for Pacific Northwest of US and west coast of British Columbia, Canada (PNW) watersheds. It is typically used at a several hundred square kilometre scale and run at a sub-daily time interval where it provides detailed information on the spatial pattern and specific location of water and energy fluxes. The model has evolved significantly from the original version described in Wigmosta et al. (1994). Canopy snow interception and release simulation, three dimensional overland flow representation, and a one-dimensional channel flow model have been added. Additionally, a more accurate two-layer ground snowpack representation has replaced the original one-layer representation (Wigmosta et al., 2002). In this study DHSVM 2.0.1 was used to simulate the hydrologic responses of Marmot Basin.

2.6 Applications of DHSVM

The Distributed Hydrology Soil Vegetation Model (DHSVM) is a physically based distributed parameter model that provides an integrated representation of watershed processes at the spatial scale described by digital elevation model (DEM) data (Wigmosta et al., 1994; Bowling and Lettenmaier, 1997). DHSVM has been utilized in a number of research activities involving hydrologic analysis and modeling (Wigmosta et al., 1994; Kenward and Lettenmaier, 1997; Wigmosta and Lettenmaier, 1999; Westrick et al., 2000). DHSVM was first applied to the Middle Fork Flathead catchment in Montana (Wigmosta et al., 1994). Since then it has been applied to a number of catchments with a variety of objectives. Perkins et al., (1996) applied it to Carnation Creek, British Columbia to test its road network algorithm. As a part of Boreal Ecosystem-Atmospheric Study (Boreas), it was applied to the Boreal forest in Canada (Haddeland and Lettenmaier, 1995; Nijssen et al., 1997). Bowling and Lettenmaier, (1997) used the model to study the effects of forest roads in Hard and Ware Creeks, Washington. Strock et al., (1998) used DHSVM to investigate two rain-on-snow floods on the North Fork Snoqualmie and on the Little Naches River, Washington to investigate spring snow melt. Storck (2000) applied DHSVM to the Snohomish River, Washington in a study on snow accumulation and melt. The model has also been used to study the interactions between climate and hydrology (Wigmosta et al., 1995; Arola and Lettenmaier, 1996) and the potential impacts between climate changes on water resources (Leung et al., 1996; Leung and Wigmosta, 1999 and 2000). There has been significant use of DHSVM for basic and applied research concerning forest management activities on watershed processes (Storck et al., 1995, Lamarche and

Lettenmaier, 1998; Storck et al., 1999, Bowling et al., 2000; Bowling and Lettenmaier, 2001; Wigmosta and Perkins, 2001).

There are several recent applications of DHSVM, Cuo et al., (2006) used DHSVM to study road effect on hydrological processes. Jost et al., (2009) applied DHSVM to the Cotton Creek watershed, south-eastern British Columbia to predict the effect of forest clear-cutting.

Chapter 3

Research Methodology

3.1 Introduction

Researchers are interested about DHSVM for a number of reasons. The most attractive feature of DHSVM, from a research perspective, is that it is a physically-based and fully-distributed model. Its distributed nature captures the spatial variability of landscape features and complex meteorological conditions presented by mountainous, forested terrain. Additionally, because it is physically-based, there is theoretically little need for model calibration. This amplifies the potential research utility of DHSVM to ungaged catchments and its use in climate studies. Detail representations of multi-layer canopy, soil, wind profile, and snowpack makes DHSVM superior to landscape representations used in other hydrologic models. This level of detail should theoretically enhance DHSVM's ability to address the actual physical processes driving the hydrologic cycle at the watershed scale. The ability of DHSVM to operate at sub-daily time steps is another essential feature for watershed scale modeling. DHSVM calculates the full water and energy balance for every pixel and for every time step. This level of complexity is necessary to capture the highly dynamic processes affecting snow accumulation and ablation in a snow-dominated system.

The model design also lends itself to incorporation of a wide variety of spatial data types. While the inputs are extensive, they are also somewhat flexible. The appeal lies in the adaptability of the model. The user defines the spatial and temporal resolution of DHSVM based on the data available for the particular research application.

Finally, DHSVM holds promise as a potential management tool. The preprocessing of the spatial inputs required by DHSVM is time consuming. However, once the data are collected and formatted for a geographic area, and the model is compiled and running on a specific computer system, then the ease of use is relatively high. The extensive list of output options has the potential for a wide range of management applications involving the simulation of hydrologic processes at a watershed scale.

This chapter describes Distributed Hydrologic Soil Vegetation Model (DHSVM) which was used in this study. A general overview of the model is provided first, followed by a more detailed discussion of model's representation of hydrologic variables.

3.2 Overview of DHSVM model

The Distributed Hydrology-Soil-Vegetation Model (DHSVM) is a spatially explicit hydrologic model that accounts for the physical processes affecting the movement of water on and through the landscape with a distributed, deterministic approach. In general, the model dynamically represents the spatial distribution of evapotranspiration, snow cover, soil moisture, and runoff across a watershed (Wigmosta et al., 2002). A DEM provides the foundation for the model structure, and typical spatial resolutions for model applications range from 10 to 100 m (VanShaar et al., 2002). Characterization of soil and vegetation at the DEM resolution derives the topographic controls on absorbed solar radiation, precipitation, air temperature, and downslope water movement in the model (Wigmosta et al., 1994). DHSVM utilizes both a two-layer vegetation representation and a multi-layer soil profile representation. For each pixel within the watershed boundary, a single vegetation and soil class is assigned. However, the

modeler has ultimate control of the parameterization of each soil and vegetation type defined. Any combination or number of individual soil and vegetation classes may incorporate, thereby enhancing the ability of the modeler to capture landscape variability. The model operates at the time step of the meteorological inputs. It functions at the sub-daily level up to a 1-hr temporal resolution. Figure 3-1 shows DHSVM inputs and outputs, including data processing.

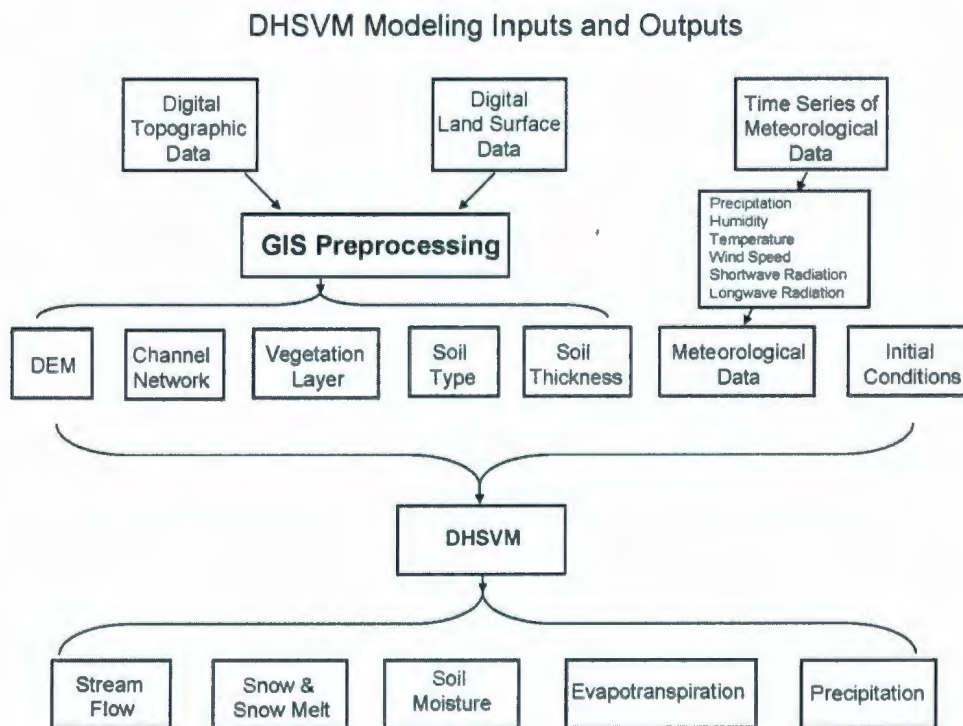


Figure 3-1: Schematic representation of DHSVM inputs, preprocessing requirements, outputs and interaction with GIS software (Storck, 2000)

Once the land surface attributes have been assigned (Figure 3-2), meteorological forcings are applied to each grid cell. DHSVM solves full water and energy balance equations at the resolution of a digital elevation model (DEM) for multiple vegetation and soil layers (Figure 3-3).

DHSVM incorporates a sophisticated two-layer snow accumulation and ablation model (Figure 3-4). Surface and subsurface flow routing algorithms channel water to the watershed outlet and allow grid cells to exchange water with adjacent neighbors (Wigmosta et al., 2002) (Figure 3-5). While DHSVM is not directly linked to any particular Geographical Information System (GIS), the inputs and outputs are best managed within a GIS.

DHSVM Model Representation

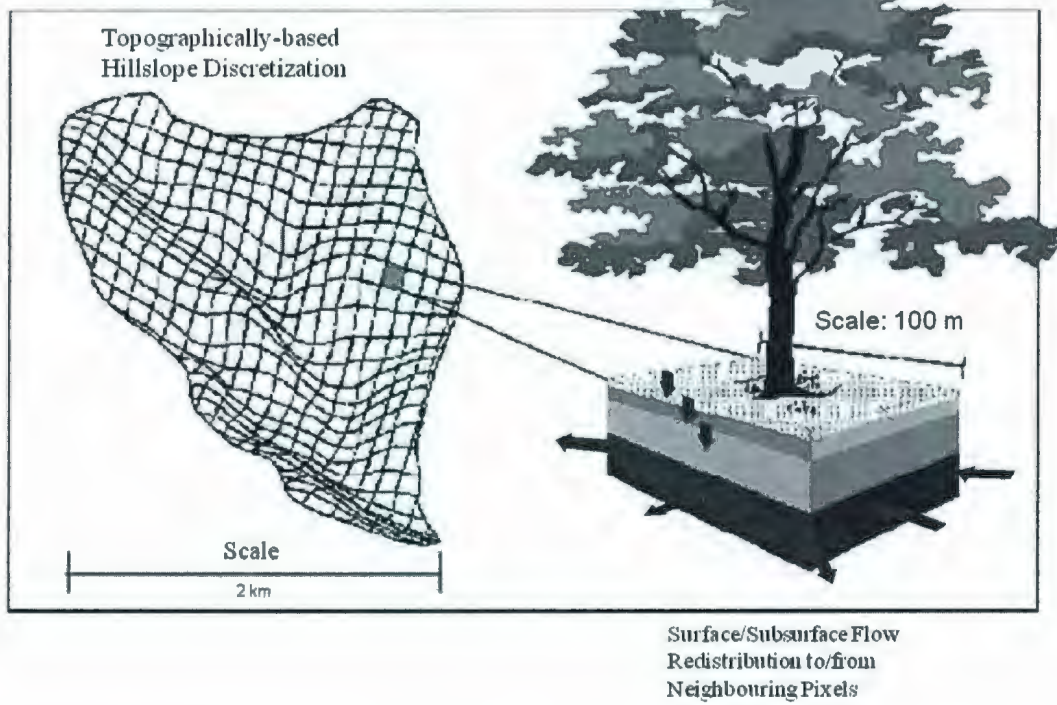


Figure 3-2: DHSVM: Model representation (Wigmosta, et al., 1994)

1-D Vertical Water Balance

Evaporation (E)

Interception (E_{io} , E_{iu})
Soil (E_s)

Transpiration

Overstory (E_{to})
Understory (E_{tu})

Storage (S)

Overstory (S_{io})
Understory (S_{iu})
Soil layer 1 ($\theta_1 d_1$)
Soil layer 2 ($\theta_2 d_2$)

Rooting Zones

$$S_e = \theta_1 d_1 + \theta_2 d_2$$

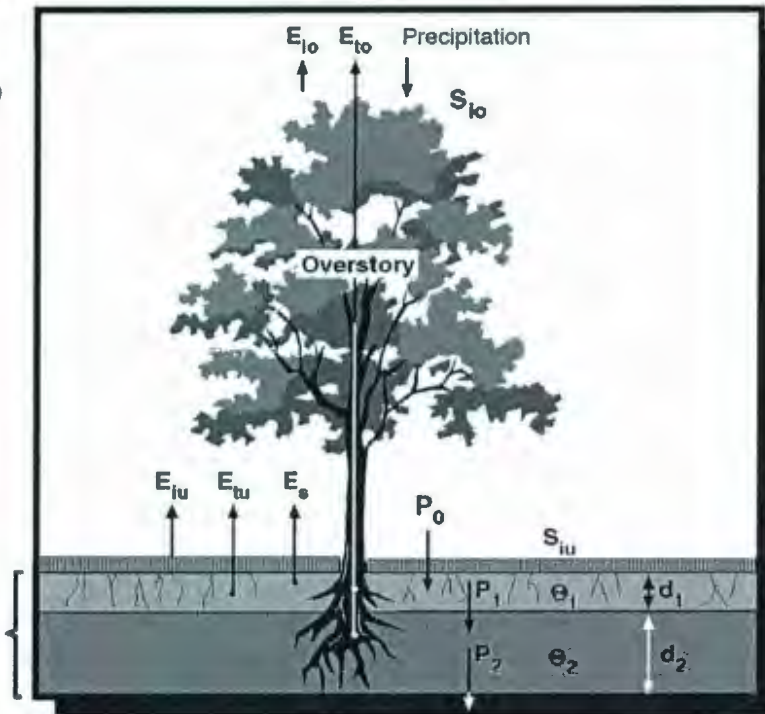


Figure 3-3: DHSVM: One-dimensional vertical water balance (Wigmosta, et al., 1994)

DHSVM: Snow Model

Required Forcings: Above-canopy meteorology

Air Temperature
Relative Humidity
Wind Speed
Shortwave Radiation
Longwave Radiation
Precipitation

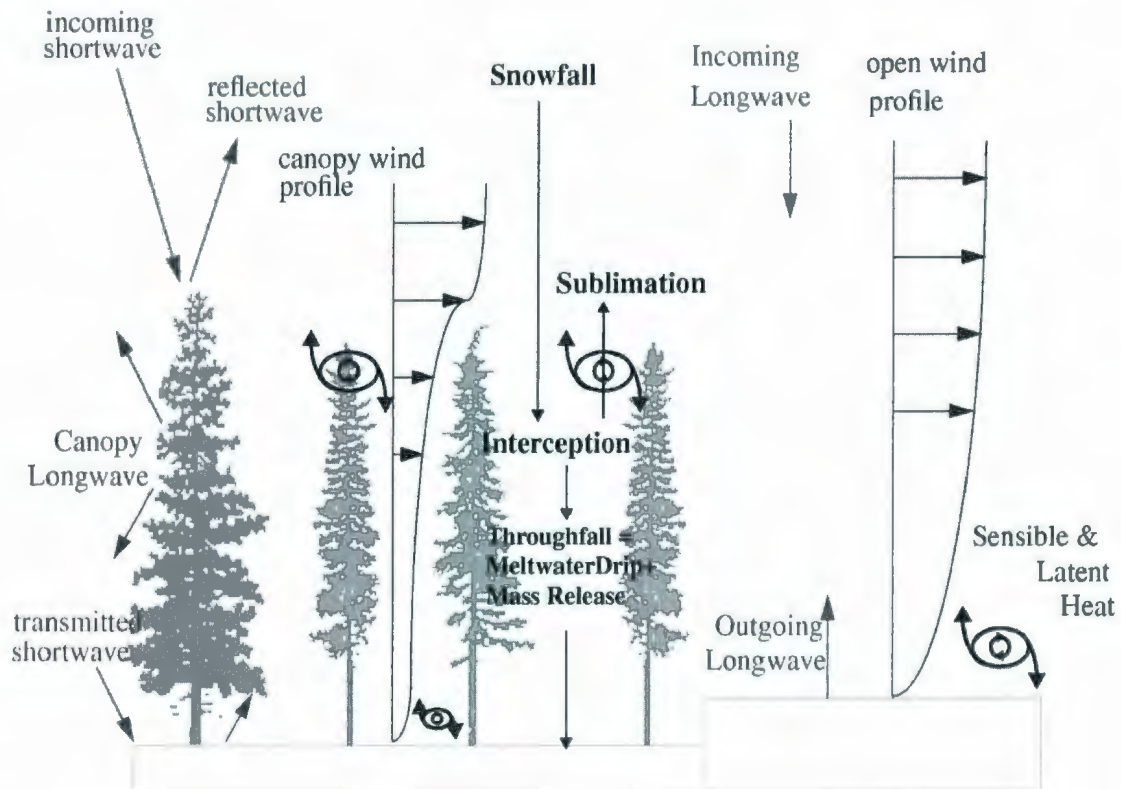
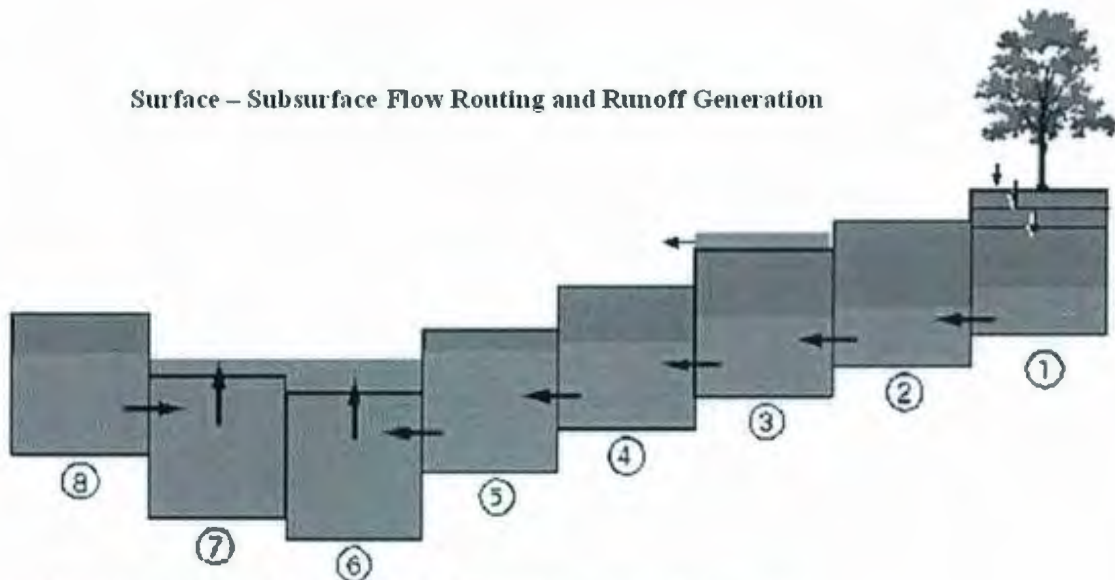


Figure 3-4: DHSVM: Snow model (Storck, 2000)

Surface – Subsurface Flow Routing and Runoff Generation



Pixels (1-5 and 8): Subsurface flow redistribution based on local water table slope

Pixels (6,7): Runoff Production (Saturation Excess)
Surface water routed to downslope neighbor

Pixel (3): Runoff Production (Infiltration Excess)
Surface water routed to downslope neighbor

Channel Network Segments (including road ditches)
May intercept subsurface flow (depends on channel depth)
Intercept all surface flow
Route water between segments using linear reservoir scheme

Figure 3-5: DHSVM: Runoff production (Wigmosta and Perkins, 1997).

Generally, inputs into DHSVM can be categorized into three separate groups: i) time series data, ii) spatial data including raster and vector inputs, and iii) associated text files that serve as look-up tables during the modeling process. The time series inputs consist of meteorological data at a specified time step for the period that the model is to be run. Spatial inputs involving raster data include a digital elevation model, a watershed mask, and grids of the vegetation type, soil type, and soil depth, each with the same extent and grid cell resolution. The vector data include arc coverages of the stream networks. The text file look-up tables provide information about the types of

meteorological, soil, and vegetation data used. Different modules of the model warrant more discussion than is included in this overview. A more detailed description of the individual modules within the main DHSVM is as follows.

3.3 Evapotranspiration

DHSVM uses a two-layer vegetation system to represent both the canopy and understory. Accurate representation of the vegetation is important with respect to evapotranspiration calculations because vegetation presence and structure influence the temperature, moisture, wind and radiation regimes of both the air and soil (Campbell and Norman, 1989). Evapotranspiration is modeled through step-wise calculations in order to ensure that the total evaporation from both vegetation layers does not exceed the rate of potential evaporation from the overstory layer. This approach also allows DHSVM to account for the presence and percent coverage of a canopy, the existence of wet and dry fractions within the overstory, the ability of any wet fraction to dry during a time step, and the presence of a ground snowpack and its effects on plant transpiration. When a snowpack is present, it is assumed to cover the entire grid cell; therefore, no evapotranspiration from the soil surface or understory is calculated while a snowpack exists on any grid cell. The partitioning of the vegetative layers into wet and dry fractions enables the model to account for interception, storage, and throughfall. DHSVM first calculates evaporation from the wet fraction of the vegetation at the potential evaporation rate. If the intercepted water remains at the end of the time step, then a Penman-Monteith approach models transpiration from dry vegetative surfaces. In the absence of an understory, evaporation from the upper soil layer is calculated as a

function of the potential evaporation rate, the soil moisture content, soil type, and antecedent moisture conditions (Wigmosta et al., 2002).

Wigmosta et al. (1994) describe the methods used to calculate canopy resistance. Values for both the understory and overstory are calculated separately as function of stomatal resistance, leaf area index (LAI), a species dependent minimum resistance factor, air temperature, vapor pressure deficit, photosynthetically active radiation flux, and soil moisture values (Dickinson et al., 1993)

Storck (2000) describes the specifics of the methods used to model aerodynamic resistance through the overstory canopy. Three different wind profiles are calculated. These include the profiles above the overstory (from the reference height down to the roughness layer just above the canopy top), through the canopy, and through the region comprised of the overstory trunk space. Aerodynamic resistance for the understory, soil, or snow surface is also calculated according to Storck (2000), and is a function of the displacement height of wind measurements and the roughness height of the surface over which the measurements are taken.

DHSVM calculates independent radiation budgets for both shortwave and longwave radiation for the overstory, the understory, and the soil surface. The overstory receives incident shortwave radiation. The understory below an existing overstory receives attenuated shortwave radiation and exposed understory receives direct shortwave radiation. The exchange of longwave radiation takes place between the overstory and the sky, between the overstory and the understory, and between the understory and the ground (Wigmosta et al., 2002).

3.4 Two-layer Ground Snowpack Model

DHSVM models the processes associated with snowpack morphology as described by Storck and Lettenmaier (1999; 2000) and Storck (2000) using a two-layer ground snowpack representation of snow accumulation and melt. This snowpack model utilizes separate energy and mass balance components to represent the various physical processes affecting the snowpack. It also accounts for energy exchanges taking place between the atmosphere, overstory canopy, and main snowpack. The energy balance components of the model address snowmelt, refreezing, and changes in snowpack heat content, while the mass-balance equations address the snow accumulation and ablation processes, transformations in the snow water equivalent, and snowpack water yield (Wigmosta et al, 2002).

DHSVM represents the two-layer snowpack as a thin surface layer and a main pack layer. Albedo of the snow surface affects the radiation budget. An exponential function based on the number of days since the last snow accounts for the decay of the snow surface albedo (Laramie and Schaake, 1972). Sensible heat flux is calculated for the surface snow layer as function of aerodynamic resistance, air temperature, snow surface temperature, and snow density. The model uses the bulk Richardson's number to correct aerodynamic resistance for atmospheric stability (Anderson, 1976). The net energy exchange for the snow surface layer determines the amount of available energy to refreeze water or melt existing snow. If this energy balance is negative, then any liquid water present may be refrozen. If it is positive, and the cold content of the snowpack has been satisfied, then this excess energy will begin to produce snowmelt (Storck and Lettenmaier, 2000).

Additional mass is added to the snowpack in both liquid and solid phases, and the delivery of this water is affected by the presence of an overstory. Snow delivered to the surface layer accumulates until the depth of snow exceeds a defined maximum thickness threshold. At that time, excess snow and its associated cold content is transferred to the pack layer. Liquid water in excess of the liquid water holding capacity of the surface layer drains into the pack layer. Snowpack temperature determines whether that volume of water will refreeze or whether it will be routed to the soil as snow melt outflow (Wigmosta et al., 2002).

3.5 Canopy Snow Interception and Release

DHSVM simulates canopy snow interception and release via a one-layer mass and energy balance model (Storck and Lettenmaier, 1999; 2000; Storck, 2000). This snowpack model explicitly accounts for the topographic and vegetative influences on the energy and mass exchanges taking place on the snow surface (Wigmosta et al., 2002), specifically the processes governing snow interception, sublimation, mass release, and melt from a forest canopy. Precipitation is partitioned into rain and snow based on atmospheric temperature per pixel and time step, and according to user defined minimum and maximum temperatures for rain and snow occurrence. A step-wise calculation dictates snow interception patterns. The volume of intercepted snow is determined by the maximum interception storage value. This is directly correlated to the leaf area ratio of each pixel and is based on field observations by Storck (2000). Snow in the canopy may subsequently intercept rainfall up to its water holding capacity. Bare

branches of deciduous vegetation types may also intercept rain. Excess rainfall becomes canopy throughfall.

Snowmelt from intercepted canopy snow is calculated similarly to ground snowpack melt, utilizing a modified energy balance approach for each time step. As the snow in the canopy melt, it is converted into liquid canopy water until the water holding capacity of the canopy snowpack is met. Snowmelt in excess of this value results in meltwater drip. Mass release of canopy snow is linearly related to meltwater drip in DHSVM. If sufficient snow is available in the canopy, and sufficient meltwater drip is occurring, then mass release of canopy snow occurs for that pixel (Storck, 2000; Wigmosta et al., 2002)

3.6 Unsaturated Soil Moisture Movement

Movement of water through an unsaturated multi-layer soil profile is represented dynamically in DHSVM, as described by Wigmosta et al. (1994). Water is delivered to the soil surface by way of the mechanisms of throughfall, snowmelt, or surface runoff from adjacent cells. DHSVM calculates infiltration into the upper soil layer based on the maximum infiltration rate defined by the user. Any water in excess of the infiltration capacity is then managed by the surface routing components of the model. Water that has infiltrated into the unsaturated soil profile percolates through the additional layers according to Darcy's Law. A unit hydraulic gradient calculated according to the Brooks-Corey relationship is used to calculate hydraulic conductivity (Brooks and Corey, 1964). This relationship describes the portion of the water-retention curve only for pressures at

which air will enter the soil. The Brooks-Corey hydraulic conductivity equation is:

$$\frac{K(\theta)}{K_s} = \left[\frac{(\theta - \theta_r)^n}{(\phi - \theta_r)} \right]$$

Where $K(\theta)$ is the hydraulic conductivity for a given water content (cm/h), K_s is the fully saturated hydraulic conductivity (cm/h), θ is the volumetric water content, θ_r is the residual water content, ϕ is the total porosity, and $n = [3 + (2/\text{pore size distribution index})]$ (Maidment, 1993).

Water may be removed from the unsaturated profile via three pathways. First, evapotranspiration may take place from the upper soil layer. Transpiration also occurs from within the soil profile according to the total percent of plant roots in a soil layer for both vegetation layers. Finally, desorption from the top soil layer may occur and is calculated for every time step as a function of the potential evaporation demand at the soil surface and soil desorptivity.

DHSVM first calculates infiltration into the upper layer. Next, the calculations address the downward vertical moisture transfer moving from top to bottom through the soil profile. The net flux of any lateral flow is added to the bottom layer. The model then calculates soil moisture in a step-wise fashion as it moves up through the individual layers of the soil profile. If the moisture exceeds the porosity for an individual layer, then the moisture is set equal to the porosity. If the calculated soil moisture is less than the porosity value, then that available water is added to the overlying layer until the uppermost soil layer is reached.

3.7 Saturated Subsurface Flow

DHSVM routes saturated subsurface flow downslope using both a kinematic and a diffusion approach. The kinematic method uses slopes to approximate the hydraulic gradient for those cells representing steep areas with thin, permeable soils. In contrast, the diffusion assumption approximates hydraulic gradients using local water table slopes, specifically for areas of low vertical relief (Wigmosta and Lettenmaier, 1999; Wigmosta et al., 2002).

The rate of subsurface flow per time step is calculated for each pixel and in each of eight directions. Saturated subsurface water movement is controlled in DHSVM by the transmissivity of an individual grid cell, as determined by the lateral saturated hydraulic conductivity of the soil profile. This value is assumed to decrease exponentially with depth, according to a user-defined exponential decay coefficient. Subsurface water moving downslope may be intercepted by a stream segment. Stream interception occurs when a stream depth exceeds the depth to the water table. When the water table rises above a streambed, that water is intercepted by the channel (Wigmosta et al., 2002).

3.8 Surface Overland Flow

DHSVM addresses this physical process on a per pixel basis. Generation of overland flow occurs when at least one of three physical conditions is met. First, overland flow occurs when the sum of throughfall and snowmelt exceeds the user-defined infiltration capacity of the soil. Surface flow may also be generated if throughfall or snowmelt occurs for a cell that already represents a fully saturated soil layer. Finally, return flow from a water table rising above the soil surface will generate surface water for routing in DHSVM (Wigmosta et al., 1994; Wigmosta et al., 2002). Surface water is routed on a cell-by-cell basis downslope in a similar fashion to subsurface routing (Wigmosta et al., 2002).

3.9 Channel Flow

DHSVM routes flow through the network of stream channels using a cascade of linear channel reservoirs. The stream channel networks comprise of any number of individual segments, each of which have its own hydraulic parameters. These constants imply a uniform flow velocity per channel segment and time step (Wigmosta et al., 2002). Lateral inflow to a channel segment, from the watershed cells through which it passes, consists of overland flow and subsurface flow intercepted by channels. Outflow from a segment may drain to another segment or exit the watershed.

A robust linear storage routing algorithm is available for channel routing. Each channel reach is treated as a reservoir of constant width with outflow linearly related to storage.

The linear storage-discharge relationship implies a constant flow velocity that is calculated from Manning's equation using a reference flow depth and corresponding hydraulic radius, allows calculate the storage at each time step (Wigmosta and Perkins, 2001).

Chapter 4

Data Acquisition and Model Setup

Construction of the data sets and choices of model parameters setting for the prediction of streamflow, and snow water equivalent by DHSVM is outlined in this chapter. Hydrologically modified DEM generation by ANUDEM is also outlined in the last section of this chapter.

4.1 Study Area

General Overview

Marmot Creek watershed is located at latitude 50°57'N and longitude 115°10'W on the West side of the Kananaskis River Valley, about 40 km southeast of Banff, Alberta (Figure 4-1). The total area of the basin is approximately 9.4 square kilometres. The basin ranges in elevation between 1,585 to 2,805 m with a mean elevation of approximately 2,112m. There are three identified sub basins namely Cabin Creek, Middle Creek and Twin Creek having areas of 2.12, 2.85, and 2.64 km², respectively. The three major streams flowing from these sub basins combine to form a single larger stream (Main Marmot) which drains into the Kananaskis River. Topography is moderately to steeply sloping throughout. Slopes vary from about 24 percent in the lowest reaches of the basin to over 50 percent above treeline. The average slope for the basin as a whole is 39 percent.

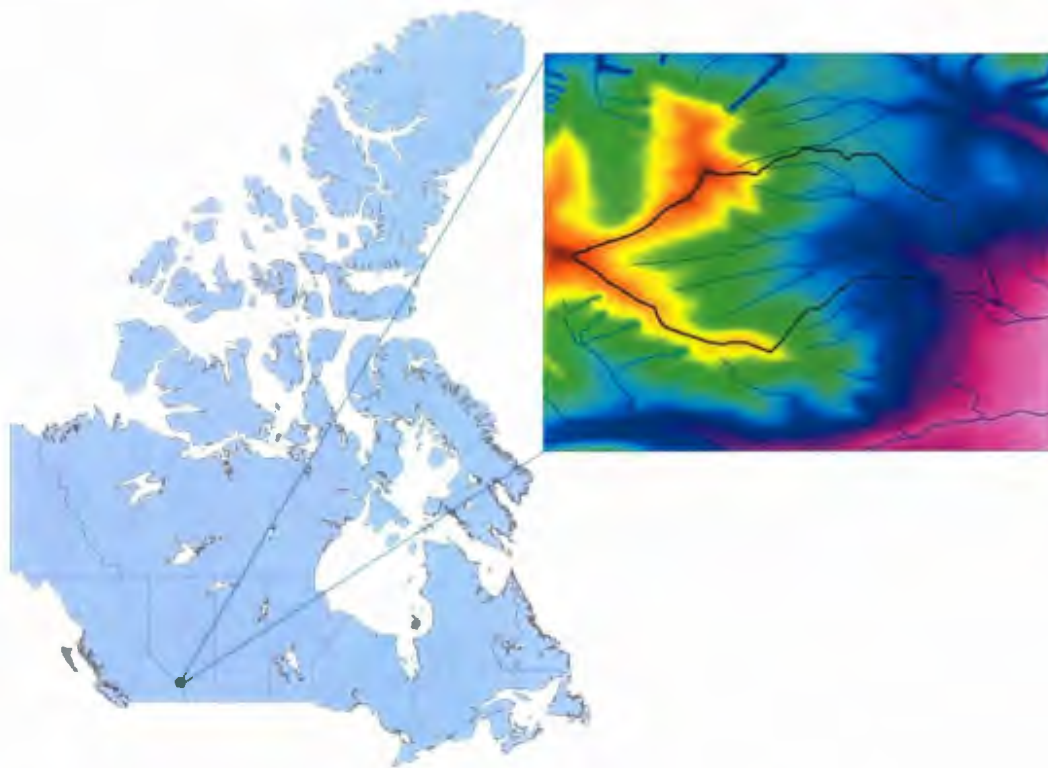


Figure 4-1: Marmot Creek Basin location on the Canadian map.

The main types of soil are brunisolic grey-wooded, podzolic, regosolic, local gleysolic and organic soils (Telang et al., 1981). The basin is underlain by Mesozoic formations consisting mainly of shale and sandstone with lesser amounts of limestone, conglomerate, and coal. The stream bed is composed of sands, gravels and boulders, and is inhabited by stream microflora including benthic invertebrates, algae, and bacteria (Telang et al., 1981). Topographic boundaries between sub-basins, while well-defined in the upper reaches of the basin, tend to be rather indefinite in some parts of the lower portions (Jeffrey, 1965). In the Cabin Creek sub-basin limestone appears to

be the dominant bedrock, whereas bedrock in the other basins is dominantly clastics (Telang et al. 1981).

The Marmot basin is representation of much of the Subalpine and Alpine zone of the Bow Valley-Kananaskis region. Forest cover is mainly old spruce-fir with a scatter of trembling aspen. The lower tip of the basin is covered with even-aged lodgepole pine. Alpine larch occupies a narrow band just below tree line. About 40 % of total basin area lies above tree line (Bernier 1986). Rapid elevation changes are responsible for the large number of vegetation types, and most of the conifers are capable to hybridization where they overlap. The upper regions of the basin consist largely of Englemann Spruce and sphagnum moss below the treeline. Willow, Larch, and Fir along with a number of grasses and sedges dominate alpine regions above the treeline (Wallis et al., 1981).

The climate is characterized by short, cool summers and long, cold winters. Annual precipitation averages 900 mm, increasing from 600 mm in the lower basin to over 1140 mm in the upper reaches of Twin Forks Creek (Storr, 1967) and average annual evapotranspiration is about 440 mm. Approximately 75 percent of the precipitation occurs as snow, none of which is stored from one year to the next. Snow pack accumulation is affected by elevation, aspect, slope and forest density, with total mean snow pack increasing at a predictable rate with elevation (Golding, 1969). Rain occurs during the June-September period. The average July temperature ranges from 18 to 2^oC; average January temperature ranges from -6 to -18^oC (Kirby and Ogilvie, 1969); recent observations corroborate these values (DeBeer and Pomeroy, 2010).

Minimum stream flow occurs in late March. Spring snowmelt begins at low elevations and gradually moves upslope, into heavier snowpack areas. Snowmelt typically starts in late April to early May and peaks in early June, continuing into mid-summer from sheltered high elevation sites, notably Marmot cirque. Through spring and summer, stream flow is derived from snowmelt, rainfall, storm seepage and groundwater storage. Flows from late fall through winter were slow but steady. Fifty percent of annual precipitation is accounted for as stream flow (Swanson et al., 1986).

Storr (1974) correlated groundwater storage to stream flow. Where there was no surface flow to the streams, the rate of stream flow was set as an index of the amount of groundwater reservoir, the greater the proportion of discharge from groundwater to the stream at all points along the channel.

The coarse glacial deposits usually had minimum infiltration rates higher than maximum reported storm intensities (Beke, 1969). Swanson et al., (1986) concluded that most of the Marmot Creek stream flow was fed by transient subsurface flow from glacial deposits which had a moderating effect on storm peaks.

The Marmot Creek basin forms an unconfined groundwater system, where water is stored and moves in surficial deposits draped over bedrock. Groundwater that discharges from joints in exposed bedrock is fine seepage, suggesting low matrix porosity; however localized folding and faulting have the potential to create hydraulically significant fracture networks. The bedrock has minimal interaction with the groundwater in the overlying drift, although its structure influences stream geometry. Water table divides closely approximate topographic divides, and groundwater flow mostly parallels the slope of topography. Near the top of the basin where slopes are steep and surficial deposits are thin to nonexistent, most precipitation is converted to runoff and shallow

lateral flow. Recharge occurs in spring and early summer from snowmelt, spring rains and occasional late season storms. For most of the basin, surficial deposits have a high infiltration capacity and surface runoff is negligible. The level of the water table rises and falls in direct response to precipitation and is close to the land surface. Seepage and springs are common in low-lying areas, breaks in slope and in the v-shaped creek valleys. Water is continuously removed from the groundwater system by evapotranspiration and by baseflow seepage to the creeks. Stream flow is derived almost entirely from baseflow and interflow. Fluctuations on most of the groundwater hydrographs correspond directly to fluctuations on stream flow (Davis, 1964; Stevenson, 1974).

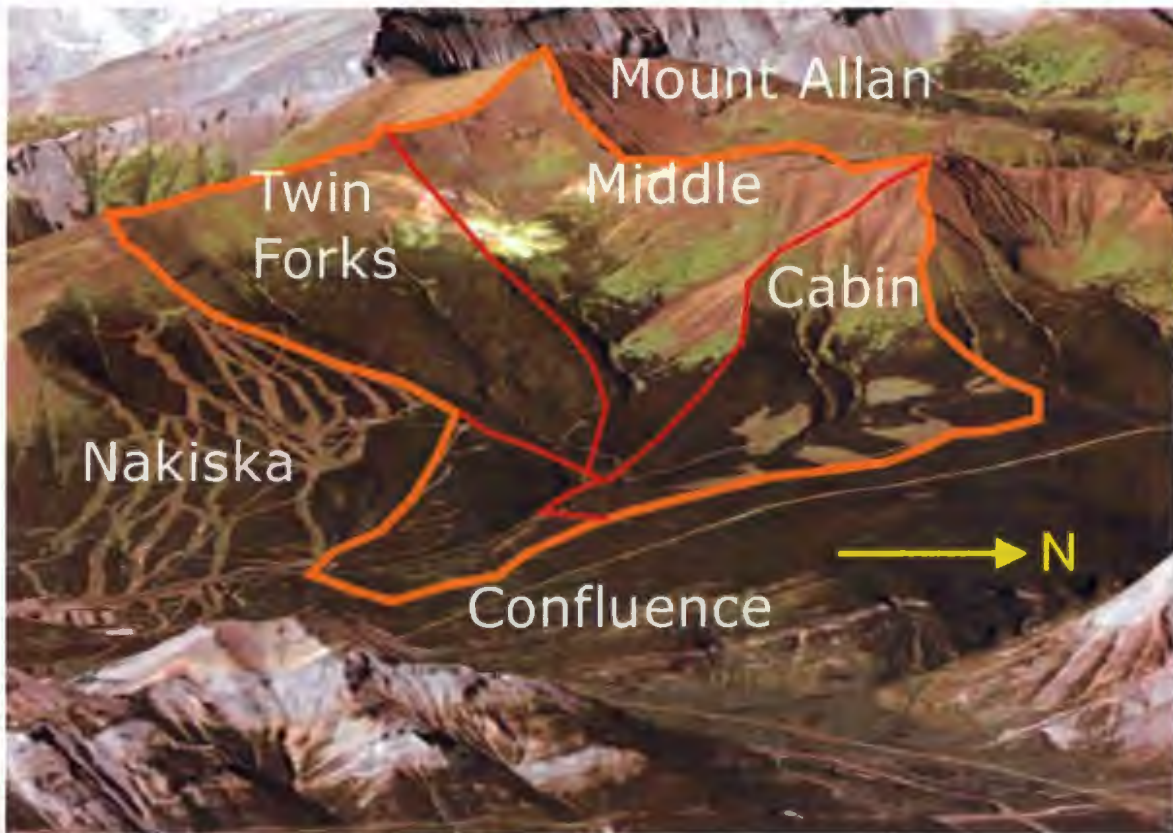


Figure 4-2: Aerial view of the Marmot Creek Basin (Swanson et al., 1986).

4.2 Data Preparation

The research required a progression of stages in order to integrate all of the data set required by the DHSVM. The manipulation and analysis of the data along with the development of the final data set for the model are all described below.

4.2.1 Processing with GIS

DHSVM spatial inputs were compiled, edited, and formatted using ArcGIS9.3, specifically using ArcMap, ArcCatalog, and ArcInfo Workstation interface. A requirement of DHSVM requires that the same spatial resolution is used. Land cover maps were converted using the reclassify tool of ArcInfo.

4.2.2 Raster Inputs

A seamless 90 meter resolution digital elevation model was obtained for the Marmot Creek watershed from the USGS shuttle Radar Topography Mission (SRTM). A depressionless DEM is required to generate a stream network. The input DEM was filled using the spatial analyst tools in ArcInfo in order to produce a depressionless DEM for hydrologic simulations. This formatting enforces a linear drainage pattern onto the DEM grid. This is completed through two basic processes that includes, i) filling in sinks in the drainage area by raising the elevations of those grid cells, and ii) lowering the elevations of the cells corresponding with vector drainage network.

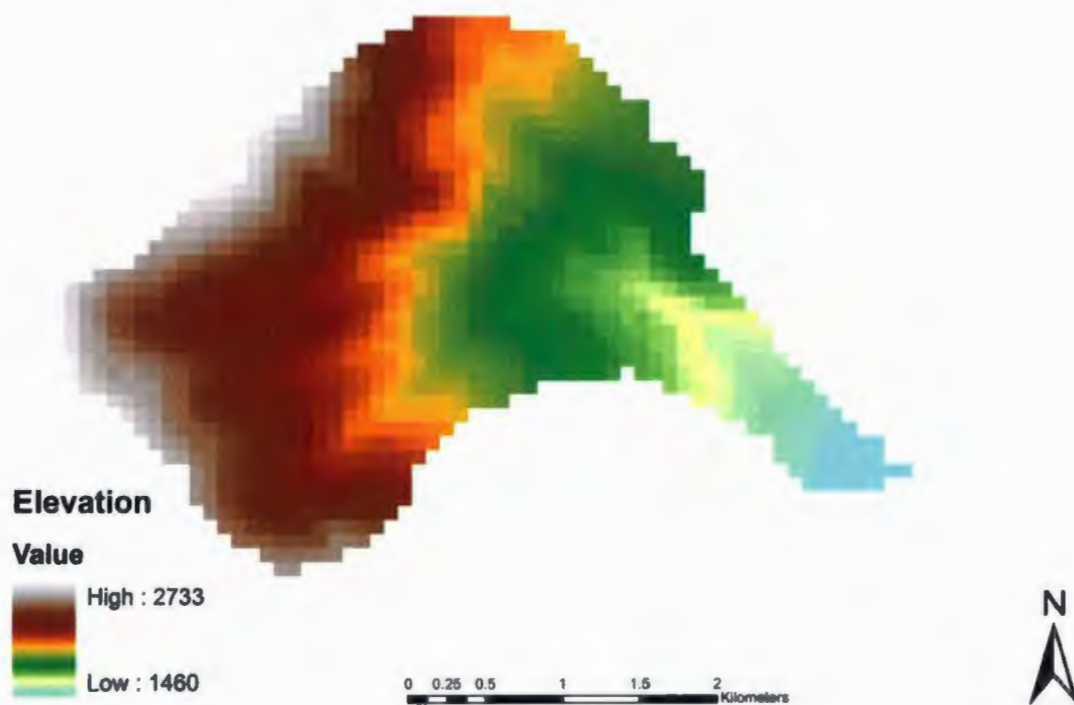
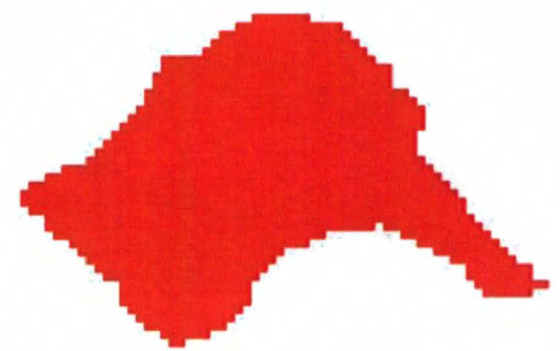


Figure 4-3: Digital Elevation Model of Marmot Creek Watershed from USGS SRTM data.

As there is no high-resolution soil maps available for the Marmot Creek basin, considering small mountainous basin one soil type was applied for the simulation. In order to obtain soil raster for DHSVM input, a raster map is generated from ascii file with same resolution of DEM in ArcMap 9.3. The soil was generalized with one value (Figure 4-4). A soil profile that represents the class in the watershed boundary was used to describe the soil properties in the DHSVM input file.



Soil Type

 Organic (as loam)

Figure 4-4: Marmot Creek Soil type.

Table 4-1: Soil input parameters for DHSVM

Parameter	Description	Unit	Value	Source
Lateral conductivity	Lateral saturated hydraulic conductivity	m/s	3.5E-04	Cuo et al.,2006 Ziegler 2000
Exponential decrease	Exponent for change of lateral conductivity with depth	Unitless	0.5	Cuo et al.,2006
Maximum infiltration	Maximum infiltration rate	m/s	2.5E-05	Model default
Surface albedo	Albedo of bare soil surface	m/s	0.15	Model default
Number of soil layers	Number of soil layer described in soil profile	Unitless	3	Model default
Porosity	Porosity of each soil layer	Unitless	0.59	Model default
Pore size distribution	% of bulk volume of various sizes of soil pores for each soil layer	Unitless	0.19	Model default
Bubbling pressure	Air entry value for each soil layer	M	0.11	Model default
Field capacity	Water retained at -1500 kPa for each soil layer	Unitless	0.29	Model default
Wilting point	Water retained at -33kPa for each soil layer	Unitless	0.14	Model default
Bulk density	Mass dry soil per unit bulk volume for each soil layer	Kg/m ³	1485	Model default
Vertical conductivity	Vertical saturated hydraulic conductivity for each soil layer	m/s	0.01	Model default
Thermal conductivity	Thermal conductivity of dry soil for each soil layer	W/m°C	6.923-7.114	Model default
Thermal capacity	Thermal capacity of dry soil for each soil layer	J/m ³ C	1.4E06	Model default

A soil depth grid is also a necessary spatial input. While the depth of the soil profile corresponding to specific soil types is generally known, this is not a readily available spatial data layer. DHSVM provides AML script that generates a soil depth grid in ArcInfo Workstation for input into the model. This raster is created as a function of the watershed slope and a range of soil profile depths based on the soil type.

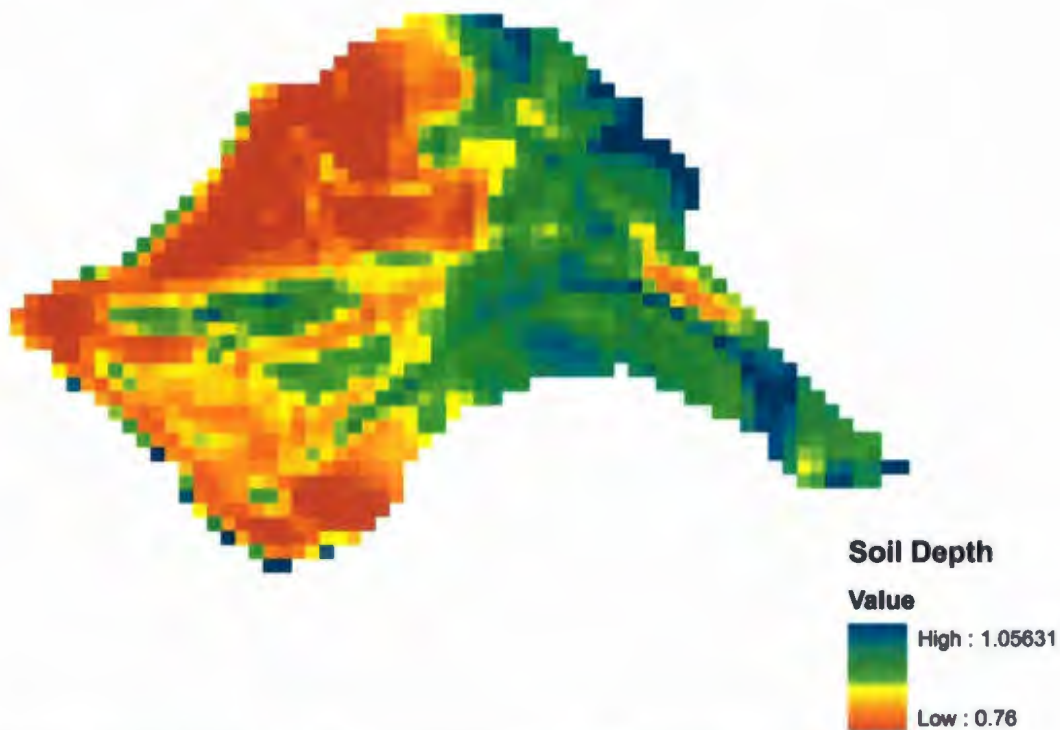


Figure 4-5: Marmot Creek Soil depths generated by AML script

Two vegetation scenarios are used in this study: one vegetation cover data that has a spatial resolution of one kilometre was obtained from the USGS Land Cover Institute (LCI). To make this input file same spatial resolution of input DEM raster, the vegetation grid was reclassified into 90-m resolution using ArcMap (Figure 4-6). Another vegetation cover data set was taken from Earth Observation for Sustainable Development (EOSD) and has a 25-m resolution. The EOSD vegetation cover was resample onto a 90-m grid using ArcMap (Figure 4-7). Table 4-2 and 4-3 represent the physical details of these different vegetation types, as well as the percent distribution by class. Table 4-4 outlined input parameter settings of land-cover for DHSVM.

Table 4-2: Vegetation type descriptions of USGS land cover map.

Land cover classes	Vegetation Class ID	Proportion (%) in the basin
Evergreen Neddleleaf	1	0.64
Woodland	6	0.27
Wooded grassland	7	0.09

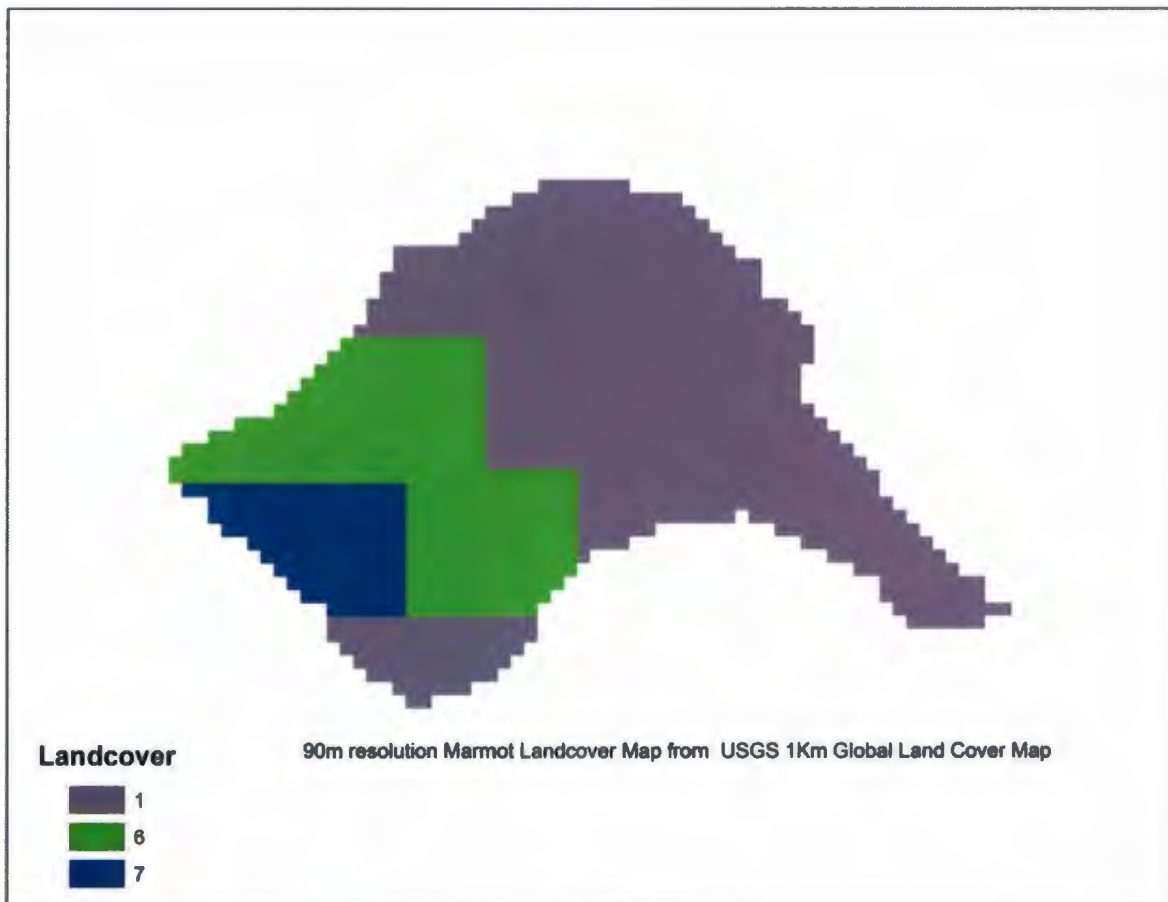


Figure 4-6: Land Cover classification from USGS.

Table 4.3: Land cover classes in Marmot Creek basin used in DHSVM

Land cover classes	Vegetation Class ID	No of grid cell with in the basin
Broadleaf Dense	4	9
Shrub	8	206
Wetland shrub	9	1
Herb	10	233
Rock	12	103
Exposed land	13	1
Coniferous Open	17	16
Coniferous Dense	18	646

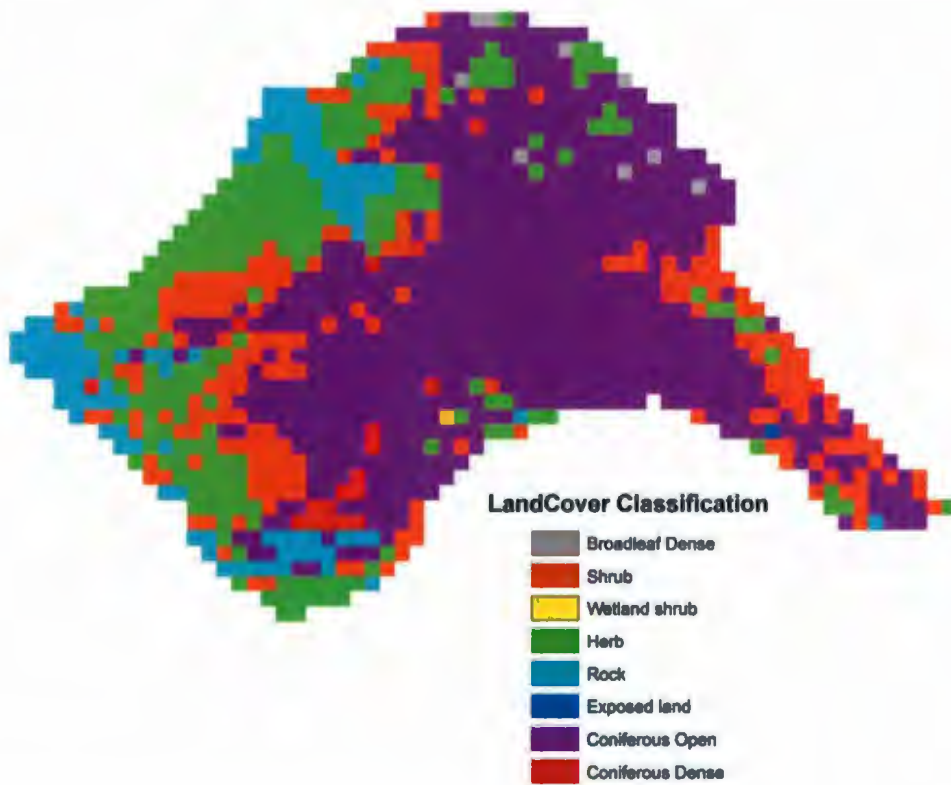


Figure 4-7: Land Cover Classification from EOSD.

Table 4-4: Vegetation input parameters used for DHSVM

Parameter	Description	Unit	Reference
Fractional coverage	The fraction of total area occupied by the overstory	Unitless	Cuo et al., 2006
Trunk space	Distance from the ground to the start of the crown	M	Cuo et al., 2006
Aerodynamic attenuation	Canopy attenuation coefficient for the wind profile	s/m	Cuo et al., 2006
Radiation attenuation	Radiation attenuation by the overstory	Unitless	Wigmosta et al., 1994
Maximum snow interception capacity	Maximum snow interception capacity for the overstory	m	Storck, 2000
Max release drip ration	Ratio of mass release to meltwater drip from to meltwater drip from intercepted snow	M	Storck, 2000
Snow interception efficiency	Percentage of snowfall intercepted until the maximum snow interception capacity has been met	Unitless	Storck, 2000
Height	Height of each vegetation layer	M	Cuo et al., 2006
Maximum resistance	Maximum stomatal resistance for each vegetation layer	s/m	Cuo et al., 2006
Minimum resistance	Minimum stomatal resistance for each vegetation layer	s/m	Cuo et al., 2006
Moisture threshold	Value above which soil moisture does not restrict transpiration	Unitless	Cuo et al., 2006
Vapour pressure deficit	Vapour pressure deficit threshold above which stomatal closure occurs	Pa	Cuo et al., 2006
Rpc	Fraction of shortwave radiation that is photosynthetically active	W/m ²	Model default
LAI values	Monthly LAI values for each vegetation type	Unitless	Model default
Albedo values	Monthly albedo values for each vegetation type	Unitless	G. Jost et al., 2009

DHSVM uses a mask of the watershed area (figure 4-8) to select the pixels within the watershed of the interest that have values associated with the elevation, soil type, soil depth, and vegetation type. This process ensures that the extent of the area of interest is the same for every spatial run of the model. This raster is created using ArcMap spatial Analyst tools. By working through a series of terrain preprocessing steps, each pixel in a DEM is assigned a flow direction. The 'Raster Calculator' of ArcMap can then delineate a watershed from any point specified within the raster by selecting all pixels

that collectively drain to that point. The Marmot Creek watershed was delineated using these ArcMap tools. Finally, this watershed mask raster was used in DHSVM to extract the Marmot Creek drainage basin values from the DEM, soil type, soil depth, and vegetation type raster inputs.

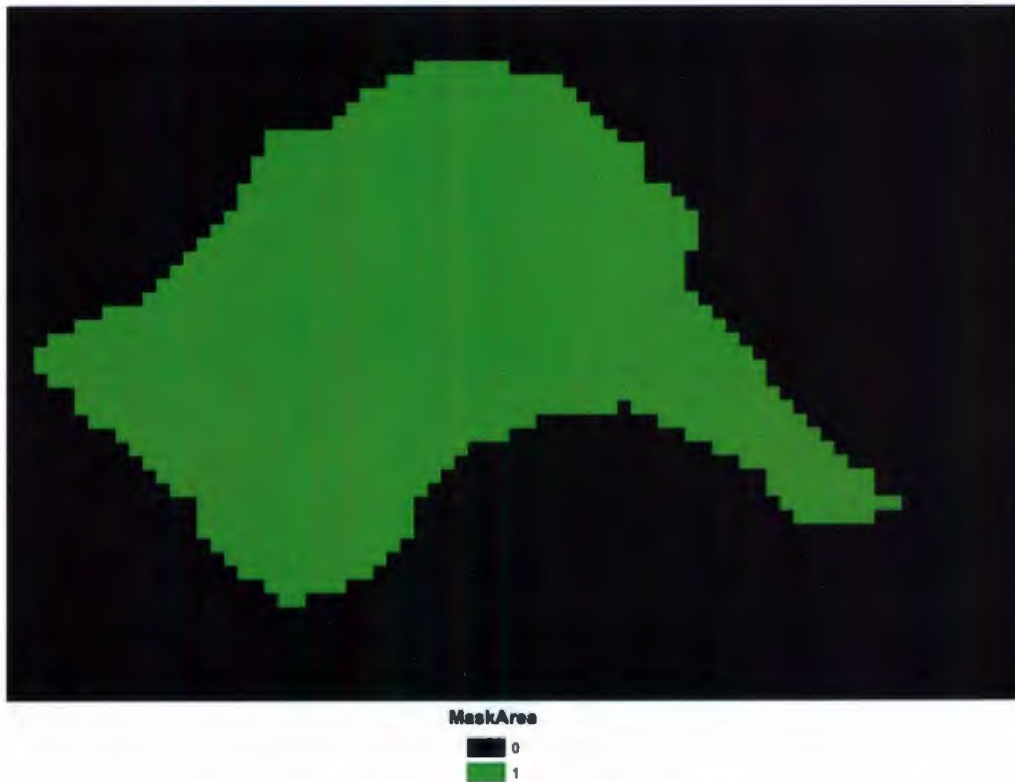


Figure 4-8: Watershed mask is used to extract analysis pixels from input grids.

4.2.3 Stream Network Input

A stream network is entered in DHSVM as a coverage clipped to the watershed extent. Digital spatial data of stream network was obtained through Natural Resources Canada (Geogratis). While these hydrology data provided a digital layer for mapping purposes, as well as locations and identity of named stream reaches, they were not used as stream coverage for input into DHSVM. Generation of a continuous stream network is a necessary preprocessing step for implementation in DHSVM. An AML script was used in ArcInfo Workstation to create a stream network with streamflow topology based on the reconditioned DEM and the watershed of interest as delineated in ArcMap. Both the delineated and Geogratis drainage network for Marmot Creek Basin are displayed below.

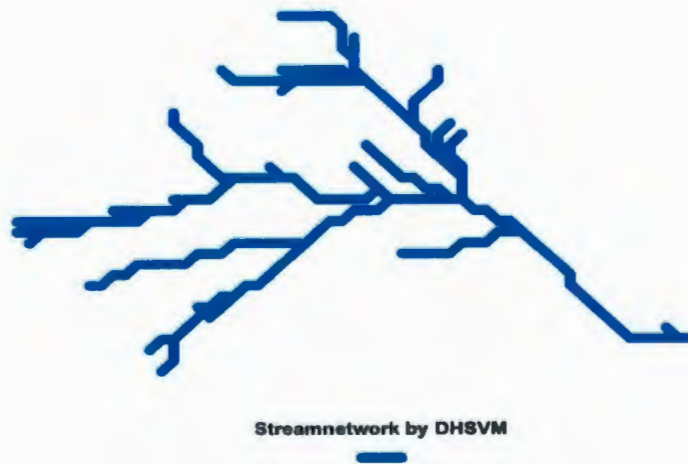


Figure 4-9: DHSVM vector coverage input of stream networks.

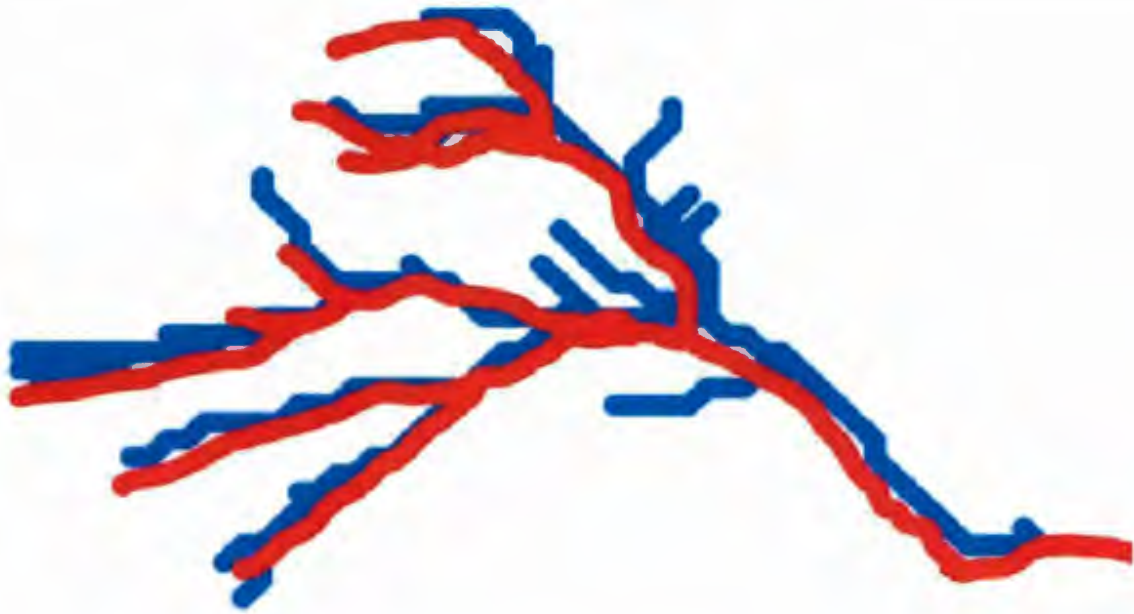


Figure 4-10: DHSVM's AML script generated stream network overlaid by Geogatis stream network.

4.2.4 Climate Forcing Inputs

DHSVM can be run using meteorological records associated with point weather stations. If available, data from multiple stations can also be incorporated into the model. In this study one meteorological station data is used for forcing the model. DHSVM distributes weather parameters across the watershed of interest, for each model time step, using one of three user-selected interpolation methods. The model requires the following meteorological variables for every time step and every weather station used: temperature ($^{\circ}\text{C}$), wind speed (m/s), relative humidity (%), incoming shortwave radiation (W/m^2), incoming longwave radiation (W/m^2), and precipitation (m/time step). A list of meteorological forcing and calibration data are outlined in table 4-5.

Table 4-5: Time-dependent field measurements at field sites in Marmot Creek basin by IP3 network

Variable	Sensor	Location	Purpose
Incoming Long wave radiation	CNR1(4-component radiation sensor)	Upper Clearing	Forcing
Incoming short wave radiation	CNR1(4-component radiation sensor)	Upper Clearing	Forcing
Air temperature	HMP35C	Upper Clearing	Forcing
Humidity	HMP35C	Upper Clearing	Forcing
Wind speed	NRG 3-cup anemometer and direction vane	Upper Clearing	Forcing
Precipitation	Geonor T200B accumulating precipitation gauge	Upper Clearing	Forcing
Snow depth	SR50 sonic ranging snow depth sensor	Upper Clearing	Calibration
Stream discharge ¹	Recorder Gauge	Marmot Creek main stem Station ID 05BF016	Calibration

¹ Seasonal (May to October) stream discharge recorded by Environment Canada.

Meteorological records associated with Marmot creek particularly temperature, precipitation, wind speed, relative humidity, incoming shortwave and longwave radiation were taken from IP3 network website, specifically Upper Clearing (50°57'24"N, 115°10'31"W) meteorological station located 1844.6 m above sea level. Upper Clearing meteorological station is a good representation of the whole basin (Figure 4-11). Constant temperature lapse rate is applied over the basin. The hourly time series of the data is created from the 15-minutes data by using an AWK Unix code. The hourly precipitation time series is created from adding up four 15-min data. The hourly temperature, humidity, wind speed, short wave radiation and long wave radiation are generated from averaging the 15-min data.

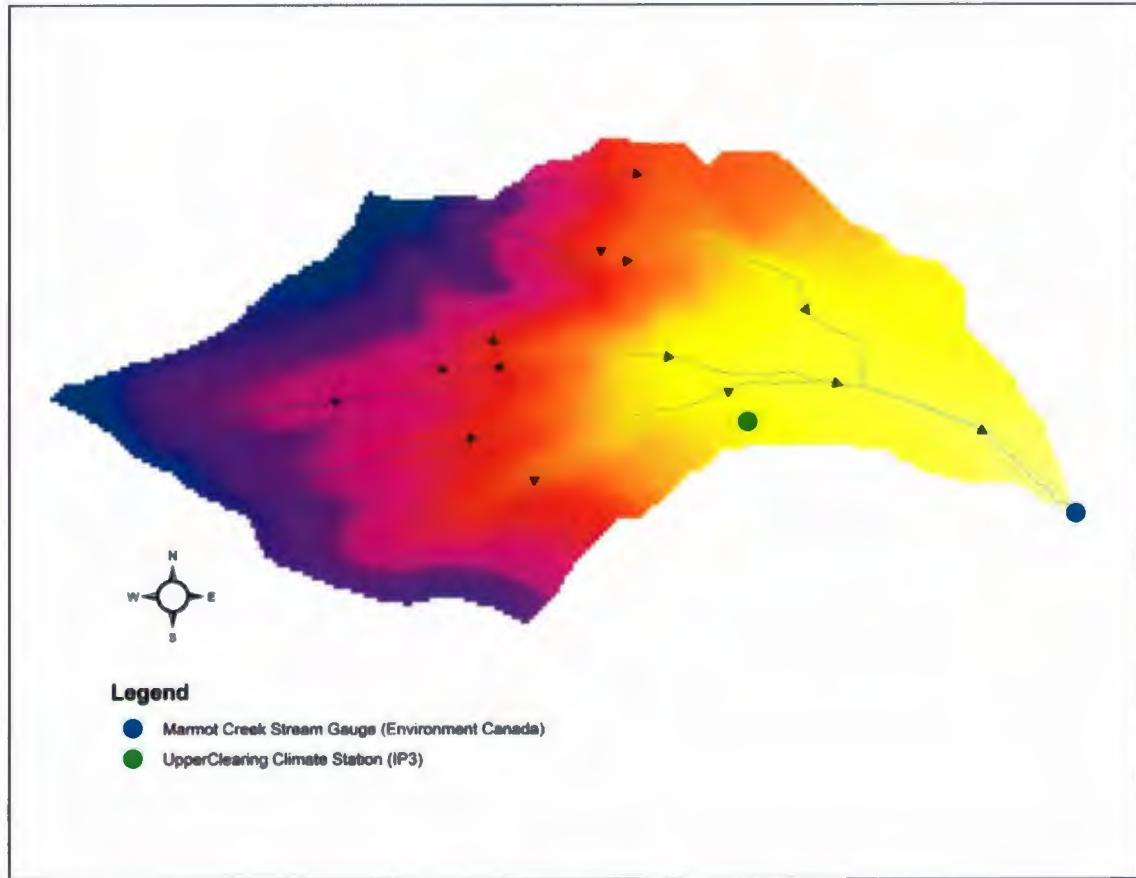


Figure 4-11: Climate and Stream gauge station site locations. Different colors showing elevation difference.

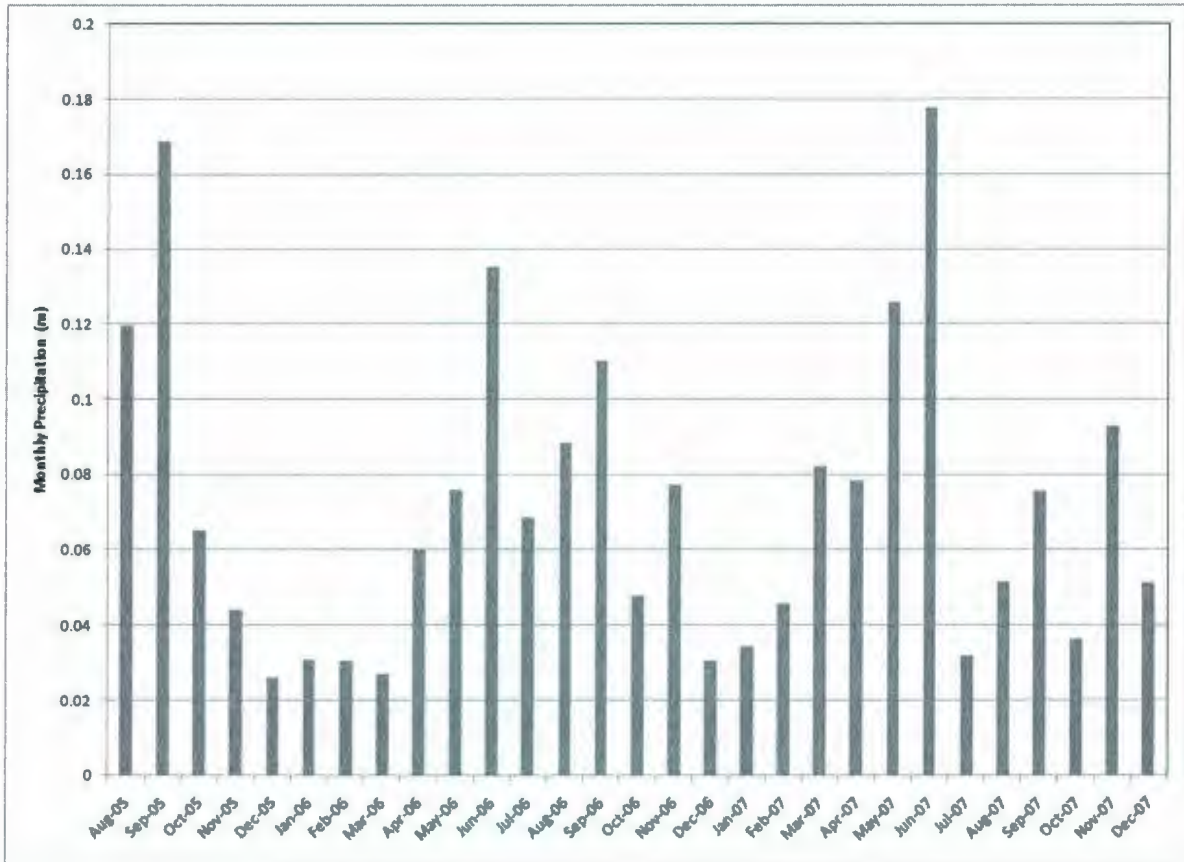


Figure 4-12: Monthly hyetograph for the Marmot Creek basin.

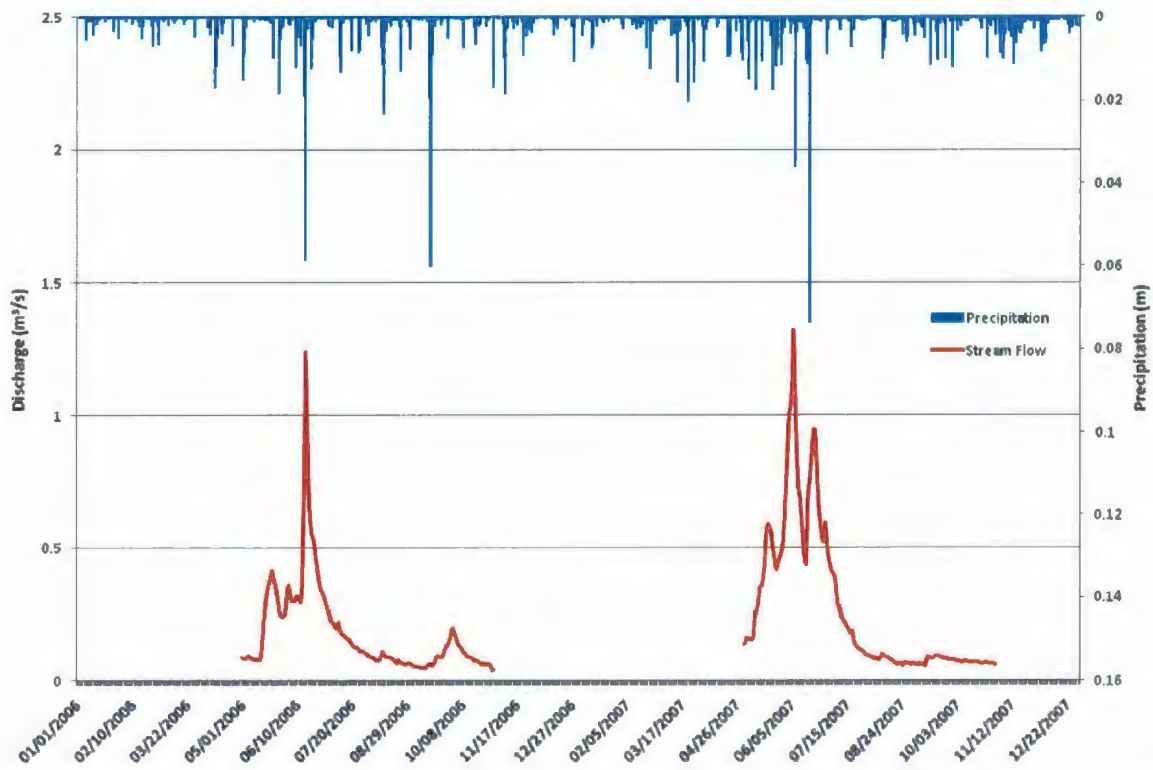


Figure 4-13: Daily hyetograph and seasonal (May-October) stream flow for the Marmot Creek watershed, for the year 2006 to 2007.

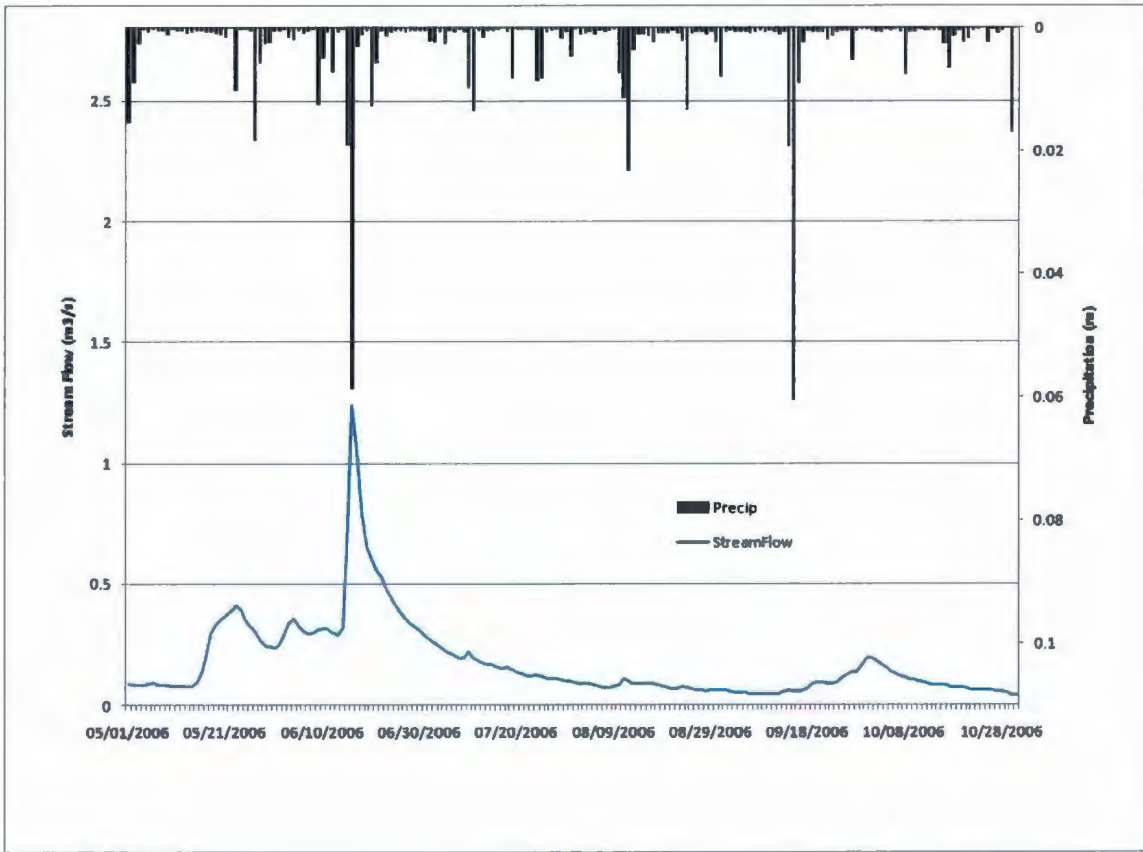


Figure 4-14: Daily discharge and precipitation for the Marmot Creek watershed, seasonal (May-October) year 2006.

Table 4-6 Parameter files used in DHSVM

File	File composition
Soil class	Distributed over user-defined grid
Land cover class	Distributed over user-defined grid
Soil depth	Distributed over user-defined grid, depth unit: meter
Stream class file	Channel class ID Hydraulic width (m) Hydraulic depth (m) Manning's number
Stream network file	Channel segment ID Segment routing order Segment slope (ratio) Segment length (m) Channel segment ID Segment title in stream output file
Stream map file	Cell grid column number Cell grid row number Channel segment ID Straight line length of the channel segment lying within the cell (m) Cut/bank height (m) Stream channel width (m) Azimuth of straight line of segment within cell (degree) Sink identifier
DEM	Distributed over user-define grid, elevation unit : meter
Watershed mask file	Distributed over user-define grid

4.3 Hydrologically Modified DEM Generation

The goal of this section is to generate a 90 meter digital elevation model for the Marmot Creek watershed based on 1:50,000 scale digital topographic maps.

As mentioned in chapter two, the ANUDEM program has been applied in this study to generate hydrologically correct digital elevation models (DEMs). ANUDEM has an interpolation method specifically designed for the creation of hydrologically correct DEMs from comparatively small, but well selected elevation and stream coverages (Hutchinson 1988, 1989).

Water is the primary erosive force determining the general shape of the most landscapes. For this reason, most landscapes have many hilltops and few sinks, resulting in a connected drainage pattern. ANUDEM uses this knowledge about surfaces and imposes constraints on the DEM interpolation process that result in connected drainage structure and corrected representation of ridges and streams. This imposed drainage condition produces higher accuracy surfaces with less input data.

The drainage enforcement algorithm attempts to clear spurious sinks by modifying the DEM, by inferring drainage line via the lowest saddle point in the drainage area surrounding each spurious sink. It does not attempt to clear real sinks that are identified as such in the input. Since sink clearance is subject to a defined elevation tolerance, the program is conservative when attempting to clear spurious sinks.

4.3.1 Creating the ANUDEM Input Data

Canvec data of 1:50,000 scale was obtained from the Geogratis website. These vector data are the digital version of Canada's National Topographic System (NTS) maps. The Canvec data contains many entities, however, only contours and hydrographic lines were used as input to the DEM generation process. This section describes the creation of inputs required to run ANUDEM, while next section tests the quality and accuracy of ANUDEM generated DEM.

During the processing of data over the Marmot Creek area, a problem with the source datasets were observed and subsequently resolved. Primarily, it was observed that some streamlines were flowing in the wrong direction (i.e., flowing uphill) (Figure 4-15). This stream directionality problem caused canyon anomalies in the DEM. Correct stream directions were manually identifying based on the elevation of the area, and the flip command in Arc Map was used to correct the problem (Figure 4-16).



Figure 4-15: Stream flow direction error. Steam segment is flowing in the wrong direction.



Figure 4-16: Corrected directions of streamflow.

4.3.2 DEM Generation

The default values provided in the ANUDEM 5.2 manual were used for all parameters to generate DEM. A thumb rule developed by M.F. Hutchinson is that the output DEM x and y resolution is 10^{-3} of the map scale. For example, using contour data at a scale of 1:100,000 the output grid resolution should be 100m, whereas contour data generated from a 1:250,000 scale map should result in a 250m resolution grid cell.

Once vector data are pre-processed, they are used as input into the ANUDEM program to generate the DEM. Firstly, ANUDEM reads input elevations, windows the data to the specified map limits, and then generates a grid at 90m intervals. Elevation data are generalized by accepting a maximum of 4 data points per grid cell and discarding any remaining points. Contour and streamline data are generalized by accepting a maximum of one line per grid cell. The program then employs a multi-grid method that calculates grids at successively finer resolutions until the specified grid resolution is achieved. During this process, drainage conditions are imposed to remove sinks where possible. Values at grid points not occupied by data points are calculated by Gauss-Seidel iteration with over relaxation subject to an appropriate roughness penalty and ordered chain constraints. The ordered chain constraints are obtained from the streamline and contour line data and through automatic drainage enforcement as calculated by the program. Starting values for the first coarse grid resolution are calculated from a least squares plane fit to the data points. Values for each succeeding grid are linearly interpolated from the preceding grid.

The profile curvature, defined as the curvature of the fitted surface in the downslope direction (Gallant and Wilson, 2000). The profile curvature, which is locally adaptive (Hutchinson, 2000), can be used to partly replace the total curvature. This is controlled by the user specifying the 2nd roughness penalty. Values for the 2nd roughness can range from 0.0 to 0.9; a value of 0.0 (default) means only total curvature is used, whereas a value of 0.9 means that 0.1 of total curvature and 0.9 of profile curvature is used.

The full set of ANUDEM parameters used to develop the Marmot Creek DEM is give in Table 4-7.

Table 4-7: The following user directives were applied to ANUDEM version 5.2 using the contour and stream data from Canvec data set to construct the DEM for the Marmot Creek.

ANUDEM User Directive	Value	Remarks
Drainage option	1	Drainage enforced where possible
Contour data	1	Data mainly consists of contours
Discretisation error factor	1.0	
Vertical standard error	0.0	
1 st roughness penalty	0.0	Determines how much planar (or contour) curvature is used in addition to the default total curvature. Set to 0.0 for contour data.
2 nd roughness penalty	0.0	Determines how much profile curvature is used in addition to the default total curvature.
Elevation tolerance	10	Half of the contour interval of 20m.
Maximum number of iterations	20	Number of iteration for final DEM generation
Elevation units	1	Elevation unit in meter
Height minimum	0	Data points lower than this value ignored, and fitted cells cannot be lower than this.
Height maximum	5000	Data points higher than this value ignored, and fitted cells cannot be higher than this
Centring option	1	Grid points located at the centre of the pixels.
Position units	5	Position units in degree decimal
X lower	-115.5	Data points below this value are ignored
X upper	-115.0	Data points above this value are ignored
Y lower	50.76	Data points below this value are ignored
Y upper	51.0	Data points above this value are ignored
Grid spacing	0.0008	Final grid resolution is 0.0008 degree (90m),
Grid margin	0.016	This corresponds to twenty 90m (0.0008) resolution output grid cells.

Once final DEM of 90 m resolution is generated for the Marmot Creek basin it used in determining hydrologic variable including stream flow and snow water equivalent.

4.3.3 DEM Comparison

USGS and ANUDEM generated DEMs were compared to determine the range and nature of their differences. Elevation and elevation-dependent topographic parameters were examined numerically and spatially. ARC/INFO program were used for digital terrain analysis and to calculate basin topographical parameters.

4.3.4 Watershed Area and Elevation

Arc/Info was used to determine the watershed area and elevation of the basin as defined by each DEM. For each DEM, drainage area was determined as the contributing area upstream of the outlet. Table 4-8 summarise the two DEMs drainage contributing area and elevations.

Table 4-8: Watershed area and elevation

	USGS DEM	ANUDEM DEM
Watershed Area (sq. km)	9.98	9.25
Elevation Range (m)	1419-2785	1407-2798.32
Average Elevation (m)	1994.38	1991.68
Standard deviation of Elevation	338.295	344.464

Visual inspection of the DEMs reveals similarity in the USGS DEM (Figure 4-17). Both DEMs generated sharp images that clearly defines the valley river network whereas the elevation ranges is more scattered ANUDEM generated DEM at the same resolution. The watershed boundaries differ considerably between the two images.

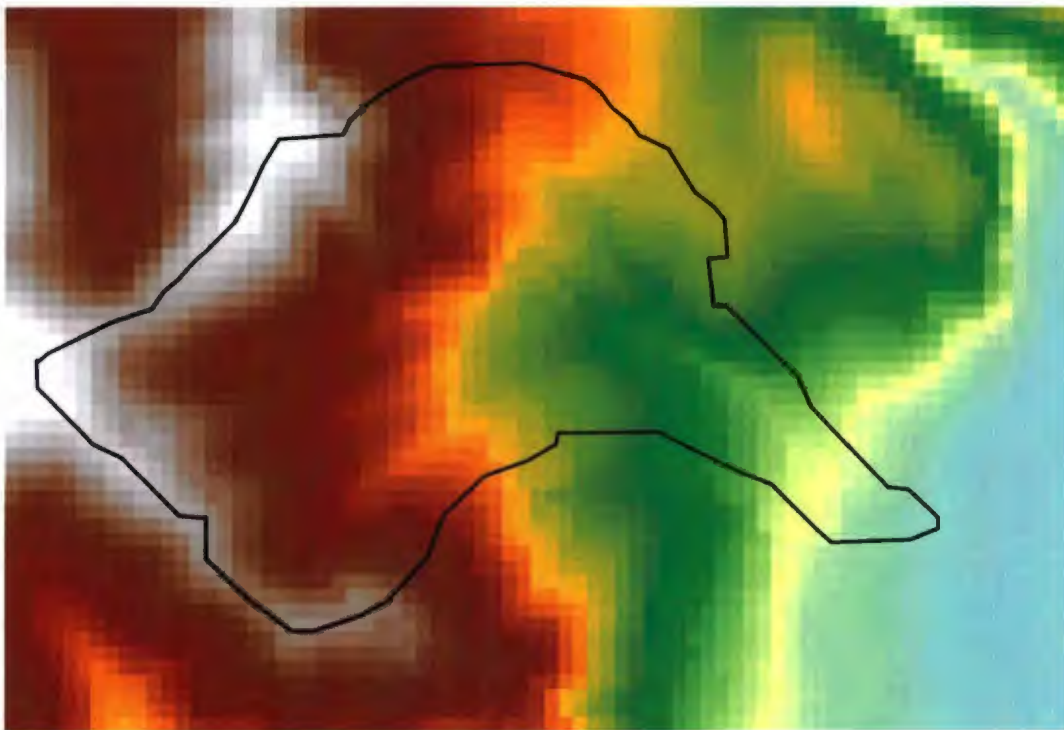


Figure 4-17: USGS DEM showing the Marmot Creek boundary.

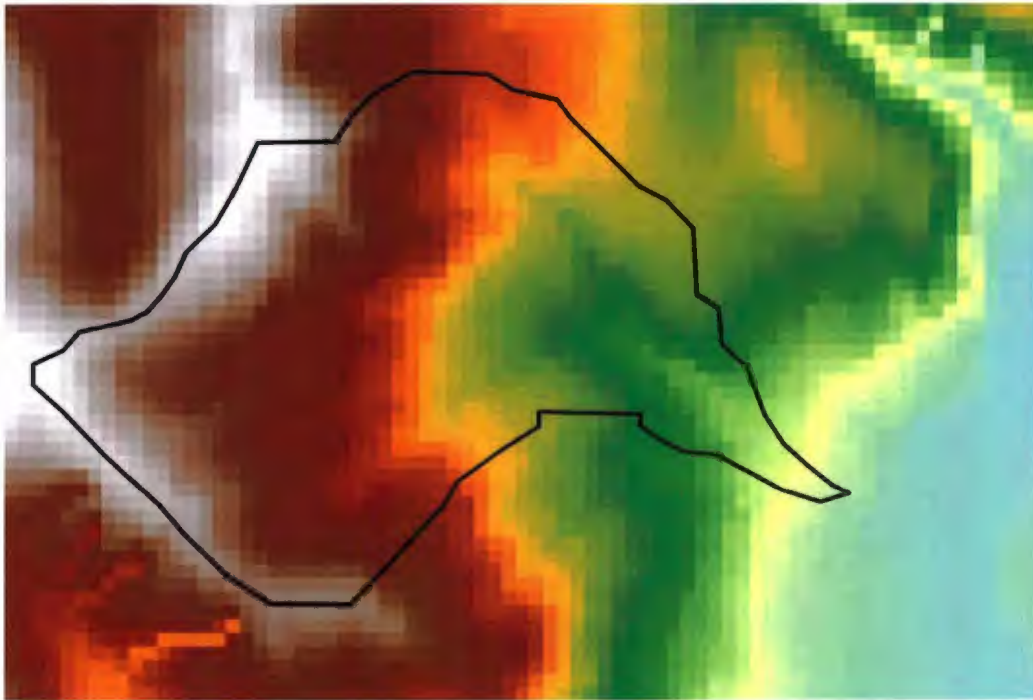


Figure 4-18: ANUDEM DEM showing the Marmot Creek boundary

Application and result of this approach for Marmot Creek basin are described in this chapter and the following chapter.

5.1 Calibration of Model

The process of distributed model calibration involves the optimization of parameter values to provide the best possible fit between measured and simulated hydrologic response (Grayson and Blöschl, 2000). A description of specific steps applied to calibrate DHSVM to the Marmot Creek watershed is described below.

5.1.1 Calibration Process

In this application, calibration of DHSVM includes both qualitative and quantitative assessments of simulated streamflow to observed streamflow. An Environment Canada stream gauge is located $50^{\circ}57'1''\text{N}$, $115^{\circ}9'10''\text{W}$, which records seasonal (May-October) daily discharge in cubic meter per second. These gage data were obtained through the Water Survey of Canada web interface (www.wsc.ec.gc.ca). The model was run with a starting date of July 27, 2005 and the initial simulation results were discarded to account for the necessary model spin up. The first run generated initial file was used to simulate the final streamflow. The daily mean was obtained by averaging one hourly simulated streamflow values. These values were then plotted against the daily observed values, and the input parameters were adjusted to achieve improved Nash-Sutcliffe efficiency, Nash-Sutcliffe efficiency relative and Index of Agreement. Visual assessment of the graphed results identified the best simulations, and statistical analysis of these selected results quantitatively identified the most accurate simulations.

Because DHSVM is physically based, a thorough understanding of how streams are routed through a watershed in DHSVM is fundamental factor for successful model calibration. Systematic trial and error proved to be the most effective calibration method (Stonesifer, 2007). The general strategy involved several model runs dedicated to the investigation of the sensitivity of a single input parameter with respect to streamflow at the gauge location. All other inputs were held constant while the input of interest was adjusted to address the range of referenced values. Any improvement or decline in the simulation results was noted. Investigation of the next possible input was selected both by suggestions made in the literature of the most sensitive model parameters, and visual observation of the general shape of the simulated hydrograph with respect to the measured values. This process was repeated until the model simulation could be improved no further based on the available input data.

5.1.2 Statistical Judgment

As suggested by Krause et al. (2005), three statistical measures were applied for quantitative assessment for the goodness of model fit. The statistics used include the Nash Sutcliffe efficiency (E), the relative efficiency E_{rel} and Index of Agreement. Root mean square errors (RMSEs), mean and standard deviation of stream flow and snow water equivalent were also compared with their measured variables, where:

$$RMSE = \sqrt{\frac{1}{N} \sum_{i=1}^N (P_i - O_i)^2}$$

Where N = sample size, P_i = simulated value, and O_i = measured value.

This method was used by Wigneron, et al. (1999) to evaluate the Interactions between Soil-Biosphere-Atmosphere (ISBA) schemes. Model efficiency (Nash and Sutcliffe, 1970) indicates a model's ability to explain the variance of observed streamflow and is able to describe how well calculated and observed flows compare in both volume and shape (Kokkoken and Jakeman, 2001; Beckers and Alila, 2004). Model efficiency is defined as one minus the sum of the absolute squared differences between the predicted and observed values normalized by the variance of the observed values during the period under investigation. It is calculated as below

$$E = 1 - \frac{\sum_{i=1}^n (O_i - P_i)^2}{\sum_{i=1}^n (O_i - \bar{O})^2}$$

E values may range from 1.0 to $-\infty$, and higher values indicate a better fit of the simulated data. An E value equal to zero indicates that the mean of the observed discharge is as good of a predictor of flow as the modeled results. A value below zero suggests that the mean value of the observed flows would have been a better indicator of flow (Krasue et al., 2005).

The relative efficiency E_{rel} (Krause et al., 2005) is a modified form of the model efficiency E (Nash and Sutcliffe, 1970), measures the goodness of model fit by comparing both the volume and shape of the discharge profile. The rationale for using E_{rel} is because E calculates the differences between the two time series as squared values. Consequently, an over or under estimation of higher values in the time series has greater influence than that of lower values (Krause et al., 2005). E_{rel} enhances the

lower absolute differences during the low flow period since they are substantial where considered relatively. Relative efficiency can be calculated as

$$E_{rel} = 1 - \frac{\sum_{i=1}^n \left(\frac{O_i - P_i}{O_i}\right)^2}{\sum_{i=1}^n \left(\frac{O_i - \bar{O}}{O_i}\right)^2}$$

The index of agreement “d” was proposed by Willmot (1984) to overcome the insensitivity of E and r^2 to differences in the observed and predicted means and variances (Legates and McCabe, 1999). The index of agreement represents the ratio of the mean square root and the potential error (Willmot, 1984) and is defined as

$$d = 1 - \frac{\sum_{i=1}^n (O_i - P_i)^2}{\sum_{i=1}^n (|P_i - \bar{O}| + |O_i - \bar{O}|)^2}$$

The potential error in the denominator represents the largest value that the squared difference of each pair can attain. With the mean square error in the numerator d is very sensitive to peak flows and insensitive for low flow conditions. The range of d is between 0 (no correlation) and 1 (perfect fit).

5.2 Validation of Model

Testing of modeled simulations using a calibrated model against real data that were not a part of the calibration process, generally called as model validation (Grayson and Bloschl, 2000). In this research validation of DHSVM was done assessing stream flow and snow accumulation in forested, snow dominated watershed of Alberta, Canada.

This goal was met through the comparison of measured to modeled streamflow and snow water equivalent using the calibrated DHSVM in Marmot Creek watershed.

DHSVM version 2.0.1 was run using a 1-hr time step from July 2005 to Dec 2006. Calibrated results of these streamflow simulations were compared to measured streamflow data collected for the 2005 to 2006 summer (May-October) seasons. These data were obtained from Water Survey of Canada web site. They have daily stream stage data during the summer months for Marmot Creek basin. Using AWK code 1-hr step streamflow converted into daily streamflow (m^3/s), which were used to assess the performance of the simulated results. After that calibration model is run for the year 2007 for validation.

5.3 Results

DHSVM performed well with respect to the calibration of the model to the Marmot Creek watershed. The results of the simulation with measured streamflow data are shown in figure 5-1. Visual assessment of these results suggests that the model performed considerably well for the year 2006 and in year 2007 although some peak flows simulated are high when compared with the measured data. The 2006 hydrograph is shown separately to highlight it as the most accurate during the simulated period. Statistical analysis of the simulated data will help to quantify the performance of DHSVM.

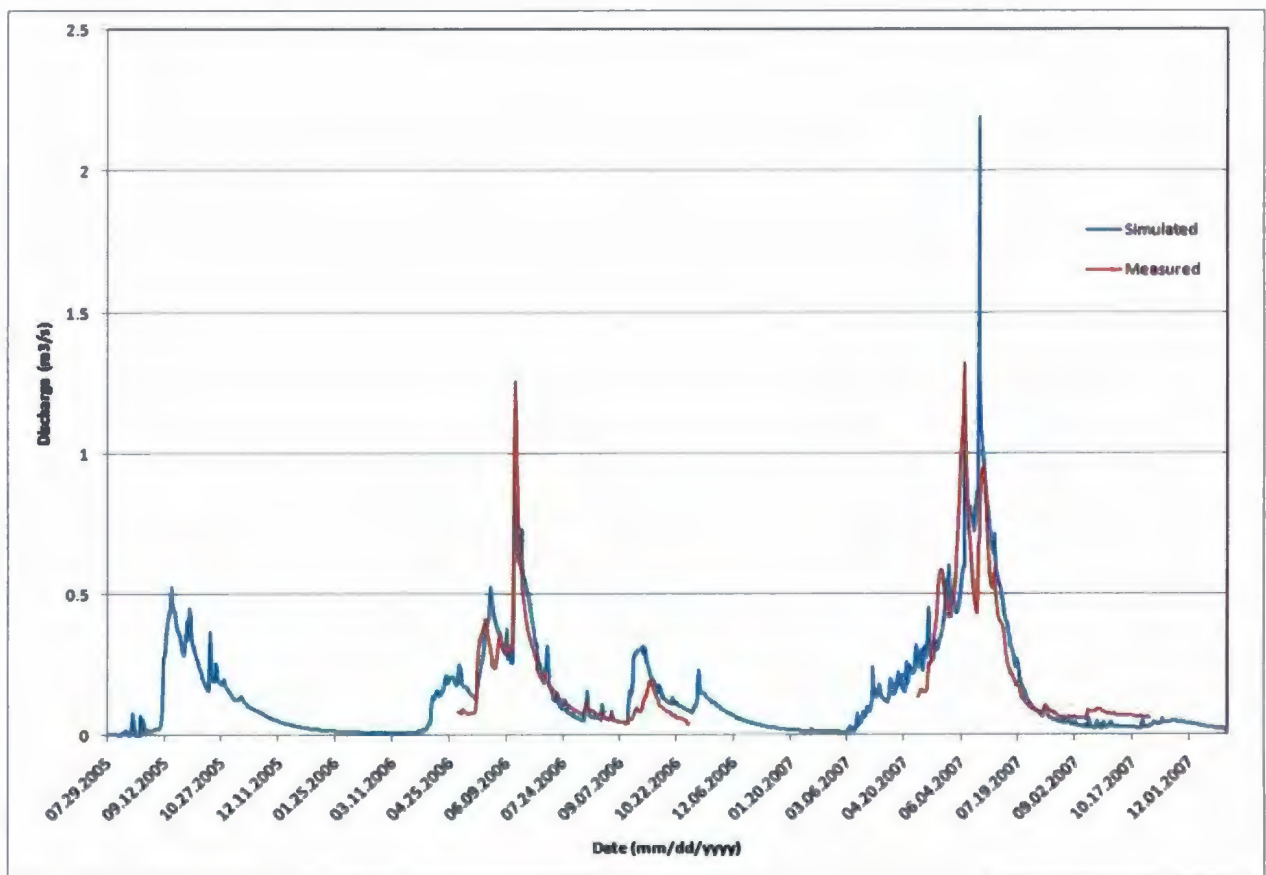


Figure 5-1: Calibrated results for the Marmot Creek basin. Simulated daily streamflow (m^3/s) versus measured streamflow. Broken lines are due to measured streamflow only available from May to October.

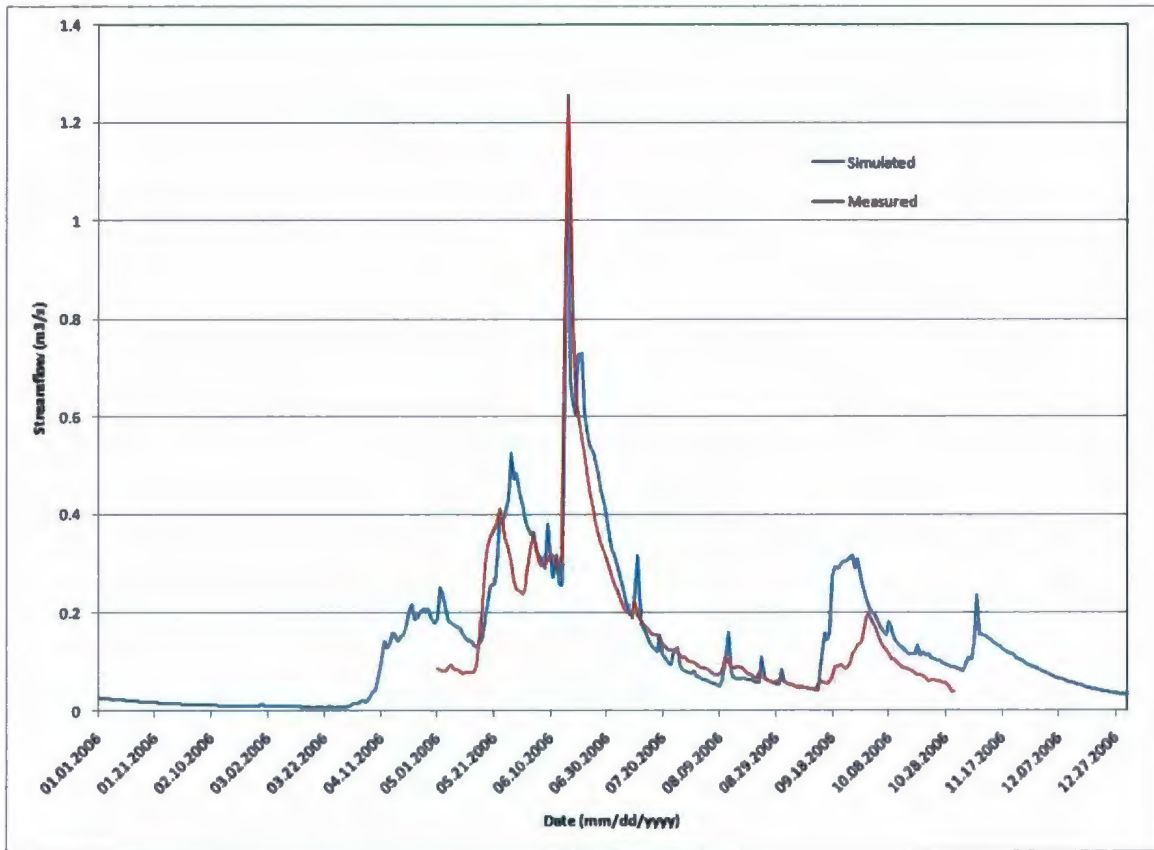


Figure 5-2: Precise simulation period for the year 2006.

5.3.1 Statistical Analysis

For both observed and simulated datasets, descriptive statistics were calculated. As describe in previous section measures of goodness of fit for hydrologic simulation namely Nash-Sutcliffe efficiency, Nash-Sutcliffe efficiency relative and Index of agreement were also calculated for the individual years. Descriptive statistics calculation includes the sample mean, and standard deviation for each of the observed and simulated datasets. Table 5.1 summarizes the individual year statistics by presenting the Nash and Sutcliffe efficiency, Nash and Sutcliffe efficiency relative, and Index of agreement of simulated and observed data. These measures of range for independent datasets provide an idea of how well the distribution of the simulated data matches the distribution of the measured data. When compared to the measured data, DHSVM simulations generally had a higher mean and standard deviation. These statistics illustrate that the DHSVM simulated yearly hydrograph was characterized by a more wider distribution with slightly higher peaks, a early runoff, and more steeply sloping rising and recession limbs when compared to the distribution of the measured flows. These patterns are readily apparent in the figure 5.2, depicting the modeled versus measured streamflow for the year 2006.

During model calibration, simulated total stream discharge was kept as close as possible to the measured total, while also minimizing RMSE between simulated and measured streamflow. Peak flows are consistently slightly overestimated in the early, middle and end of the summer season. Total discharge is simulated very well in the

calibration period. RMSE is lower than the measured standard deviation (Table 5.1). Model efficiency is acceptable at 0.734.

The streamflow simulation in 2006 is better than in 2007 in general (Figure 5.1). RMSE is lower than the measured standard deviation in the year 2007 as well (Table 5.2); total discharge is over estimated by 2.5% for the summer months (May-Oct); model efficiency is 0.621 (Table 5.1). In the early summer season, peaks were captured quite accurately but in the late summer season one peak was overestimated in 2007. However, in the early part of 2007 and at the end of the year, streamflow is simulated well by the model (Figure 5.1). Index of agreement for both years shows good results for the model performance.

Table 5-1 Statistics of observed and simulated stream discharge during calibration and validation periods

Year	RMS E	Mean		Standard deviation		Nash- Sutcliffe efficiency	Nash- Sutcliffe efficiency- relative	Index of agreement
		Measured	Simulated	Measured	Simulated			
2006	0.088	0.177	0.21	0.171	0.171	0.734	0.426	0.932
2007	0.171	0.264	0.27	0.278	0.321	0.621	0.798	0.912

Figure 5-3 shows the scatter plot of daily simulated versus measured stream discharge for the study period. The figure clearly shows that the measured and simulated streamflow have positive correlation and only few outliers observed.

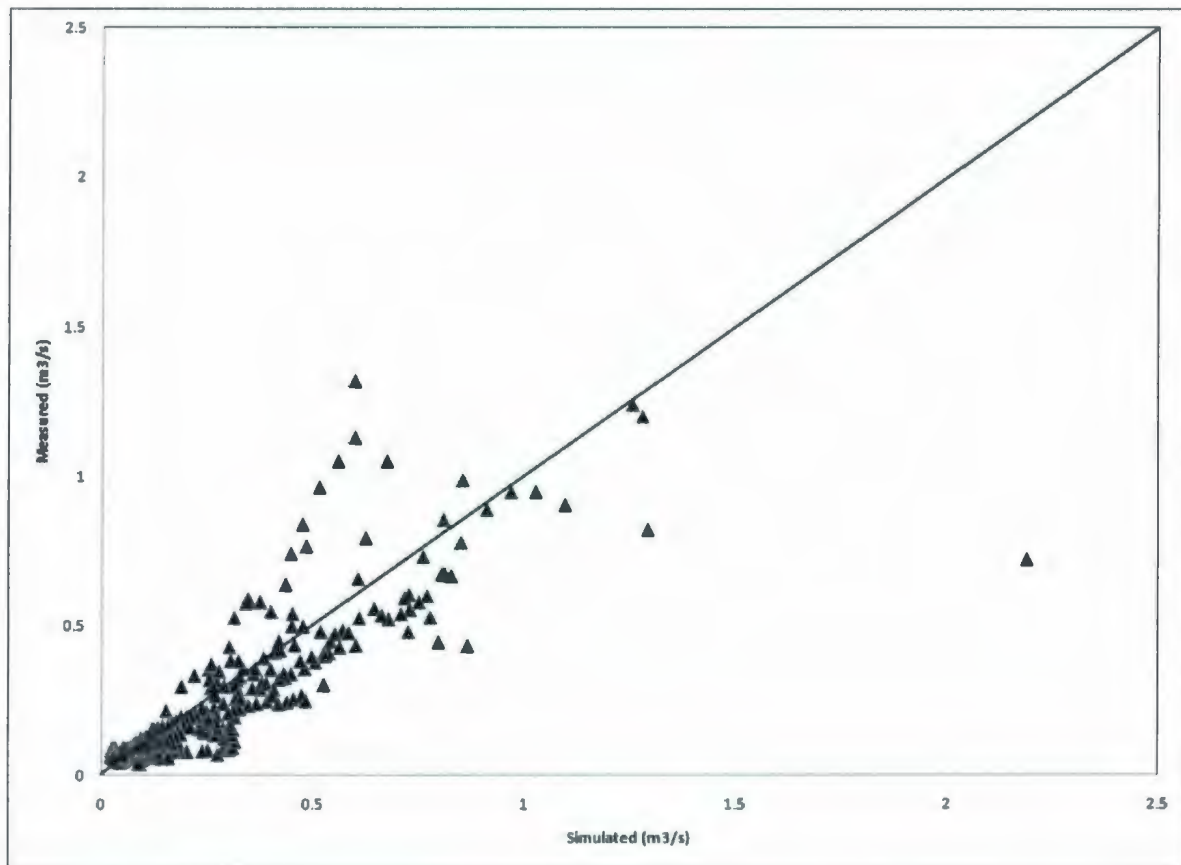


Figure 5-3: Scatter plot of daily average simulated streamflow versus measured data.

5.3.2 Snow Water Equivalent (SWE)

Snow water equivalent at Marmot Creek basin in general simulated well for the two simulated years (Figure 5-4). Snow water equivalent is simulated very well at the end of the both years; but it is underestimated in the beginning of the each year, and there is a discrepancy between simulated and measured during the summer season of the year. Visual assessment of the simulated SWE indicates snowmelt timing was capture well for both years.

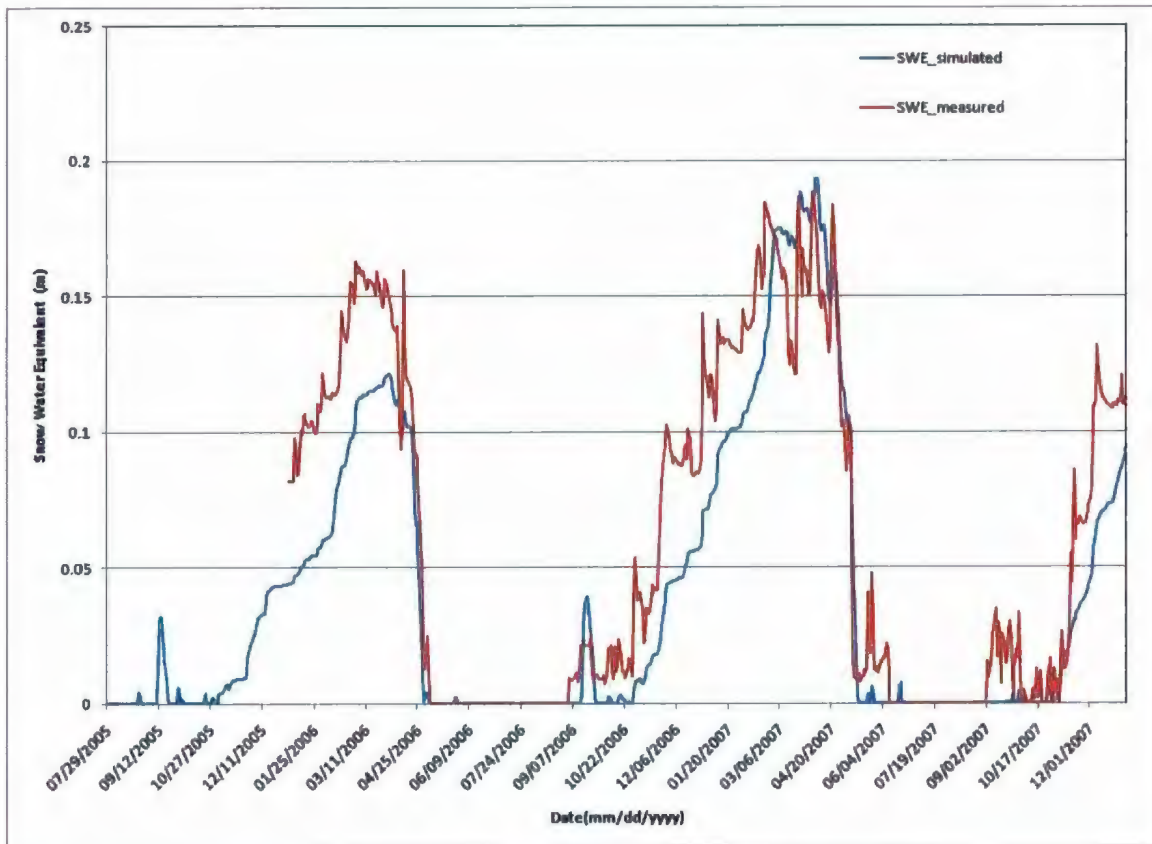


Figure 5-4: Simulated and measured snow water equivalent for the Marmot Creek basin. Measured data started from Jan 01,2006.

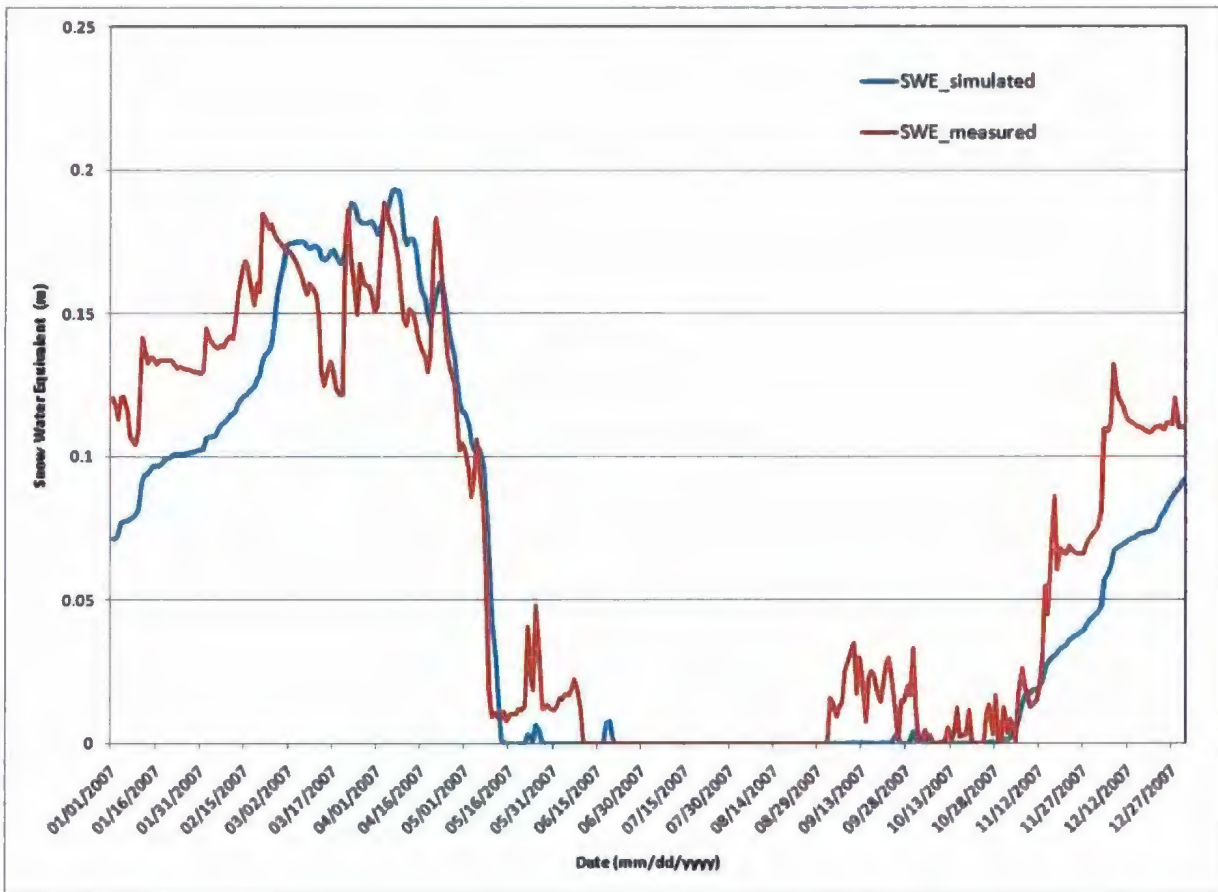


Figure 5-5: Simulated and measured snow water equivalent for the Marmot Creek basin for the year 2007.

Statistical investigation shows that RMSEs are smaller than measured variability represented by mean and standard deviation of the data (Table 5-2). In 2006, SWE has a RMSE of 0.029, the highest among the two-year simulations. Simulated and measured standard deviation of SWE shows good agreement of peak snow accumulation for the year 2007. Model efficiency is 0.736 and 0.874 for the year 2006 and 2007 respectively, is acceptable. Simulated co-efficient of determination (R^2) are 0.962 and 0.948 for year 2006 and 2007 respectively.

Table 5-2: statistics of snow water equivalent (SWE) simulated and measured at Marmot Creek basin in calibration and validation periods.

Year	RMSE	Mean		Standard deviation		² E	³ R ²
		Measured	Simulated	Measured	Simulated		
2006	0.029	0.055	0.034	0.057	0.041	0.736	0.962
2007	0.023	0.066	0.057	0.066	0.065	0.874	0.948

¹RMSE = Root mean square error; ²E = Nash-Sutcliffe efficiency; ³R² = Co-efficient of determination

5.4 Discussion

In general, the model accurately simulates total stream discharge and SWE. However, some of the peak discharge was captured high. Beckers and Alila (2004) applied the model in the Pacific North West region and found that the accuracy of either baseflow or storm flow estimates could not be improved together. One can be improve with expense of other. It became clear in this study as well, during the calibration of streamflow simulation. Below is the summary of model efficiency of DHSVM in previous studies.

Table 5-3: Statistics of streamflow and snow water equivalent simulation in previous studies.

Studies	Streamflow	Snow water equivalent
	Model Efficiency	Model Efficiency
Beckers and Alila (2004)	0.57-0.87	-
Leung et al., (1996)	0.41-0.86	-
Burges and Wigmosta (1998)	0.89	-
G. Jost et al., (2009)	-	0.49-0.89
Marmot Creek basin	0.73, 0.62*	0.736, 0.874*

Note: numbers with asterisks are statistics for 2006 and 2007 respectively for this study.

While the streamflow simulation is poor for 2007, perhaps due to some input data or land cover changes not represented in the model. Model efficiency for the 2006 and 2007 are comparable to those in other studies like Beckers and Alila (2004) found

model efficiency for streamflow 0.57-0.87, Leung et al., (1996) found 0.41-0.86 and Burges and Wigmosta (1998) found 0.89.

Snow water equivalent simulated model efficiency is done recently by G. Jost et al., (2009) ranges from 0.49 to 0.89 (using DHSVM 3.0), while in this study its 0.736 and 0.874 in 2006 and 2007 respectively for the Marmot Creek basin. On this basis, the model validation is accepted with caution and model will be used to investigate the effects of DEM and land cover change on watershed processes in the following chapter.

Chapter 6

DEM and Land Cover Effects

Spatial inputs of landscape characteristics into DHSVM version 2.0.1 are static. The vegetation cover, soil type, and road and stream network parameters do not change over the course of simulation. Because DHSVM is highly adaptable, the model design allows the user to manipulate landscape characteristics and run the model for different landscape scenarios. This theoretically allows the user to quantitatively assess the changes of hydrologic variables of a watershed. Specifically, a DHSVM user should be able to manipulate the landscape to reflect the soil and vegetation properties on the hydrologic responses. The results of the different simulations are analyzed to assess the effects that a particular landscape change may have on the hydrologic regime of a catchment.

The previous chapter 5 describes the DHSVM model application to simulate runoff for the Marmot Creek watershed. In this chapter, DHSVM is applied in order to compare the effect of different DEM and vegetation classification on streamflow and snow water equivalent. All model inputs parameters remained constant with the exception of the input DEM and vegetation. The results were compared to assess the effect of DEM and vegetation cover for the simulation of streamflow and snow water equivalent.

6. Results

The calibrated model for the catchment as described in Chapter 5 was used as the basis for an investigation of the hydrologic sensitivities of DEM and vegetation cover over the streamflow and snow water equivalent. Model output variables archived included time-series of basin averaged snow water equivalent, runoff hydrographs and selected spatial images of hydrologic characteristics at pre-specified times. Following the initial runs with USGS DEM and EOSD vegetation cover, the simulations were repeated using the same initial condition but with hydrologically modified DEM and alternative specification of vegetation scenarios. This chapter presents the findings of these simulations.

6.1. DEM Effects

6.1.1 Streamflow

The effect of DEM source on simulated hydrologic response was evaluated by applying DHSVM to the Marmot Creek catchment using USGS and ANUDEM generated DEM at resolution of 90 m. Each of the model runs used the calibrated parameter set developed at chapter 5, so it was expected that of the simulated streamflow, those calculated using USGS DEM would more closely resemble the observed streamflow time series. Table 6-1 lists the monthly averaged discharge modeled for each DEM scenario.

Table 6-1 Monthly averaged discharges (cms) for each DEM

Month	USGS DEM	ANUDEM	Observed	USGS DEM	ANUDEM	Observed
		DEM			DEM	
		2006			2007	
January	0.020	0.028		0.021	0.031	
February	0.012	0.017		0.013	0.020	
March	0.009	0.013		0.070	0.064	
April	0.123	0.104		0.184	0.167	
May	0.261	0.235	0.197	0.366	0.345	0.371
June	0.471	0.452	0.452	0.837	0.818	0.770
July	0.171	0.182	0.167	0.306	0.311	0.232
August	0.068	0.085	0.078	0.062	0.074	0.076
September	0.164	0.157	0.079	0.033	0.044	0.076
October	0.132	0.136	0.092	0.029	0.038	0.068
November	0.118	0.122		0.046	0.050	
December	0.052	0.061		0.029	0.034	
Total	1.601	1.592		1.996	1.966	

Table 6-2 Summary of average summer (May-Oct) flows

Year	Observed	ANUDEM DEM	USGS DEM
2006	0.1775	0.2078	0.2111
2007	0.2655	0.2717	0.2722
Average	0.2215	0.2398	0.2417

Simulated streamflow volumes were found to vary between the two DEMs in a consistent fashion. Mean runoff volumes were lowest when predicted by the ANUDEM

DEM. The ANUDEM DEM and USGS DEM predicted average annual flows that were 8.2% and 9.11% larger, respectively (Table 6.2). The increase in prediction by the USGS DEM is attributable to the higher basin area (Table 4-8) compared with ANUDEM DEM.

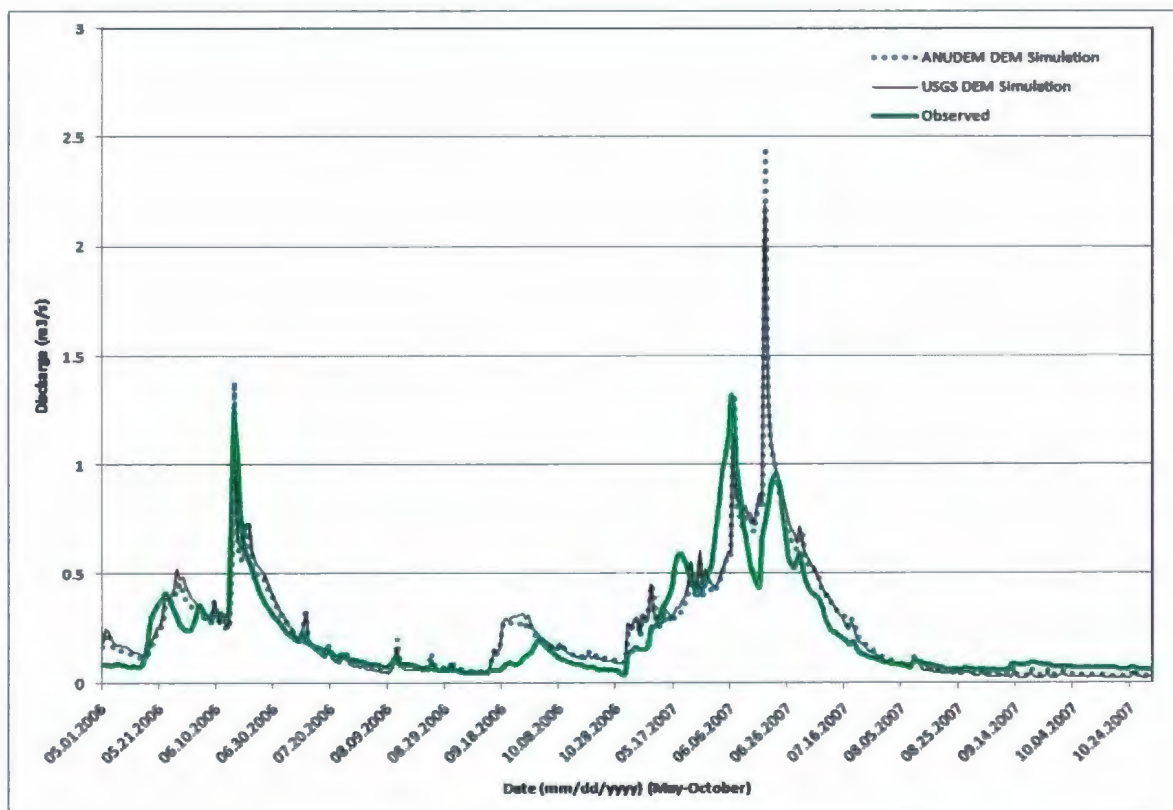


Figure 6-1: Simulated streamflows for the ANUDEM DEM and USGS DEM along with measured streamflow from May to October in year 2006 and 2007.

Time series plots were examined for an individual peak flow events series for 2006. These hydrographs showed that the ANUDEM DEM simulated had a higher peak than flows simulated with the USGS DEM. The ANUDEM DEM had a smaller watershed

area and higher standard deviation of elevation (Table 4-8) than USGS DEM which results higher peak flows.

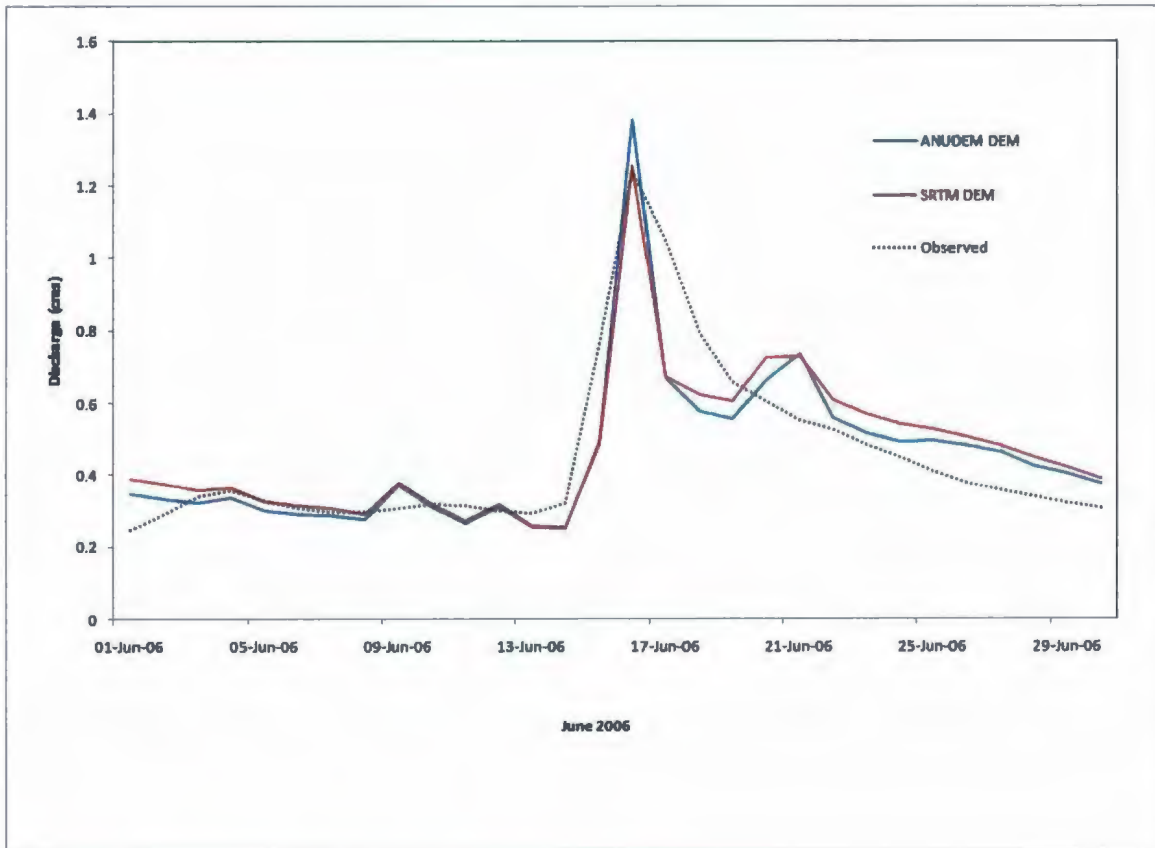


Figure6-2: Simulated high flow event, June 2006

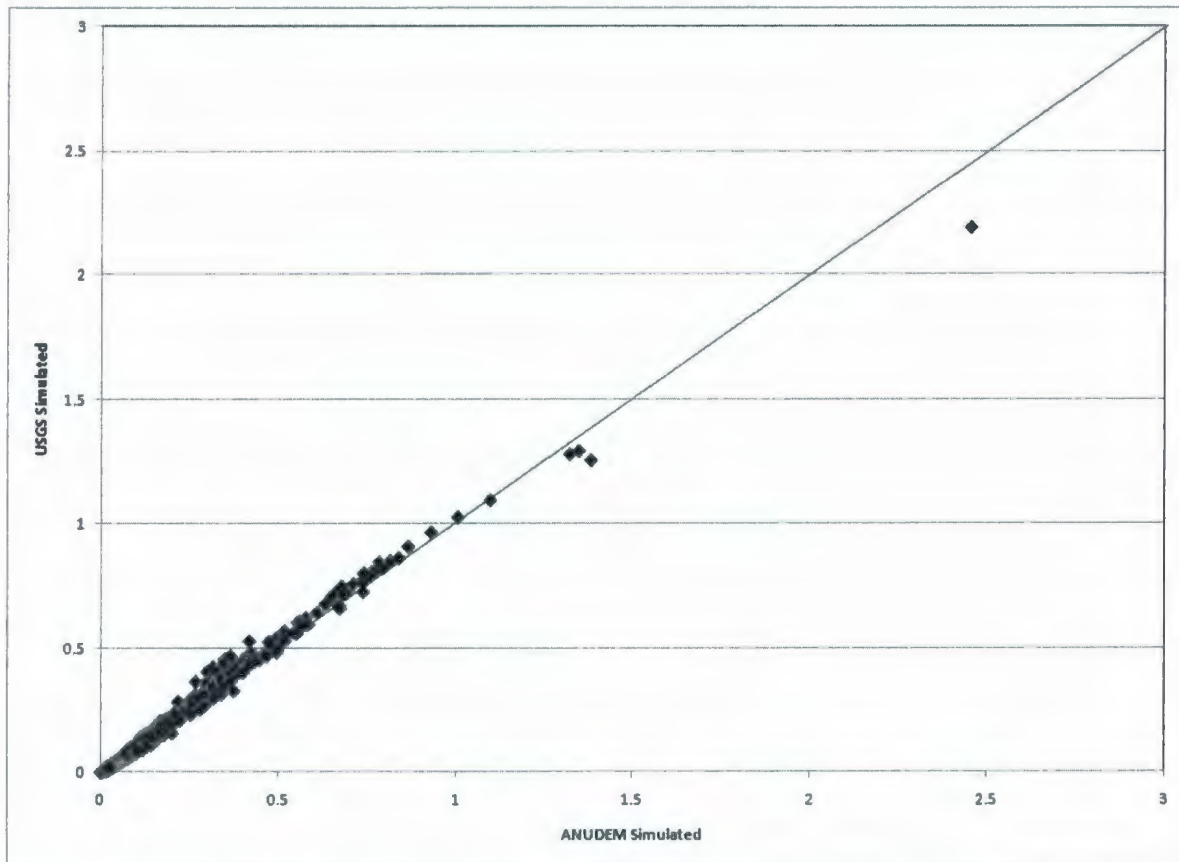


Figure 6-3: Scatter plot of daily streamflow for USGS vs. ANUDEM simulated.

Scatter plot of ANUDEM DEM simulated streamflow versus USGS simulated streamflow does not show much difference (Figure 6-3). Compared with USGS DEM simulation ANUDEM DEM simulation has decreased summer season flow for the 2006 and 2007. Winter season flow is increased slightly for 2006; the increase is only 3.3%. There is not much change in winter season flow for 2007.

ANUDEM DEM effects on peak flows, the effect is more prominent for the large sized peak flows compared to medium and small sized peak flows for the 2006 and 2007 scenarios (Figure 6-1 and 6-2)

In previous studies, Kenward and Lettenmaier (1997) found that the mean annual runoff volumes for simulations that used the USGS and SIR-C DEMs were 0.3 and 7.0 percent larger, respectively, than simulations produced using the same resolution reference DEM.

6.1.2 Snow Water Equivalent

DEM effects on basin-averaged snow water equivalent are negligible. Figure 6-4 shows daily average values of snow water equivalent for the entire study period, i.e., from July 2005 to December 2007. In general, ANUDEM DEM slightly decreases monthly SWE during some months and slightly increases SWE in other months. However, the overall increase is only 0.5% (Figure 6-5). The highest increase (0.0041 m) occurs in June 2007, and highest decrease (0.0017 m) occurs in November 2007.

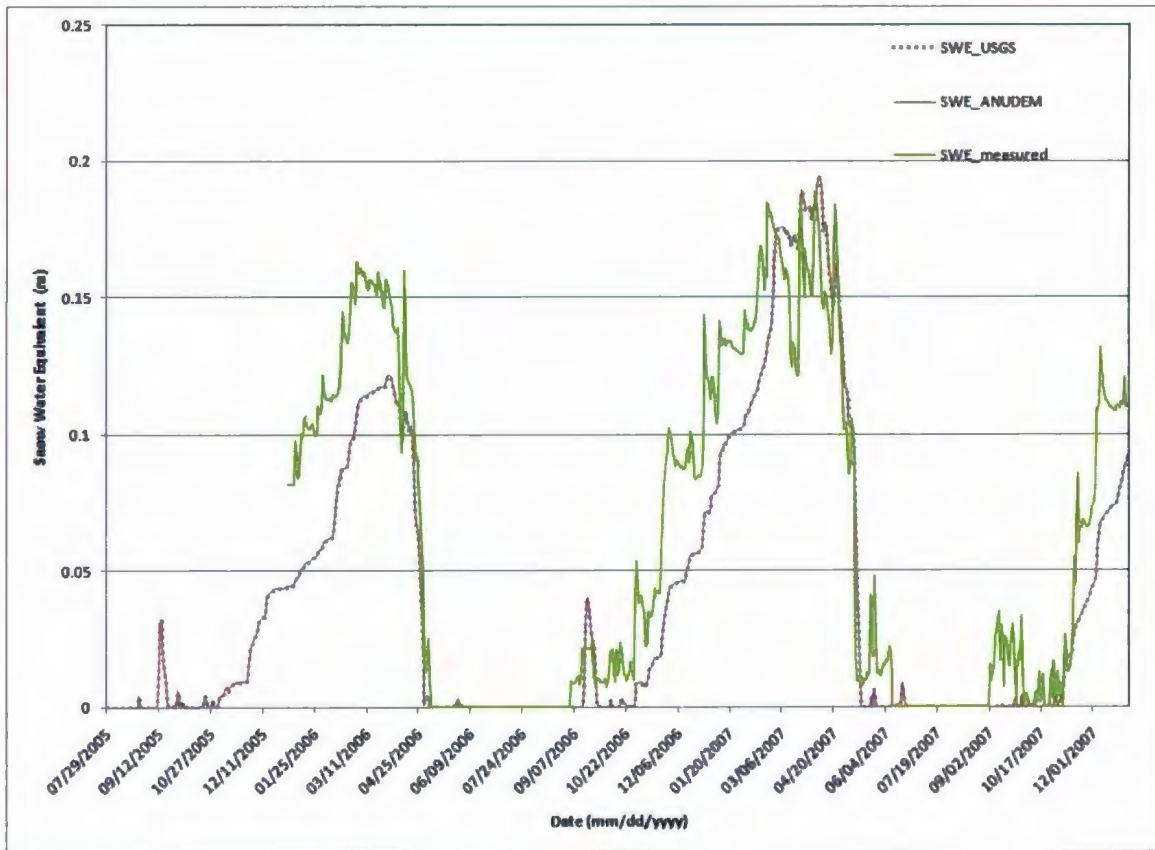


Figure 6-4: Simulated SWE generated by ANUDEM DEM and USGS DEM.

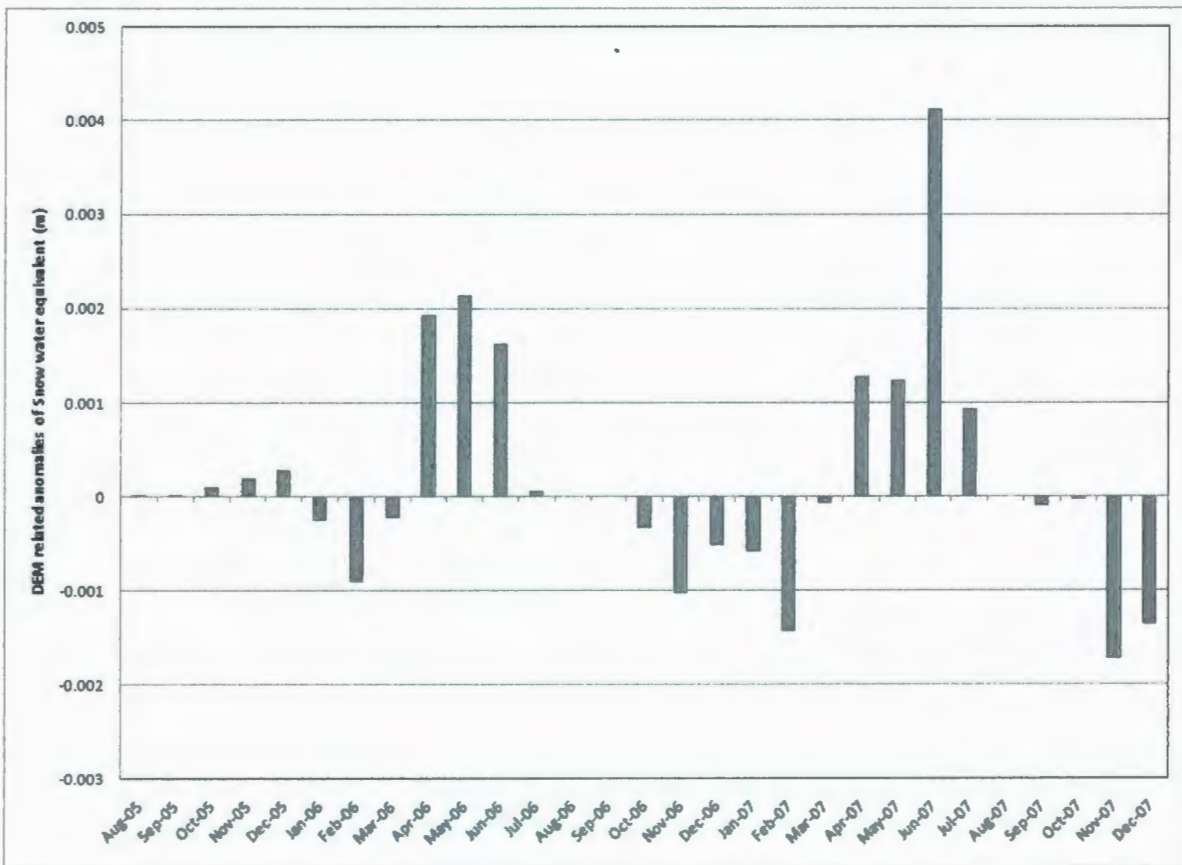
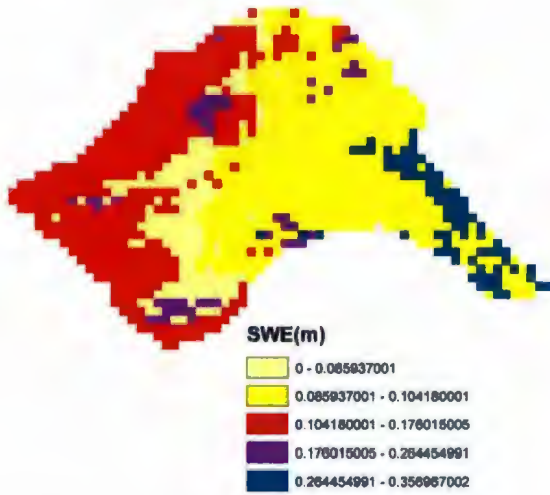


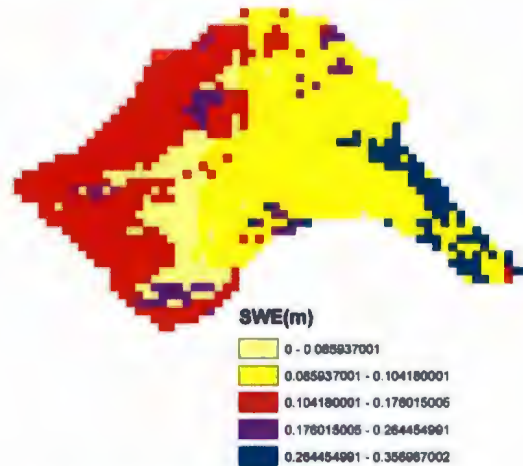
Figure 6-5: DEM-related mean monthly anomalies in snow water equivalent (SWE) during August 2005 through December 2007.

The change in spatial distribution of SWE (m) with altered DEMs taken as a snapshot on different date can be seen in Figure 6-6 which shows the variation in melt patterns of extremes from the top of the mountain and bottom. Patterns of SWE are evident and generally are not related to DEM source.

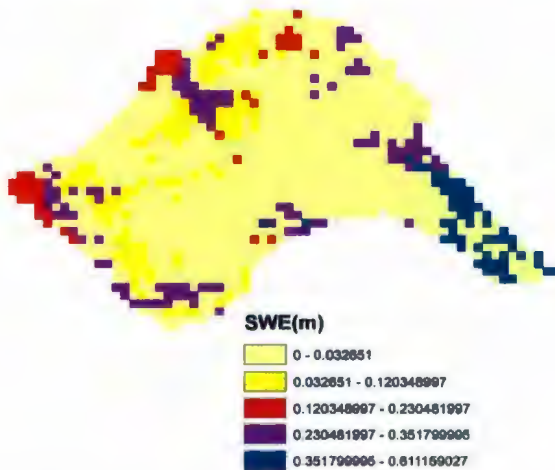
SWE with USGS DEM (March 11, 2006)



SWE with ANUDEM DEM (March 11, 2006)



SWE with USGS DEM (June 15, 2007)



SWE with ANUDEM DEM (June 15, 2007)

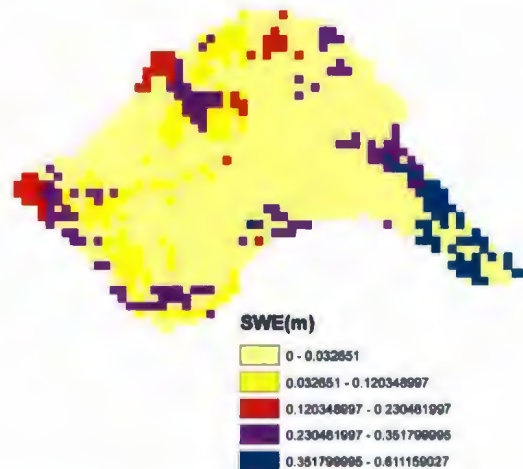


Figure 6-6: Spatial distribution of DEM source effect in SWE (m) over the Marmot Creek basin.

The effort to use different DEM source for SWE effect is probably the first among DHSVM users, hence, the SWE simulation cannot be compared to other studies. However, simulation of SWE is reasonably good as shown in figures 6-4.

6.2 Land Cover Effect

To study the effects of land cover on streamflow and snow water equivalent of the experimental scenarios, USGS vegetation classes are compared to those of the control EOSD vegetation classes. Use of USGS vegetation classes generate changes in streamflow when compared to the control scenarios (Figure 6-7). The experiment scenario under estimates stream discharge all over the year. The difference in stream discharge between the control and the experimental scenario are largest during periods of peak flows throughout the simulation. Snow water equivalent is also under estimated for the experimental scenario.

6.2.1 Streamflow

Compared to the EOSD land cover scenario, stream discharge is slightly lower for the USGS land cover scenario, with 5.8% decrease. A scatter plot of streamflow shows that the peak flows decrease for the USGS scenario (Figure 6-8). From August to February, both scenario shows similar flows. The effect of land cover change on peak flow values is in accordance with the findings of Storck et al., (1998) and La Marche and Lettenmaier (2001). This study has also found that the greatest influence of land cover is on streamflow peaks.

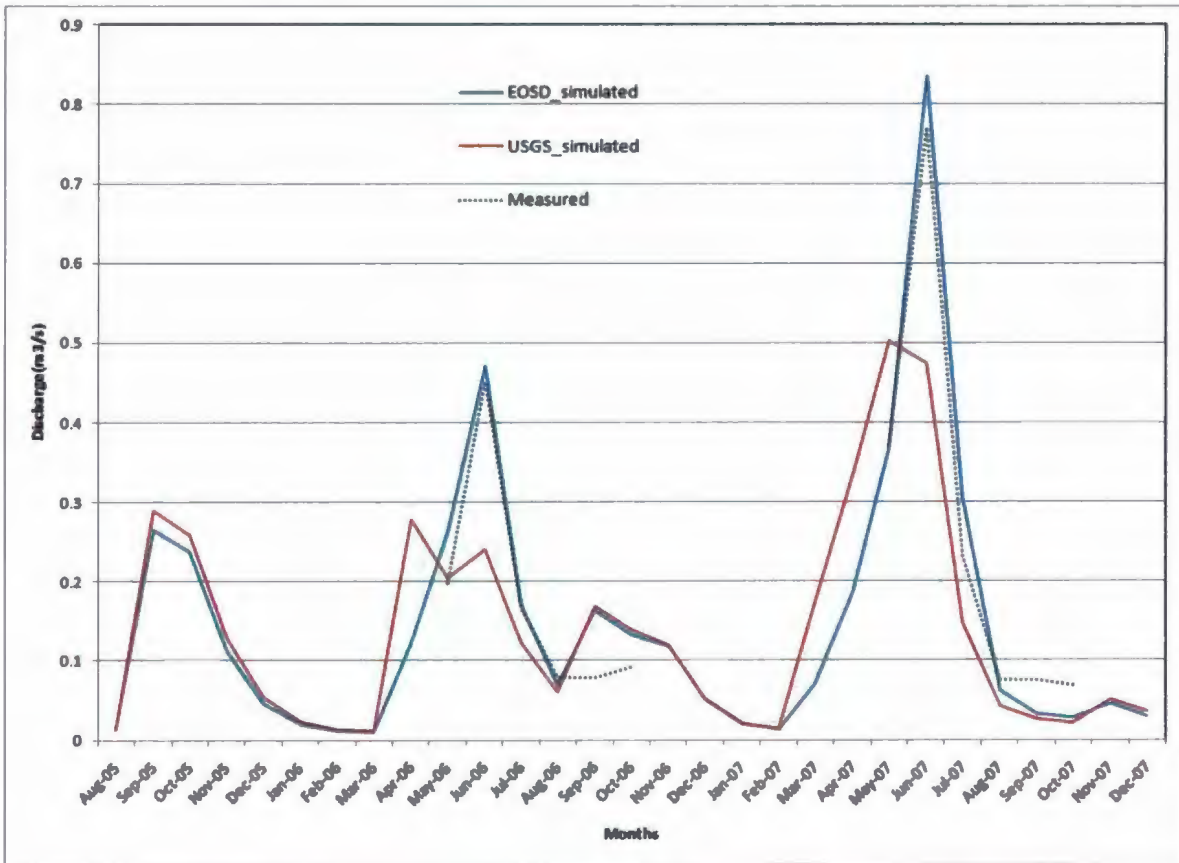


Figure 6-7: Monthly average stream discharge with E OSD land cover, and USGS land cover scenarios.

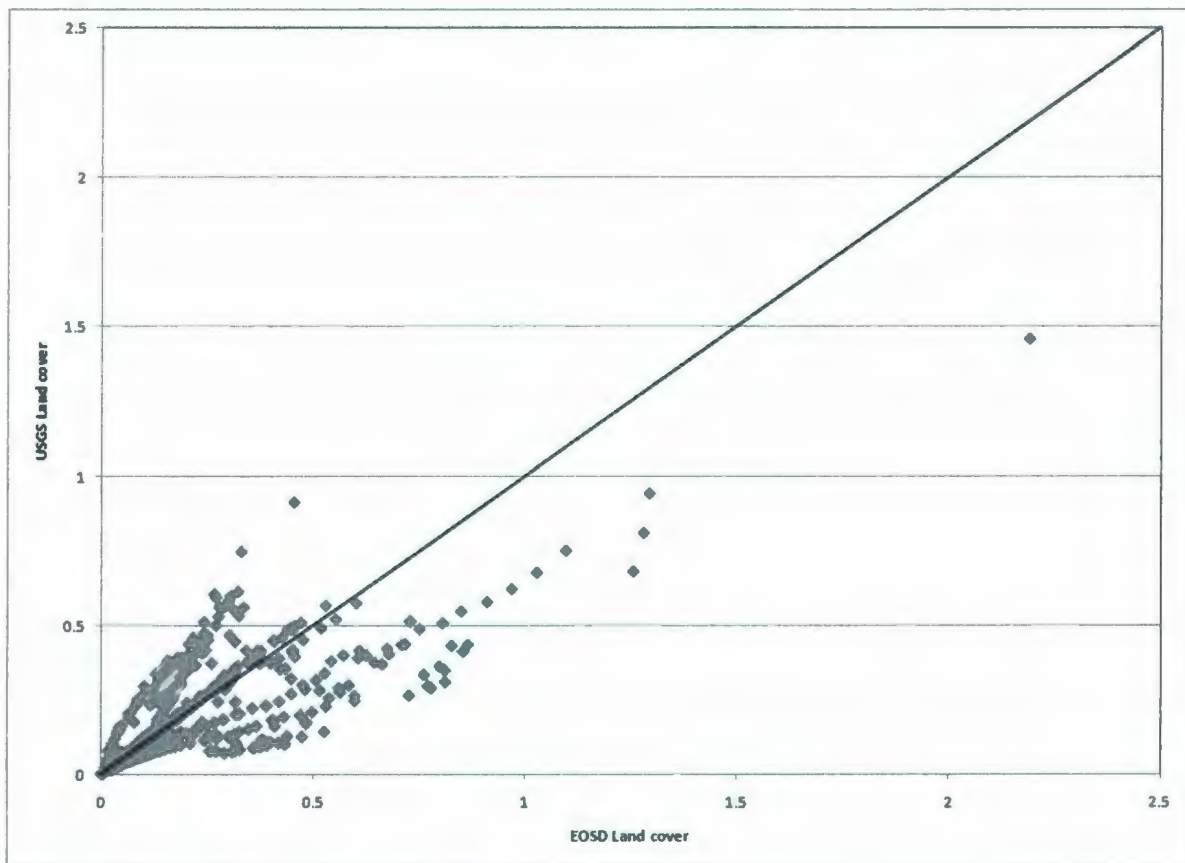


Figure 6-8: Scatter plot of daily average streamflow for the control and experimental scenarios.

6.2.2 Snow Water Equivalent

Catchment-average time series plots of snow water equivalent (SWE) show that the direction of change is consistent from year to year (Figure 6-9). The timing of SWE accumulation and ablation averaged over the basin for each month over the simulation period from August 2006 to August 2007 can be seen in Figure 6-10. In considering the effects of vegetation change on snow storage within the catchments, trend differences are not easily concluded when compared with the USGS coarse land cover map.

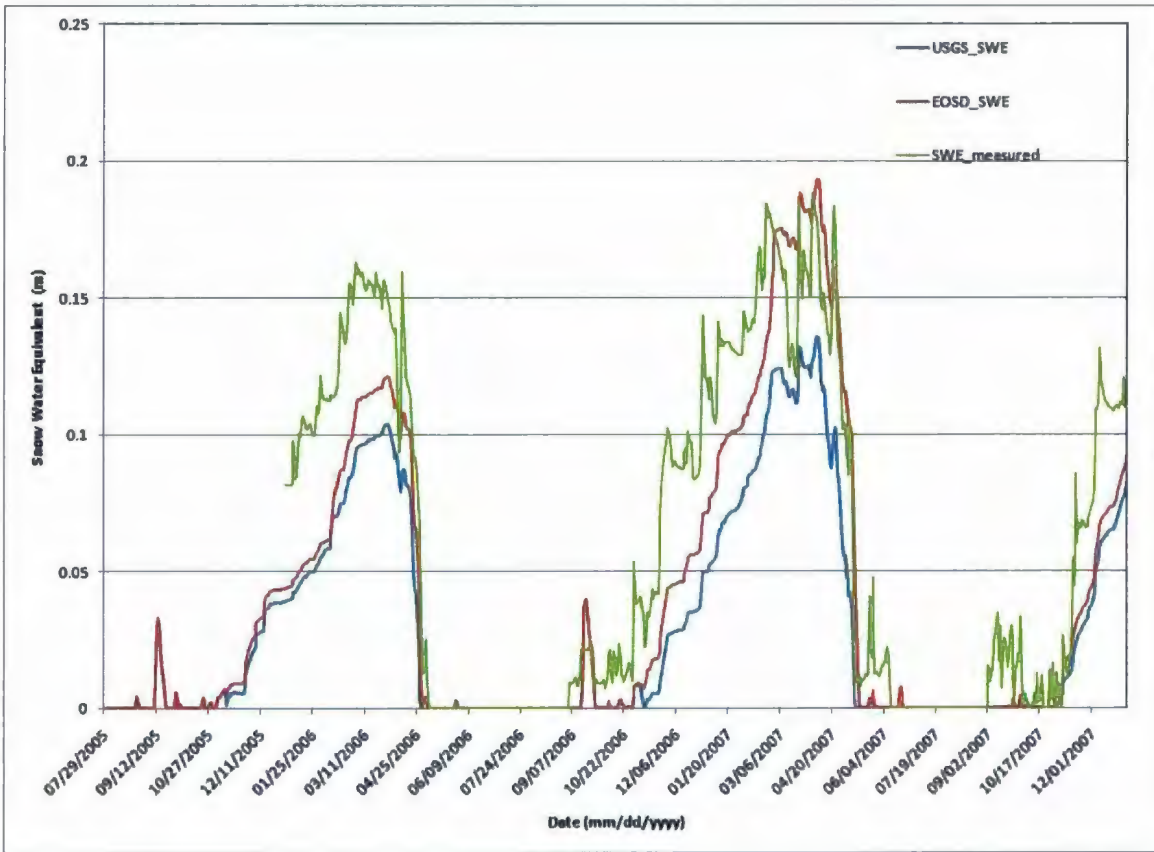


Figure 6-9: Daily SWE (m) time series for EOIS and USGS land cover simulated and measured.

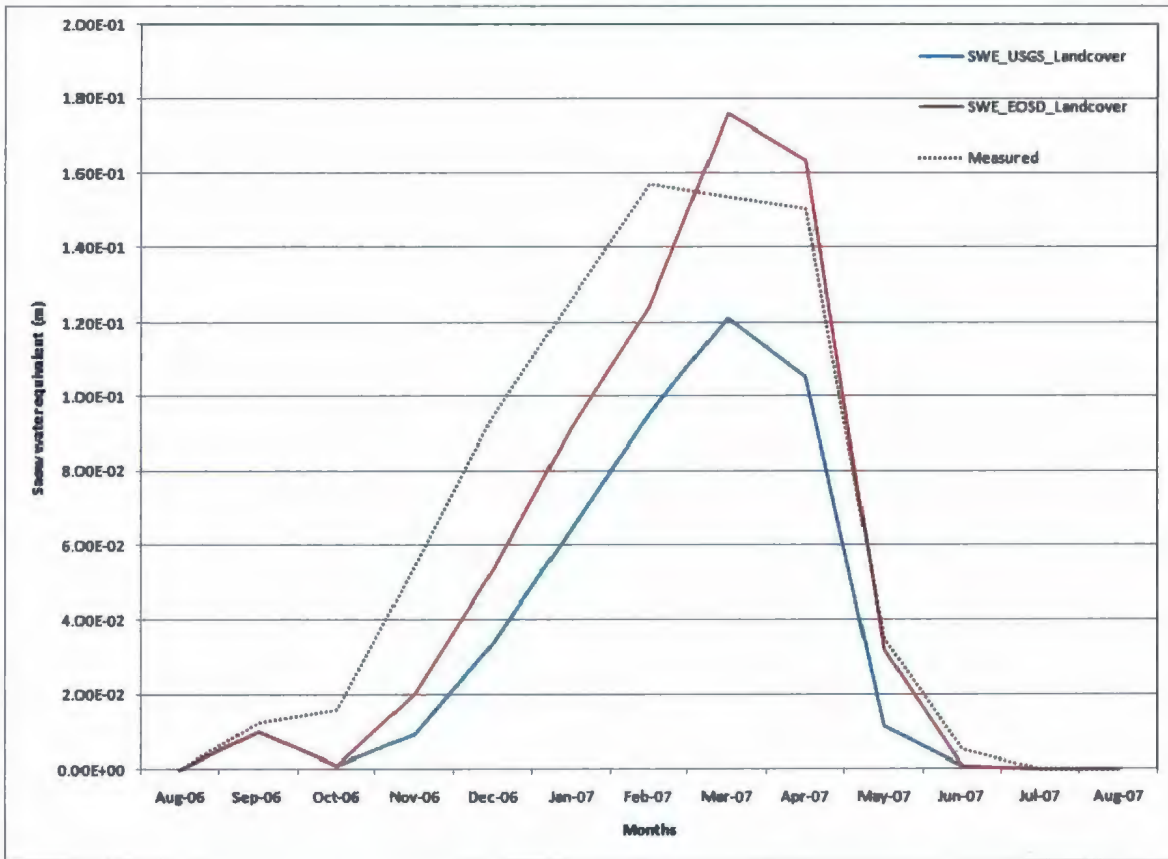
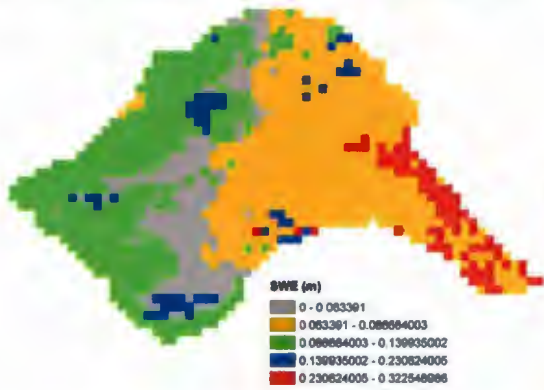


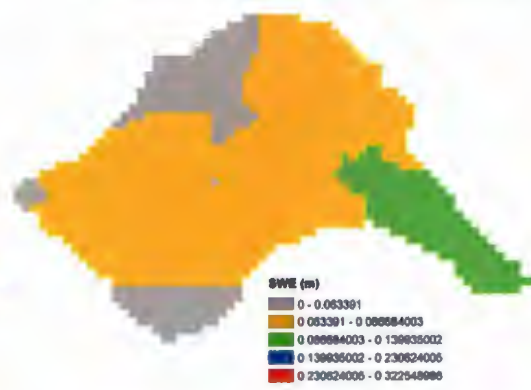
Figure 6-10: Measured and simulated SWE (m) time-series (month)

The change in spatial distribution of SWE (m) with altered land cover taken into consideration can be seen in Figure 6-11 for a number of dates which shows the variation in melt patterns of extremes from the top of the mountain and bottom. While patterns of SWE are evident and generally related to vegetation change, use of a coarser resolution land cover map is not a reliable predictor of the direction of change in SWE. However, it can be seen that the model is sensitive to the resolution of the data utilized.

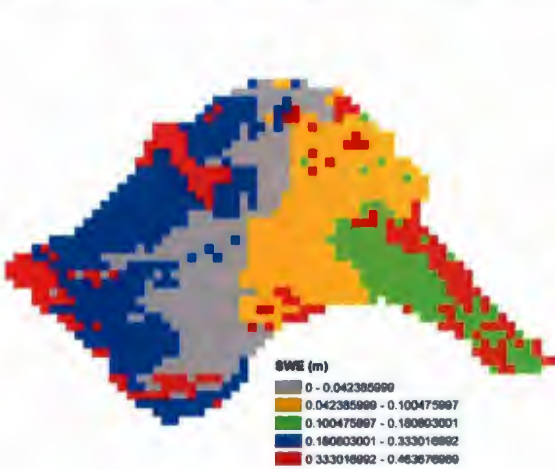
SWE with EOSD land cover (Feb 15, 2006)



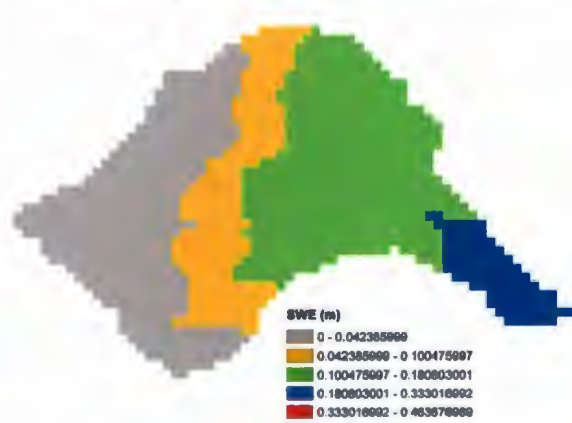
SWE with USGS land cover (Feb 15, 2006)



SWE with EOSD land cover (April 20, 2007)



SWE with USGS land cover (April 20, 2007)



SWE with EOSD land cover (Dec 03, 2007)

SWE with USGS land cover (Dec 03, 2007)

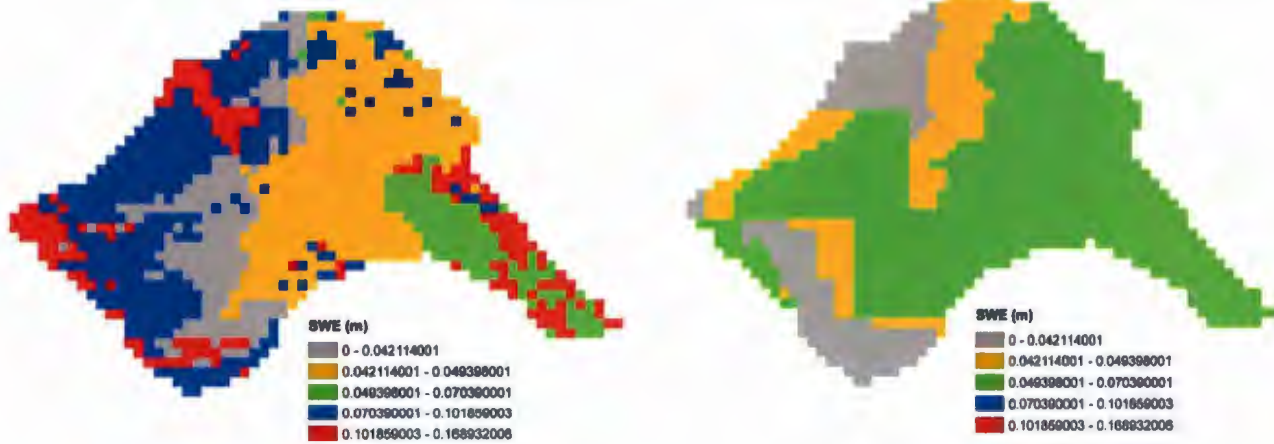


Figure 6-11: Spatial distribution of land cover change effect in SWE (m) over the Marmot Creek basin.

Figure 6-12 shows daily SWE for the EOSD and USGS land cover, the direction of change is consistent throughout the year as all the points are below the one to one line.

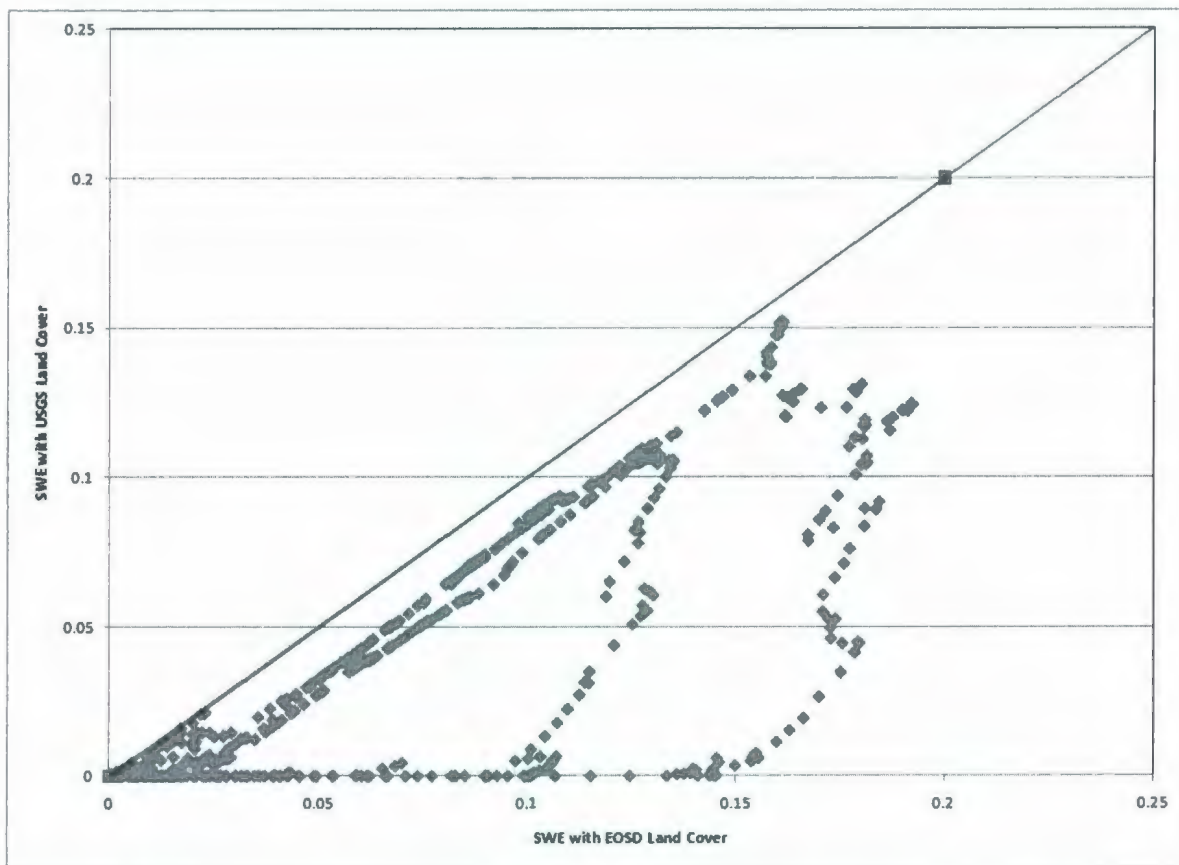


Figure 6-12: Scatter plot of SWE (m) with EOIS land cover versus SWE (m) with USGS land cover.

Change in overstory presence is highly correlated to change in SWE. Densely forested areas have lower ablation rates and accumulate less snow (Vanshaar and Lettenmaier, 2001). USGS land cover scenario represent only three type of vegetation classification among them 64% evergreen needle leaf which cause covering of overstory and less accumulation of snow. Elevation and aspect, which influence temperature and the amount of radiation input to a pixel, cloud the catchment-wide patterns related to vegetation. Changing some function such as leaf area index (LAI), elevation and aspect could predict change in SWE more effectively than changing the land cover map

resolution. SWE is clearly related to land cover data, although the effects of land cover in conjunction with local topography would be more readily visible.

Chapter 7

Conclusion

7.1 Summary of the Results

DHSVM was applied in mountainous watersheds in Western Alberta to study DEM and land cover change effects on streamflow and snow water equivalent (SWE). The model was calibrated and validated first in Marmot Creek basin. The calibrated model was then used to study the DEM and land cover effect in study basin.

Through model validation, it is found that the model was applicable to Marmot Creek basin, a mountainous watershed similar to the region where DHSVM was developed and applied. The effects of DEM and land cover change are mainly shown through streamflow and snow water equivalent (SWE). When simulating with ANUDEM derived DEM, all peak flows simulated by the model are higher than those simulated by USGS DEM. The total predicted runoff volume depended on the average elevation and basin area of DEM (Table 4-8). This implies that the model simulation is dependent on the DEM. The model simulation with ANUDEM does not have any significant effect with snow water equivalent. However, the model simulation using the USGS land cover map decrease the streamflow and SWE compared to the model simulation with EOSD land cover.

The results suggest that among variables influence by land cover, streamflow and snow water equivalent should not be neglected. Simulations also show that land cover influences on peak flow are greater than influences on total storm volume. Land cover change to the USGS product causes a greater decrease of the summer peak flow than the annual streamflow compared with the EOSD land cover simulation during the two year study period.

7.2 Implication and Recommendation

DHSVM explicitly depicts the spatial pattern of hydrologic fluxes for the Marmot Basin. When combined with a geographic information system (GIS) it makes a good choice for the study of the effects of DEM and land cover change. As mention in literature review, many previous studies of DEM and land cover change mainly focus on streamflow volume and peak flow in the temperate Pacific North-West area. Through the study of the streamflow, snow water equivalent and peak flow in mountainous watershed in Western Alberta, this dissertation broadens knowledge of the DEM and land cover effects in snow dominated mountainous watersheds. The results extend current scientific knowledge of the importance of DEM quality and land cover alterations in influencing watershed hydrology. The model simulations also give new insights of DEM and land cover effects on peak flows.

The current study confirms the results of most other studies, showing that land cover changes have large effects on streamflow and snow water equivalent. The results presented here can be used to assist understanding cold region hydrology snow accumulation and melt. The comparison of EOSD and USGS land covers, for example,

shows that annual streamflow, winter flow, summer flow and peak flows in all size categories were lower for the USGS land cover. This is due to the resolution in vegetation cover used by USGS map. This suggests a possible reduction in storm frequency, but at the expense of lower summer season flows. This result can be used in forest management strategy.

Based on the increased accuracy of simulated streamflow following rigorous model calibration, it is evident that calibration is an essential first step to the application of DHSVM to a particular watershed. Because the model is extremely sensitive to parameters such as saturated hydraulic conductivity, it is imperative that these parameters be first adjusted to reflect study area conditions in order to obtain accurate hydrologic simulations. A well-calibrated model should have some degree of regional translatability, and the calibrated parameters should theoretically be applicable to other watersheds of similar area, climatic patterns, vegetative structure, and dominant soil types. Because hydrologic models need to be calibrated to data in a particular watershed are often not available, this research suggests that in order to produce reliable simulations, at very last, DHSVM should first be calibrated to a comparable watershed with available streamflow data prior to simulating streamflow for the watershed of interest.

Uncertainty of hydrologic prediction with DHSVM could be done in future research work. DHSVM predictions with digital elevation data for a different study site could be investigated. This would help to determine whether the results of the current study are independent of basin size, topography, vegetation, soil type and climate. Additional research in this area could further investigate the impact of vertical accuracy of DEMs. Standard USGS DEMs of different classifications could be compared to give an

indication of improvement related of the newer products. The ANUDEM DEM used in this study was developed using default setting of the ANUDEM DEM generation parameter. Optimization of ANDUEM parameters, such as the number of iterations and amount of profile curvature permitted could also be investigated by comparing to the preliminary product.

Improvements could also be made to the soil map presentation of the Marmot Creek basin. Only a single soil type was used in this study. This could be improved on by defining more classes through field investigation.

Because land cover changes along with time, more recent, high resolution land cover data could be used to quantify the impact of hydrologic response.

Bibliography

Ackerman, C.T., 2002. HEC-GeoRAS 3.1. US Army Corps of Engineers, Institute for Water Resources. Hydrologic Engineering Centre, Davis, CA.

Anderson, E.A., 1976. A point energy and mass balance model of snow cover. NWS Technical Report 19. National Oceanic and Atmospheric Administration: Washington D.C.; 150.

Arola, A. and Lettenmaier, D.P., 1996. Effects of subgrid spatial heterogeneity on GCM-scale land surface energy and moisture fluxes, *Journal of Climate*, in press.

Bates, C.G. and Henry, A. J., 1928. Second phase of streamflow experiment at Wagon Wheel Gap, Colorado. *Mon. Weather Review*, 56(3), 79-85.

Beke, G., 1969. Soils of the Marmot Basin, Streeter Basin, and Red Deer Basin. PhD Thesis, University of Alberta.

Beckers, J., Alila, Y., 2004. A model of rapid preferential hillslope runoff contributions to peak flow generation in a temperate rain forest watershed. *Water Resour. Res.* 40, W03501, doi:10.1029/2003WR002582.

Bernier, P., 1986. Extrapolation snow measurements on the Marmot Creek experimental basin. *Nordic Hydrology*, 17, 83-92.

Berris, S.N. and Harr, R.D., 1987. Comparative snow accumulation and melt during rainfall in forested and clear-cut plots in the western Cascades of Oregon, *Water Resources Research*, 23 (1), 135-142.

Beven, K.J. and Kirkby, M.J., 1979. A physically based, variable contributing area model of basin hydrology, *Hydrological Sciences Bulletin*, 24, 43-69.

Beven, K., and Wood, E. F., 1983. Catchment geomorphology and the dynamics of runoff contributing areas, *J. Hydrol.*, 65, 139-158.

Black, T. A., Chen, J. M., Lee, X. and Sagar, R. M., 1991. Characteristics of short wave and long wave irradiances under a Douglas-fir forest stand, *Canadian Journal of Forest Resources*, 21, 1020-1027.

Bowling, L.C., and Lettenmaier, D.P., 1997. Evaluation of the effects of forest roads on streamflow in Hard and Ware Creeks, Washington, *Timber Fish Wild Water Resources Ser., Tech. Resp. 155*, 189 pp., Washington Dept. of Nat. Resources. Olympia.

Bowling, L. C., Storck, P. and Lettenmaier, D. P., 2000. Hydrologic effects of logging in Western Washington, USA, in press.

Bowling, L.C. and Lettenmaier, D.P., 2001. The effects of forest roads and harvest on catchment hydrology in a mountainous maritime environment, in *Land Use and Watersheds: Human Influence on Hydrology and Geomorphology in Urban and Forest Areas*, M.S. Wigmosta and S.J. Burges, eds., *AGU Water Science and Application Volume 2*, p. 145-164.

Burt, T. P., and Butcher, D. P., 1985. Topographic controls of soil moisture distributions, *J. Soil Sci.*, 36, 469-486.

Burges, S.J., and Wigmosta, M.S., 1998. Hydrological effects of land-use change in a zero-order catchment. *ASCE Journal of Hydrologic Engineering*, 3(2), 86-97.

Brooks, R.J., and Corey, A.T., 1964. Hydraulic properties of porous media. *Hydrol. Pap.* 3. Colorado State Univ.: Fort Collins; 27.

Campbell, G.S., and Norman, J.M., 1989. The description and measurement of plant canopy structure. In *Plant canopies: their growth, form, and function*, P.G. Jarvis (ed.). Cambridge University Press: Cambridge, UK; 1 – 19.

Chang, K. T., and Tsai, B. W., 1991. The effect of DEM resolution on slope and aspect mapping. *Cartogr. Geogr. Info. Sci.* 18(1): 69-77.

Claessens, L., Heuvelink, G. B. M., Schoorl, J. M., and Veldkamp, A., 2005. DEM resolution effects on shallow landslide hazard and soil redistribution modeling. *Earth Surf. Process. Landforms* 30(4), 461-477.

Cuo, L., Giambelluca, T.W., Ziegler, A.D., and Nullet, M.A., 2006. Use of the distributed soil vegetation model to study road effects on hydrological processes in Pang Khum Experimental Watershed, northern Thailand. *Forest Ecology and Management* 224, 81-94.

Davis, D. A., 1964. Collection and compilation of streamflow data in Marmot Creek Basin. In Jeffrey (1964) : Appendix I.

DeBeer, C.M., and Pomeroy, J.W., 2010. Simulation of the snowmelt runoff contributing area in a small alpine basin. *Hyrol. Earth Syst. Discuss.*, 7, 971-1003.

Dickinson, R.E., Henderson-Sellers, A., and Kennedy, P.J., 1993. Biosphere-Atmosphere Transfer Scheme (BATS) Version 1e as Coupled to the NCAR Community Climate Model: NCAR Technical Note, NCAR/TN-387+STR. National Center for Atmospheric Research: Boulder, CO; 72.

Dietrich, W. E., Wilson, C. J., Montgomery, D. R., and McKean, J., 1993. Analysis of erosion thresholds, channel networks, and landscape morphology using a digital terrain model, *J. Geol.*, 101(2), 259-278.

Doan, J.H., 2000. Geospatial Hydrologic Modelling Extension HECGeoHMS. US Army Corps of Engineers, Institute for Water Resources, Hydrologic Engineering Centre, Davis, CA.

Dunne, T., Moore, T. R., and Taylor, C. H., 1975. Recognition and prediction of runoff-producing zones in humid regions, *Hydrol. Sci. Bull.*, 20, 305-327.

Dubin, A. M., and Lettenmaier, D.P., 1999. Assessing the influence of digital elevation model resolution on hydrologic modeling, *Water Resources Series, Technical Report 159*, University of Washington, Seattle.

Eberhardt, L.L. and Thomas, J.T., 1991. Designing environmental field studies, *Ecol. Monogr.*, 61(1), 53-73.

English, P., Richardson, P., Glover, M., Cresswell, H., Gallant, J., 2004. Interpreting Airborne Geophysics as an adjunct to Hydrogeological Investigations for Salinity Management: Honeysuckle Creek Catchment, Victoria. 18/04, CSIRO Land and Water.

Fairfield, J., Leymarie, P., 1991. Drainage networks from grid digital elevation models. *Water Resources Research* 27 (5), 709–717.

Florinsky, I. V. 1998. Accuracy of local topographic variables derived from digital elevation models. *Intl. J. Geogr. Info. Sci.* 12(1): 47-61.

Gallant, J.C., and Dowling, T.I., 2003. A multiresolution index of valley bottom flatness for mapping depositional areas. *Water Resources Research* 39 (12), 1–4, ESG.

Gallant, J.C., and Hutchinson, M.F., 1997. Scale dependence in terrain analysis. *Mathematics and Computers in Simulation* 43 (3–6), 313–321.

Gallant, J.C., and Wilson, J.P., 2000. Primary Topographic Attributes. In *Terrain Analysis*. John Wiley & Sons, Inc.: New York, pp. 51-85.

Gao, J., 1998. Impact of sampling intervals on the reliability of topographic variables mapped from grid DEMs at a micro scale. *Intl. J. Geogr. Info. Sci.* 12(8): 875-890.

Golding, D.L., 1969. Snow relationships on Marmot Creek experimental watershed. *Can. Dept. Fish. For. Br. Bi-mon. Res. Notes* 25(2), 12-13.

Grayson, R., and Blöschl, G., 2000. *Spatial Patterns in Catchment Hydrology: Observations and Modelling*. Cambridge University Press: Cambridge, UK.

Gyasi-Agyei, Y., Willgoose, G., De Troch, F.P., 1995. Effects of vertical resolution and map scale of digital elevation models on geomorphological parameters used in hydrology. *Hydrological Processes* 9, 363–382.

Haddeland, I., and Lettenmaier, D.P., 1995. Hydrologic modeling of boreal forest ecosystems, Water Resources Series, Technical Report 145, University of Washington, Seattle.

Harr, R. D. and McCorison, F. M., 1979. Initial effects of clearcut logging on size and timing of peak flows in small watershed in western Oregon, Water Resources Research, 15(1), 90-94.

Hill, J. M., Graham, L. A., and Henry, R. J., 2000. Wide area topographic mapping and applications using airborne light detection and ranging (LIDAR) technology. Photogramm. Eng.Remote Sensing 66(8): 908-914.

Hutchinson, M.F., 1988. Calculation of hydrologically sound digital elevation models. In: Third International Symposium on Spatial Data Handling. International Geographical Union, Columbus, OH.

Hutchinson, M.F., 1989. A new procedure for gridding elevation and streamline data with automatic removal of spurious pits. Journal of Hydrology 106, 211–232.

Hutchinson, M.F. 2000. Optimising the degree of data smoothing for locally adaptive finite element bivariate smoothing splines. Australian & New Zealand Industrial and Applied Mathematics Journal 42(E): C774-C796.

Hutchinson, M.F., 2003. ANUDEM Version 4.6.3. Australian National University. Centre for Environmental Studies, Canberra.

Hutchinson, M.F., 2004. ANUDEM Version 5.1. The Australian National University (ANU), Canberra, Australia.

Hutchinson, M.F. 2006. Adding the Z-dimension. In: Wilson, J.P. and Fotheringham, A.S. (eds), Handbook of Geographic Information Science. Blackwell Publishing. Oxford.

Hutchinson, M.F., and Dowling, T.I., 1994. A continental hydrological assessment of a new grid-based digital elevation model of Australia. *Hydrological Processes* 5 (1), 45–58.

Hutchinson, M.F., and Gallant, J.C., 2000. Digital Elevation Models and Representation of Terrain Shape. *Terrain Analysis* pp. 51-85.

Jefferey, W.W., 1965. Experimental watersheds in the rocky mountains, Alberta, Canada. Publication 66, Symposium of Budapest of IASH.

Jenson, S. K., and Domingue, J. O., 1988. Extracting topographic structure from digital elevation data for geographic information system analysis. *Photogramm. Eng. Remote Sensing* 54(11): 1593-1600.

Jenson, S. K., 1991. Application of hydrologic information automatically extracted from digital elevation models. *Hydrol. Proc.* 5(1): 31-44.

Jones, K.H., 1998. A comparison of algorithms used to compute hill slope as a property of the DEM. *Computers and Geosciences* 24 (4), 315–323.

Jones, J. A. and Grant, G. E., 1996. Peak flow responses to clear-cutting and roads in small and large basins, western Cascades, Oregon, *Water Resources Research* 32(4), 959-974.

Jost, G., Moore, R.D., Weiler, M., Gluns, D.R. and Alila, Younes, 2009. Use of distributed snow measurements to test and improve a snowmelt model for predicting the effect of forest clear-cutting. *Journal of Hydrology* 376, 94-106.

Kattelman, R., 1990. Effects of forest cover on a snowpack in the Sierra Nevada, Watershed planning and analysis in action. American Society of Civil Engineers, New York.

Kenward, T., and Lettenmaier, D.P., 1997. Assessment of required accuracy of digital elevation data for hydrologic modeling, Water Resources Series, Technical Report 153, University of Washington, Seattle.

Kirkby, M. J., and Chorley, R. J., 1967. Throughflow, overland flow and erosion, Bull. Int. Assoc. Sci. Hydrol., 12, 5-21.

Kirby C.L., and Ogilvie R.T., 1969. The forest of Marmot Creek watershed research basin, Can.For.Ser.Publ.No.1259.

Kokkonen, T.S. and Jakeman, A.J., 2001. A comparison of metric and conceptual approaches in rainfall-runoff modeling and its implications. Water Resources Research, 37(9), 2345-2352.

Krause, P., Boyle, D.P., and Base, F., 2005. Comparison of different efficiency criteria for hydrological model assessment, Advances in Geosciences, 5, 89-97, European Geosciences Union.

LaMarche, J.L., and Lettenmaier, D.P., 1998. Forest road effects on flood flows in the Deschutes River basin, Washington, Water Resources Series, Technical Report 158, University of Washington, Seattle.

Laramie, R.L., and Schaake, J.C., Jr. 1972. Simulation of the continuous snowmelt process. In Ralph M. Parsons Laboratory Report Number 143. Massachusetts Institute of Technology: Cambridge.

- Legates, D. R. and McCabe Jr., G. J., 1999. Evaluating the use of "goodness-of-fit" measures in hydrologic and hydroclimatic model validation, *Water Resour. Res.*, 35, 1, 233–241.
- Leung, L.R., Wigmosta, M.S., Ghan, S.J., Epstein D.J., and Vail, L.W., 1996. Application of subgrid orographic precipitation/surface hydrology scheme to a mountain watershed, *Journal of Geophysical Research*, 101, 12, 803-812, 817.
- Leung, L.R., and Wigmosta, M.S., 1999. Potential climate change impacts on mountain watersheds in the Pacific Northwest. *J. Amer. Water Resour. Assoc.*, 35, 1463-1471.
- Leung LR, and Wigmosta, M.S., 2000. "The roles of subgrid topography on land-atmosphere interactions." In 15th Conference On Hydrology, pp. 194-197. American Meteorological Society, Boston, MA.
- Liu, X., 2008. Airborne LiDAR for DEM generation: Some critical issues. *Prog. Phys. Geogr.* 32(1): 31-49.
- Maidment, D.R., 1993. *Handbook of Hydrology*. McGraw-Hill: New York; 1424.
- Martz, L., De Jong, E., 1998. CATCH: A FORTRAN program for measuring catchment area from digital elevation models. *Computers and GeoSciences* 14 (5), 627–640.
- Matheussen, B., Kirshbaum, R.L., Goodman, I.A., O'Donnell, G.M., and Lettenmaier, D.P., 2000. Effects of land cover change on streamflow in the interior Columbia River Basin (USA and Canada), *Hydrologic Processes*, 14, 867-885.
- McKenzie, N., Gallant, J., and Gregory, L., 2003. Estimating water storage capacities in soil at catchment scales. 03/03, CRC Catchment Hydrology.

Megahan, W. F., 1972. Subsurface flow interception by a logging road in mountain of central Idaho, paper presented at Symposium on watersheds in transition, American Water Resources Association, Ft. Collins, Colorado.

Megahan, W. F., 1983. Hydrologic effects of clearcutting and wildfire on steep granitic slopes in Idaho, *Water Resources Research*, 19(3), 81-119.

Murphy, P. N. C., Ogilvie, J., Meng, F. R., and Arp, P., 2008. Stream network modeling using lidar and photogrammetric digital elevation models: A comparison and field verification. *Hydrol. Proc.* 22(12): 1747-1754.

Moore, I., Grayson, R., and Ladson, A., 1991. Digital terrain modelling: a review of hydrological, geomorphological, and biological applications. *Hydrological Processes* 5, 3-30.

Nash J.E., and Sutcliffe J.V., 1970. River flow forecasting through conceptual models part I — A discussion of principles, *Journal of Hydrology*, 10(3):282-290.

Nijssen, B., Haddeland, I., and Lettenmaier, D.P., 1997. Point evaluation of a surface hydrology model for BOREAS, *J. Geophys. Res.*, 102, 29,367-29,378.

O'Callaghan J.F., and Mark D.M., 1984. The extraction of drainage networks from digital elevation data, *Computer Vision, Graphics and Image Processing*, 28:323-344.

O'Loughlin, E. M., 1981. Saturation regions in catchments and their relations to soil and topographic properties, *J. Hydrol.*, 53, 229-246.

O'Loughlin, E.M., 1986. Prediction of surface saturation zones in natural catchments by topographic analysis. *Water Resources Research* 22 (5), 794-804.

Peucker, T., Douglas, D., 1975. Detection of surface-specific points by local parallel processing of digital terrain elevation data. *Computer Graphics and Image Processing* 4, 375–387.

Perkins, W.A., Wigmosta, M.S. and Nijssen., B., 1996. Development and testing of road and stream drainage simulation within a distributed model, *EOS Transactions AGU*, 77(46) Fall Meeting Supplement H22A.

Pomeroy, J. W. and Dion, K., 1996. Winter radiation extinction and reflection in a boreal pine canopy: measurements and modeling, *Hydrological Processes*, 10, 1591-1608.

Quinn, P., Beven, K., Chevallier, P., Planchon, O., 1991. The prediction of hillslope flow paths for distributed hydrological modelling using digital terrain models. *Hydrological Processes* 5, 59–79.

Renschler, C. S., and Harbor, J., 2002. Soil erosion assessment tools from point to regional scales: The role of geomorphologists in land management research and implementation. *Geomorphology* 47(2-4): 189-209.

Rothacher, J., 1965. Streamflow from small watersheds on the western slope of the Cascade range of Oregon. *Water Resources Research*, 1(1), 124-134.

Rothacher, J. 1970. Increases in water yield following clear-cut logging in the Pacific Northwest *Water Resources Research* 6(2) : 653 - 658.

Rowe, J.S., 1972. *Forest Regions of Canada*. Can. For. Serv. Pub. No. 1300.

Schoorl, J. M., Sonneveld, M. P. W., and Veldkamp, A., 2000. Three dimensional landscape process modeling: The effect of DEM resolution. *Earth Surf. Process. Landforms* 25(9): 1025-1034.

Singh, V.P., and Frevert, D., 2002. *Mathematical Models of Large Watershed Hydrology*. Water Resources Publications: Chelsea, MI; 891.

Stevenson D.R., 1967. *Geological and groundwater investigations in the Marmot Creek experimental basin of southwestern Alberta, Canada*, M.Sc. thesis, University of Alberta, Edmonton, Alberta.

Stevenson, D. R., 1974. *Preliminary analyses of the groundwater flow systems in Marmot Creek and Streeter Basins, Alberta, Canada*. Unpublished report - Research Council of Alberta.

Stonesifer, C., 2007. *Modeling the Cumulative Effects of Forest Fire on Watershed Hydrology: A Post-fire Application of the Distributed Hydrology-Soil-Vegetation Model (DHSVM)*. M.S. Thesis. U. Montana: Missoula.

Storr, D., 1967. *A Frequency Analysis of Maximum Two-Day and Three-Day Rainfalls in Saskatchewan, Alberta and Northeastern British Columbia*. Tec 654, Meteorological Branch, Dept. of Transport, Toronto.

Storr D., Tomlain J., Cork H.F., and Munn R.E., 1970. *An energy budget study above the forest canopy at Marmot Creek, Alberta, 1967*, *Water Resources Research*, 6(3).

Storr, D., 1974. *Monthly and annual estimates of evapotranspiration at Marmot Creek, Alberta, by the energy budget method.*. Environment Canada, Canadian Met. Research Report. No. 6/74 p. 18.

Storck, P., 2000. *Trees, snow and flooding: an investigation of forest canopy effects on snow accumulation and melt at the plot and watershed scales in the pacific northwest*, *Water Resources Series, Technical Report*, 161, University of Washington, Seattle.

Storck, P., Lettenmaier, D.P., Connelly, B.A., and Cundy, T.W., 1995. Implications of forest practices on downstream flooding, phase II final report, University of Washington, Seattle.

Storck, P., Bowling, L., Wetherbee, P., and Lettenmaier, D., 1998. Application of a GIS-based distributed hydrology model for prediction of forest harvest effects on peak stream flow in the Pacific Northwest, *Hydrol. Process.*, 12, 889-904.

Storck, P., Bowling, L., Wetherbee, P., and Lettenmaier, D., 1999. Application of a GIS-based distributed hydrology model for prediction of forest harvest effects on peak stream flow in the Pacific Northwest, in *Hydrological Applications of GIS*, A.M. Gurnell and D.R. Montgomery (eds.), John Wiley and Sons.

Storck, P., and Lettenmaier, D.P., 1999. Predicting the effect of a forest canopy on ground snow pack accumulation and ablation in maritime climates, in C. Troendle and K. Elder (Eds.), *proceedings of the Western Snow Conference*, pp 1-12.

Storck, P., and Lettenmaier, D.P., 2000. Trees, snow and flooding: An investigation of forest canopy effects on snow accumulation and melt at the plot and watershed scales in the Pacific Northwest, *Water Resources Series, Technical Report 161*, University of Washington, Seattle.

Swanson, R.H., Golding, D.L., Rothwell, R.L., and Bernier, P.Y., 1986. Hydrologic effects of clear-cutting at Marmot Creek and Streeter watersheds, Alberta. *Can. For. Serv., North. For. Cent., Edmonton, Alberta. Inf. Rep. NOR-X-278.*

Tarboton, D.G., 1997. A new method for the determination of flow directions and upslope areas in grid digital elevation models. *Water Resources Research* 33 (2), 309–319.

Tarboton, D.G., 2002. *Terrain analysis using digital elevation models (TauDEM)*, Utah State University, Logan, UT, USA.

Telang, S. A., Baker, B. L., Costerton, J. W., and Hodgson, G. W., 1975. Water quality and forest management: the effects of clear cutting on organic compounds in surface waters of the Marmot Creek drainage basin. Report to Environment Canada, Inland Waters Directorate.

Telang, S.A., Hodgson, G.W., and Baker, B.L., 1981. Effects of forest clear-cutting on abundances of oxygen and organic compounds in a mountain stream of the Marmot Creek basin. *Can. J. For Res.* 11: 545-553.

Troendle, C. A. and King, R. M., 1985. The effect of timber harvest on the Fool Creek Watershed, 30 years later, *Water Resources Research*, 21 (12), 1915-1922.

Vanshaar, J., and Lettenmaier, D.P., 2001. Effects of land cover change on the hydrologic response of Pacific Northwest forested catchments, *Water Resources Series, Technical Report 165*, University of Washington, Seattle.

VanShaar, J.R., Haddeland, I., and Lettenmaier, D.P., 2002. Effects of land cover changes on the hydrologic response of interior Columbia River Basin forested catchments, *Hydrol. Process.*, 16, 2499-2520.

Vertessy, R. A., Wilson, C. J., Silburn, D. M., Connolly, R. D., and Ciesiolka, C. A., 1990. Predicting erosion hazard areas using digital terrain analysis, IAHS AISH Publ., 192, 298-308.

Wahba, G., 1990. Spline Models for Observation data. Vol. 59 in the CBMS-NSF Regional conference series in applied mathematics. SIAM, Philadelphia, 169-181.

Wallis, P.M., Hynes, H.B.N., and Telang, S.A., 1981. The importance of groundwater in the transportation of allochthonous dissolved organic matter to the streams draining small mountain basins. *Hydrobiologia* 79:77-90.

Ward, A.D., and Elliot, W.J., 1995. *Environmental Hydrology*. Lewis Publishers: New York; 496.

Westrick, K.J., and Mass, C.F., 2000. An evaluation of a high resolution hydrometeorological modeling system for prediction of a cool-season flood event in a coastal mountainous watershed, *J. Hydrometeorol.*, 2, 161-180.

Wetherbee, P. and Lettenmaier, D. P., 1996. Application of the distributed hydrology-soil-vegetation model (DHSVM) to the little naches basin in the context of watershed analysis, Report to Plum Creek Timber Company and the National Council of the Paper Industry for Air and Stream Improvement.

Wetherbee, P., and Lettenmaier, D. P., 1997. Cabin Creek hydrology assessment report using the distributed hydrology soil vegetation model (DHSVM), Report to Plum Creek Timber Company and National Council of the Paper Industry for Air and Stream Improvement.

Wechsler, S.P., 2007. Uncertainties associated with digital elevation models for hydrologic applications: A review. *Hydrol. Earth Syst. Sci.* 11(4): 1481-1500.

Wigmosta, M.S., Leung, L.R., and Rykiel, E., 1995. Regional modeling of climate-terrestrial ecosystems interactions, *J. Biogeography*, (22), 453-465.

Wigmosta, M.S., and Burges, S.J., 1997. An adaptive modeling and monitoring approach to describe the hydrologic behavior of small catchments, *J. Hydrology*, 202, 48-77.

Wigmosta, M.S., and Lettenmaier, D.P., 1999. A Comparison of Simplified Methods for Routing Topographically-Driven Subsurface Flow, *Water Resource Research*, 35, 255-264.

Wigmosta, M.S., Nijssen, B., Storck, P., and Lettenmaier, D.P., 2002. The Distributed Hydrology Soil Vegetation Model, In *Mathematical Models of Small Watershed Hydrology and Applications*, V.P. Singh, D.K. Frevert, eds., Water Resource Publications, Littleton, CO., p. 7-42.

Wigmosta, M.S., and Perkins, W.A., 1997. A GIS-based modeling system for watershed analysis: Final Report to the National Council of Paper Industry for Arid and Stream Improvement.

Wigmosta, M.S., and Perkins, W.A., 2001. Simulating the effects of forest roads on watershed hydrology, in *Land Use and Watersheds, Human Influence on Hydrology and Geomorphology in Urban and Forest Areas*, M.S. Wigmosta and S.J. Burges, eds., AGU Water Science and Application Volume 2, p. 127-143.

Wigmosta, M.S., Vail, L., and Lettenmaier, D. P., 1994. A distributed hydrology-vegetation model for complex terrain, *Wat. Resour. Res.*, 30, 1665-1679.

Wigneron, J.P., Olioso, A., Calvet, J.C., and Bertuzzi, P., 1999. Estimating root zone soil moisture from surface soil moisture data and soil-vegetation-atmosphere transfer modeling. *Water Resour. Res.* 35 (12), 3735–3745.

Willmot, C. J., 1984. On the evaluation of model performance in physical geography, in: *Spatial Statistics and Models*, edited by: Gaile, G. L. and Willmot, C. J., D. Reidel, Dordrecht, 443–460.

Wolock, D.M., Hornberger, G.M., Beven, K.J., and Campbell, W.G., 1989. The relationship of catchment topography and soil hydraulic characteristics to lake alkalinity in the northeastern United States, *Water Resour. Res.*, 25, 829-837.

Wolock, D. M., Hornberger, G. M., and Musgrove, T. J., 1990. Topographic effects on flow path and surface water chemistry of the Llyn Brianne catchments in Wales, *J. Hydrol.*, 115, 243-259.

Wolock, D.M., and Price, C.V., 1994. Effects of digital elevation model map scale and data resolution on a topography-based watershed model. *Water Resources Research* 30, 3041–3052.

Yeh, G., Huang, G., Cheng, H., Zhang, F., Lin, H., Edris, E., and Richards, D., 2006. A first principle, physics-based watershed model: WASH123D. In *Watershed Models*, V.P. Singh and D.K. Frevert (eds.). Taylor and Francis: Boca Raton, FL; 211 – 244.

Ziemer, R. R., 1981. Storm flow response to road building and partial cutting in small streams of northern California, *Water Resources Research*, 17, 907-917.

Ziegler, A.D., 2000. Toward modeling erosion on unpaved roads in mountainous Northern Thailand. Ph.D. Dissertation. University of Hawaii at Manoa, Hawaii, US.

Zhang, W., and Montgomery, D., 1994. Digital elevation model grid size, landscape representation and hydrologic simulations. *Water Resources Research* 30, 1019–1028.



